Université Catholique de Louvain
Faculté des Sciences Appliquées

Centre d'Ingénierie des Systèmes,
d'Automatique et de Mécanique Appliquée

Avenue Georges Lemaître 4
B-1348 Louvain-la-Neuve
Belgique

Connecting Prediction Error Identification and Robust Control Analysis: a new framework

Xavier Bombois

Thèse présentée en vue de l'obtention du titre de **Docteur en Sciences Appliquées**

Promoteur: **Michel Gevers**

Novembre 2000

Université Catholique de Louvain
Faculté des Sciences Appliquées

Centre d'Ingénierie des Systèmes,
d'Automatique et de Mécanique Appliquée

Avenue Georges Lemaître 4
B-1348 Louvain-la-Neuve
Belgique

Connecting Prediction Error Identification and Robust Control Analysis: a new framework

Xavier Bombois

Jury:

Prof. G. Bastin (president), Université Catholique de Louvain, Louvain-la-Neuve, Belgium
Prof. V. Blondel, Université Catholique de Louvain, Louvain-la-Neuve, Belgium
Prof. M. Gevers (supervisor), Université Catholique de Louvain, Louvain-la-Neuve, Belgium
Prof. L. Ljung, Linköping University, Linköping, Sweden
Prof. P. Van den Hof, Delft University of Technology, Delft, The Netherlands
Dr. G. Scorletti, Université de Caen, Caen, France

A ma petite soeur Nathalie

Abstract

The main purpose of this thesis is to propose a new framework that connects Prediction Error Identification and Robust Control Theory. Prediction error identification using an unbiased model structure delivers an estimated model for the true plant and a confidence ellipsoid for its parameter vector. This model information can be obtained either through direct identification of the system or through the identification of the model error, and the identification itself can be performed either in open loop or in closed loop. The ellipsoidal parametric uncertainty region U contains the parameters of the true system at a certain probability level that we can fix at, say, 95%; and defines an equivalent uncertainty region $\mathcal{D}$ in the space of transfer functions. Such uncertainty description is different from the classical *frequency domain* uncertainty descriptions used in robust control analysis and design. However, our results connect these two sets of tools in a coherent way. These results cover two distinct aspects.

- The first aspect is "PE identification for robust control". We present a measure for the size of the uncertainty set $\mathcal{D}$, resulting from prediction error identification, that is directly connected to the size of the set of model-based controllers that is guaranteed by the ν-gap theory to stabilize all systems in this uncertainty set. This allows us to establish that one uncertainty set is better tuned for robust control design than another, leading to guidelines for the design of the identification experiment.

- The second aspect is "controller validation". We develop a necessary and sufficient condition for a specific controller to stabilize all systems in $\mathcal{D}$ and we present an optimization problem that computes exactly the worst case performance achieved by a controller over all systems in an uncertainty set $\mathcal{D}$ delivered by prediction error identification.

This thesis presents also results (restricted to linearly parametrized systems) about the image of the uncertainty set $\mathcal{D}$ in the Nyquist plane. The image in the Nyquist plane of such a set of plants is made up of ellipses at each frequency. However, the connection between different frequencies makes the mapping nontrivial. We show that the probability level linked to this image in the Nyquist plane is larger than that of the confidence region in the parameter space. This is due to the fact that the mapping between the parametric and frequency domain spaces is not bijective.

In the last part of this thesis, we extend our framework to the case of biased model structures, provided that the model structure is linearly parametrized. For this purpose, we use the stochastic embedding assumptions. First, we show that these assumptions allow one to construct a frequency domain uncertainty region $\mathcal{L}$ containing the true system at a certain probability level, as well for open-loop as for closed-loop identification. Then, we show that a necessary and sufficient condition can be found for the stabilization of all plants in $\mathcal{L}$ by a given controller and a procedure can be found to compute the worst case performance achieved by a controller over all plants in $\mathcal{L}$.

Preface

This thesis is divided in ten chapters:

Chapter 1:	Introduction
Chapter 2:	Uncertainty region deduced from PE identification with unbiased model structures
Chapter 3:	A measure of robust stability for the uncertainty region $\mathcal{D}$
Chapter 4:	A necessary and sufficient robust stability condition for $\mathcal{D}$
Chapter 5:	Worst case performance in $\mathcal{D}$
Chapter 6:	Practical simulation examples
Chapter 7:	Frequency domain image of a set of linearly parametrized transfer functions
Chapter 8:	Extension to biased model structures using stochastic embedding
Chapter 9:	Robustness analysis of $\mathcal{L}$
Chapter 10:	Conclusions

The material presented in Chapter 3 is to be published in

> X. Bombois, M. Gevers, and G. Scorletti. A measure of robust stability for a set of parametrized transfer functions. To appear in IEEE Transactions on Automatic Control, December 2000.

However, some results of this chapter (and of Chapter 2) can also be found in

> X. Bombois, M. Gevers, and G. Scorletti. Controller validation based on an identified model. In *Proc. IEEE Conference on Decision and Control*, pages 2816–2821, Phoenix, Arizona, 1999.
>
> M. Gevers, X. Bombois, B. Codrons, F. De Bruyne, and G. Scorletti. The role of experimental conditions in model validation for control. In A. Garulli, A. Tesi, and A. Vicino, editors, *Robustness in Identification and Control - Proc. of Siena Workshop, July 1998*, volume 245 of *Lecture Notes in Control and Information Sciences*, pages 72–86. Springer Verlag, 1999.

The materials of Chapter 4 and Chapter 5 were (or are to be) published in

> X. Bombois, M. Gevers, G. Scorletti, and B.D.O. Anderson. Controller validation for stability and performance based on an uncertainty region designed from an identified model. In *CD-ROM Proc. IFAC Symposium on System Identification*, paper WePM1-6, Santa Barbara, California, 2000.
>
> X. Bombois, M. Gevers, G. Scorletti, and B.D.O. Anderson. Robustness analysis tools for an uncertainty set obtained by prediction error identification. Revised version submitted to Automatica, April 2000.

The material in Chapter 6 is an adaptation of the examples published in

> B. Codrons, X. Bombois, M. Gevers, and G. Scorletti. A practical application of recent results in model and controller validation to a ferrosilicon production process. In *CD-ROM Proc. 39th Conference on Decision and Control*, paper WeP07-6, Sydney, Australia, 2000.

M. Gevers, X. Bombois, B. Codrons, G. Scorletti, and B.D.O. Anderson. Model validation for control and controller validation: a prediction error identification approach. Submitted to Automatica.

Note that this last paper summarizes Chapters 2 to 6. A preliminary version of this summary can be found in

M. Gevers, X. Bombois, B. Codrons, F. De Bruyne, and G. Scorletti. Model validation for robust control and controller validation in a prediction framework. In *CD-ROM Proc. IFAC Symposium on System Identification*, paper WeAM1-1, Santa Barbara, California, 2000.

The material of Chapter 7 can be found in

X. Bombois, B.D.O. Anderson, M. Gevers. Frequency domain image of a set of linearly parametrized transfer functions. Submitted to the European Control Conference (ECC01), Porto, 2001.

A preliminary version of several parts of Chapters 8 and 9 can be found in

X. Bombois, M. Gevers, and G. Scorletti. Controller validation for stability and performance based on a frequency domain uncertainty region obtained by stochastic embedding. In *CD-ROM Proc. 39th Conference on Decision and Control*, paper TuM06-5, Sydney, Australia, 2000.

Remerciements

Au moment de mettre un point final à cette thèse, je tiens à remercier les personnes qui ont contribué à sa réalisation. Chacunes m'ont permis de mener cette entreprise à bon port.

La première personne à laquelle je désire exprimer toute ma reconnaissance est certainement mon promoteur le professeur Michel Gevers. Je le remercie pour toute la confiance qu'il a placée en moi, pour sa disponibilité ainsi que pour tous les conseils avisés qu'il a pu me prodiguer tout au long de ces trois ans. Son aide scientifique fut fondamentale au développement de cette thèse. De tout coeur, j'espère que cette collaboration passionnante puisse se poursuivre dans l'avenir, quitte à devenir un habitué de la liaison ferrovière entre Delft et Louvain-la-Neuve.

Toute ma gratitude va aussi à mon ami Gérard Scorletti qui m'a fait profiter de sa connaissance encyclopédique de l'automatique, en général et de la commande robuste, en particulier. Je le remercie pour son soutien dans les moments difficiles et pour sa patience. Je lui suis également reconnaissant pour m'avoir hébergé à de si nombreuses reprises à Caen ainsi que pour tous ces bons moments passés devant un bon verre de cidre ou à découvrir les verts paysages de Normandie. Si cette thèse est ce qu'elle est aujourd'hui, c'est, sans aucun doute, à Michel et à Gérard que je le dois.

Dans ces remerciements, je ne pourrais pas oublier le professeur Brian D.O. Anderson. Durant ses deux séjours au CESAME, nos rendez-vous quotidiens furent des moments riches en nouvelles idées qui sont encore loin d'avoir été toutes exploitées à leur juste valeur.

Je veux aussi remercier Benoit Codrons avec qui j'ai partagé l'aventure

de cette thèse et en particulier pour sa précieuse aide dans la mise en oeuvre d'un exemple (un tant soit peu) réaliste pour notre méthodologie.

Je remercie aussi de tout coeur les professeurs Georges Bastin, Vincent Blondel, Lennart Ljung (Tack !) et Paul Van den Hof (Hartelijk bedankt !) pour avoir accepté d'être membre de mon jury de thèse avec Michel et Gérard. Qu'ils soient tous remerciés pour leurs précieux commentaires qui m'ont permis d'améliorer considérablement ce manuscrit.

Mes remerciements vont aussi à Salima et Mohamed M'Saad qui, avec Gérard, m'ont si gentiment accueilli lors de mes nombreux séjours à Caen. Je remercie aussi Glenn Vinnicombe et son épouse pour leur accueil à Cambridge. Que Glenn soit aussi remercié pour ses nombreuses remarques pertinentes qui sont à l'origine des résultats présentés dans le chapitre 7 de cette thèse. Je désire aussi saluer tous les membres du LAP ISMRA de Caen ainsi que ceux du Control Group de Cambridge (en particulier Paresh Date et John Steele).

Je voudrais aussi mentionner la formidable ambiance de travail au CESAME. C'est avec grand plaisir que je remercie nos secrétaires Isabelle Hisette, Michel Termolle, Dominique Pigeon et Lydia De Boeck. J'adresse un merci tout particulier à Isabelle qui m'a soutenu dans les moments difficiles et a toujours été d'une efficacité sans faille pour l'organisation de mes déplacements. Je remercie aussi nos techniciens Michel Dewan, Victor Vermeulen (le spécialiste de la reproduction typographique), Guido Donders et Etienne Huens (qui m'ont si souvent aidé à résoudre mes nombreux problèmes informatiques). Je remercie aussi tous mes collègues de bureau avec lesquels j'ai passés de longs moments à discuter agréablement : Lamia Ben Naoum, Christophe Lecomte, Pierre Ansay et Uly Nasution. Merci aussi à tous les autres chercheurs et professeurs du CESAME: Guillermo, Isabelle, Benoit, Cristina, Frédéric, Abdu, Mohamed, Guy, Paul, Philippe, Vincent ...

Que soient aussi remerciés mes ami(e)s (Catherine, Sébastien, Jean-Christophe, Ahmed ...) pour leurs nombreux encouragements et les chouettes moments passés en leur compagnie.

Finalement, ma reconnaissance va de tout coeur à ma famille pour le soutien qu'elle m'a témoigné tout au long de cette entreprise, mais

aussi pour la chance qu'elle m'a donné de faire des études.

Xavier Bombois,

Louvain-la-Neuve,
le 29 septembre 2000.

Contents

Notation glossary

Abbreviations

ARX	Auto-Regressive model structure with eXogenous inputs
ARMAX	Auto-Regressive Moving-Average model structure with eXogenous inputs
FIR	Finite Impulse Response model structure
GPC	Generalised Predictive Control
LFT	Linear Fractional Transformation
LMI	Linear Matrix Inequality
LTI	Linear Time Invariant
MEM	Model Error Model
MIMO	Multi-Input Multi-Output
PE	Prediction Error
PRBS	Pseudo-Random Binary Signal
QFT	Quantitative Feedback Theory
SISO	Single-Input Single-Output

General symbols, Operators, Functions

$A > 0$	the matrix A is positive definite
$A \geq 0$	the matrix A is positive semi-definite
A^T	transpose of matrix A
$A^\star$	complex conjugate transpose of matrix A
A^{-1}	inverse of matrix A
A^{-T}	transpose of A^{-1}
$\arg\min_x f(x)$	minimising argument of $f(x)$

$diag(a_1, \ldots, a_n)$	$n \times n$ diagonal matrix with entries $a_1 \ldots a_n$
$\mathcal{E}x$	mathematical expectation of the random variable x
$G^*(z)$	$G^*(z) \stackrel{\Delta}{=} G(1/z)$ for a discrete-time transfer function $G(z)$
$Im(x)$	imaginary part of the complex number x
j	$\sqrt{-1}$
$\mathcal{N}(m, C)$	Gaussian probability density function with mean m and covariance matrix C
$Pr(x < \beta)$	probability that the random variable x is less than β
$\mathbf{R}$	space of real numbers
$\mathbf{R}^{k \times n}$	space of real $k \times n$ matrices
$\mathcal{R}H_\infty$	real rational subspace of H_∞: ring of proper and real rational stable transfer functions or matrices
$Re(x)$	real part of the complex number x
z	shift operator: $z\,f(t) = f(t+1)$, $z^{-1}f(t) = f(t-1)$, or $\mathcal{Z}$-transform variable
$\lambda_1(A)$	largest eigenvalue of the matrix A
$\sigma_1(A)$	largest singular value of the matrix A
$\chi^2(k)$	chi-square probability density function with k degrees of freedom
ω	normalised frequency
$\|x\|$	modulus of the complex number x
$\|x\|_2$	2-norm of the vector x
$A \setminus B$	the set A minus the set B
$A \subset B$	the set A is a strict subset of B
$A \subseteq B$	the set A is a subset of B
$\parallel P \parallel_H$	Hankel norm of P
$\parallel P \parallel_\infty$	∞-norm of the stable transfer function $P \in H_\infty$

Chapter 1

Introduction

1.1 General objective

System identification is the scientific exercice that consists of determining a mathematical model of an underlying real-life process, the so-called true system, based on observed data; and Prediction Error (PE) identification is the method that is generally used to compute this mathematical model. One of the major applications of the identified model is the design of a control law for the true system. During the last years, much attention has been paid to tune identification for control design. Guidelines have been established in order to design identification experiments delivering a model that is accurate for control design [38, 39, 75, 80, 2]. Most often, these guidelines have led to the design of iteratives schemes [90, 3, 60, 69, 75, 80]. A common feature of these schemes is that iterations are performed of model updates (by identification with the most recent controller applied to the true system) and of model-based controller updates (the controller design being based on the most recent model). However, during the iterative procedure, there is no guarantee that the controller designed from the identified model will form a stable loop and achieve sufficient performance when this controller is applied to the unknown true system.

In order to derive this guarantee, the framework of Robustness Theory, introduced in the early 80's in [89, 31], is an elegant solution. This framework consists of considering an uncertainty region (i.e. a set of systems) that contains the true system, and to verify the stability and performance properties over all systems in this uncertainty region. The

introduction of robustness principles in identification for control has led to robustified iterative schemes (see [81, 24]) where, at each iteration, in addition to the design of a controller, a model and an uncertainty region around this model is identified. The robustification requires thus a method to identify a model and an uncertainty region, and robustness tools to analyze this uncertainty set. As a consequence, we need frameworks that connect PE identification and robustness theory.

In this thesis, we propose a new framework that connects PE identification and Robustness Theory. This framework consists in a new method to design an uncertainty region using the tools of PE identification, coupled with robustness tools that are adapted to this uncertainty region. These robustness tools pertain both to the robusness analysis of a controller and the quality assessment of the uncertainty region. Our framework is deduced for PE identification with unbiased model structure. However, we show that our robustness analysis tools can be adapted to the case of PE identification with biased model structure.

1.2 Historical framework

The history of the considered problem is already very long. Indeed the estimation of the error between the identified model and the true system that may be the root of uncertainty region determination, is as old as PE identification itself. A reputable engineer should never deliver a product without a statement about its precision. However, the information about this error was classically presented in the time-domain via the cross-correlation between inputs and residuals. This model error representation was thus a great distance from the classical uncertainty descriptions used in mainstream Robustness Theory, namely frequency domain uncertainty descriptions. As a consequence, a huge gap appeared at the end of the 80's between Robustness Theory and PE identification as was evidenced in the 1992 Santa Barbara Workshop [76]. This huge gap drove the Control Community to develop new techniques, different from PE identification, in order to obtain, from measured data, a nominal model for control design and an uncertainty region containing the true system. Several directions have been pursued:

- In *set membership identification* or the *hard bound (or bounded error) framework*, uncertainty models have been derived under a

variety of hard bound assumptions on the measurement noise and on the impulse reponse of the true system: see e.g. [46, 45, 66].

- A second direction, initiated by Smith and Doyle [77], consists of starting with an a priori uncertainty set resulting from prior assumptions on the true system and on the noise, and of then using observed input-output data to *invalidate* (and thus delete from this prior set) those models that are found to be inconsistent with these prior assumptions. Elaborations on this approach can be found in [70, 56, 19, 16]. The concept of model invalidation, on the basis of an observed incompatibility between a model (including its uncertainty description and its assumed hard-bound on the noise) and data, was extended to *controller invalidation* in [74].

These new techniques aimed at producing one of the standard linear fractional frequency domain uncertainty regions that are generally used in mainstream Robust Control Theory (such as additive, coprime factor uncertainty regions). The drawbacks of these techniques are nevertheless the large amount of assumptions and, more fundamentally, the fact that they are not based on the mainstream framework in System Identification i.e. PE identification.

Other approaches that are based on mainstream PE identification, have also been investigated to design uncertainty regions from measured data. They are interesting for our purpose since they are a first step in the direction of the reconciliation between PE identification and Robustness Theory. The first approach is the Model Error Model (MEM) approach proposed by L. Ljung in his plenary lecture at CDC 1997 [61] (see also [62]). The stated goal of this approach was to replace the time-domain information (i.e. the cross-correlation function between inputs and residuals) on the model error by frequency domain information, to suit the requirements of Robustness Theory. The key idea was to estimate a model of the error between an a-priori given model and the true system using a simple step of PE identification with unbiased model structure. By virtue of the unbiased model structure, the error is a variance error only, and an ellipsoid containing the "true parameter vector" at a certain probability level can be constructed using the estimated covariance matrix of the parameters. In [61, 62], this ellipsoid in parameter space was then transformed into ellipses at each frequency in the Nyquist plane, using a *first order approximation* of the mapping between the parameter space and the Nyquist plane. These ellipses can

be collected together to make up a frequency domain uncertainty region made up of ellipses at each frequency.

Although the other approaches, Stochastic Embedding [48, 47] and the methods presented in [49, 50, 87, 26], preceded the MEM approach, they can nevertheless be considered as the extension of the MEM approach to the case of (linearly parametrized) biased model structures. In Stochastic Embedding, the undermodeling is considered as the noise in classical PE identification i.e. as the realization of a zero mean stochastic process. Consequently, just as in the MEM approach, the total error is a variance error only and ellipses at each frequency in the Nyquist plane can be constructed and collected together to make up a frequency domain uncertainty region. The first order approximation is here avoided by only considering *linearly parametrized* model structures. In the methods presented in [49, 50] and in [87, 26], the error due to the noise is estimated in the same way as in the MEM and stochastic embedding approaches, but the error due to the undermodeling is estimated using an assumption about the decay rate of the impulse response of the true system. These last two approaches can therefore be considered as mixed probabilistic-deterministic approaches. The uncertainty region obtained with these methods can also be represented as an uncertainty region made up of ellipses at each frequency in the Nyquist plane.

In all these approaches (MEM, stochastic embedding and mixed probabilistic-deterministic approaches), we obtain thus frequency domain uncertainty regions made up of ellipses at each frequency in the Nyquist plane.

1.3 Contribution of this thesis

In this thesis, we will develop a framework that elegantly and efficiently connects Robustness Theory and PE identification with unbiased model structures, starting from the results in [61, 62]. This framework will be extended for some of its aspects to PE identification with (linearly parametrized) biased model structures using the stochastic embedding assumptions.

The starting point for the framework developed in this thesis is two observations we made about the MEM approach in [12]. The first obser-

vation is that the identification of an *unbiased model error model* is not the only way to construct uncertainty regions using this paradigm: an easier way is the direct identification of an *unbiased model* for the true system, and this in open-loop or in closed-loop. The second observation, which is more fundamental, is that the first order approximation yielding the ellipses in the Nyquist plane is a real drawback of the method, since it introduces an error. In order to avoid this first order approximation, we decided in [12] to consider, as uncertainty region, the set $\mathcal{D}$ of parametrized transfer functions corresponding to the ellipsoid in parameter space that is constructed with the estimated covariance matrix and that contains the true parameter vector (at a certain probability level).

The first contribution of our work is thus to present uncertainty regions $\mathcal{D}$ constructed with PE identification with unbiased model structure, without using any approximation or adding any further assumptions. This uncertainty region $\mathcal{D}$ contains the true system at a certain probability level. We develop a procedure to compute such uncertainty set for open-loop identification, different types of closed-loop identication methods, but also for the MEM approach, and we derive a general expression for this uncertainty set valid for all these types of identification. This general expression takes the form of a set of parametrized transfer functions whose (real) parameter vector is constrained to lie in an ellipsoid. The center of this uncertainty region is the "identified" open-loop model.

The uncertainty region $\mathcal{D}$ is a "parametric" uncertainty region and is thus totally different from the frequency domain uncertainty regions that are generally used in mainstream Robust Control Theory. Due to the huge amount of research accomplished in Robust Control Theory, a lot of results have also been developed for parametric uncertainty sets (see e.g. [34, 35, 53, 72, 7, 23, 4, 5]). Some of these results will help us to develop robustness tools adapted to the uncertainty region $\mathcal{D}$. However, manipulations of $\mathcal{D}$ and new results will be necessary to obtain these robustness tools (for more details see Chapters 4 and 5).

The second contribution of this thesis is therefore to furnish robustness tools that are adapted to the uncertainty set $\mathcal{D}$ (i.e. without embedding it in a classical uncertainty set as we first made in [12]). We develop robust stability and robust performance analysis tools. The ro-

bust stability analysis tool is a necessary and sufficient condition for the stabilization of all plants in $\mathcal{D}$ by a given controller. This condition has been deduced from the result of [53, 72] that gives such a condition for an uncertainty set defined by a real vector and expressed in the general LFT (Linear Fractional Transformation) framework of robust analysis. Our contribution is to recast the closed-loop connections of all systems in $\mathcal{D}$ with the considered controller as an LFT. The necessary and sufficient robust stability condition for $\mathcal{D}$ follows then from the result of [53, 72]. The robust performance analysis tool is an LMI[1]-based optimization problem that we develop to compute exactly the worst case performance achieved by a given controller over all plants in the uncertainty set $\mathcal{D}$.

A third contribution is to develop preliminary steps in the direction of "PE identification for robust control". This is a design problem, where our contribution is to characterize what quality an uncertainty region $\mathcal{D}$ must possess for it to be tuned for robustly stable control design. We have indeed established a measure of size of the uncertainty region $\mathcal{D}$ that is directly connected to the size of a set of model-based controllers that stabilize all systems in $\mathcal{D}$. This measure of size is the worst case ν-gap between the nominal model and the plants in $\mathcal{D}$ and is an extention of the ν-gap metric introduced in [84]. We show that this worst case ν-gap can be computed frequency-wise using an LMI-based optimization problem at each frequency. We also show that the smaller is the worst case ν-gap between the model G_{mod} and the uncertainty set $\mathcal{D}$, the larger is the set of G_{mod}-based controllers that are guaranteed to stabilize all systems in $\mathcal{D}$. The worst case ν-gap is thus an indicator of how well an uncertainty set $\mathcal{D}$ is tuned for robustly stable controller design based on G_{mod} and can therefore be used to assess the quality of the uncertainty set $\mathcal{D}$ obtained by a PE identification experiment. Our result also gives a meaning to the concept of *PE identification for robust control*: an identification experiment is "tuned for robust control design" if the worst case ν-gap for the uncertainty set delivered by this experiment is small, because it implies that, for that uncertainty set, the set of robustly stabilizing controllers is large. In that sense, although it is restricted to stability purposes, our result is thus a first step in the direction of the establishment of a link between identification experiment design and controller robustness.

[1] Linear Matrix Inequality

In our process of understanding the properties of the parametric uncertainty region $\mathcal{D}$, the representation (i.e. the image) of this uncertainty region in the Nyquist plane is an interesting feature. Since the analysis of the image of $\mathcal{D}$ for its general structure is quite complicated, we limit our analysis to uncertainty sets where the plants are linearly parametrized. The image in the Nyquist plane of such set of plants is made up of ellipses at each frequency. However, the connection between different frequencies makes the mapping nontrivial. We show that the image in the Nyquist plane contains more plants than the parametric uncertainty set. This is due to the fact that the mapping between the parametric and frequency domain spaces is not bijective.

The last part of this thesis consists of extending our framework to the case of PE identification with a *biased model structure* in the particular case where this model structure is linearly parametrized. For this purpose, we use the stochastic embedding assumptions [48, 47]. The choice of the stochastic embedding method instead of the mixed probabilistic-deterministic approaches [50, 26] to extend our framework to biased model structures is quite arbitrary. It is nevertheless important to note that the results we develop for the stochastic embedding approach also apply to the mixed probabilistic-deterministic approaches since the uncertainty regions delivered by all these methods are similar.

The uncertainty set deduced from an open-loop PE identification procedure with stochastic embedding assumptions delivers an ellipsoidal uncertainty set in the Nyquist plane (see Section 1.2). In this thesis, we extend the stochastic embedding technique to closed-loop identification and we give a general expression of the uncertainty region $\mathcal{L}$ (valid for both the open-loop and closed-loop cases) that exposes the structural similarities of the uncertainty set $\mathcal{L}$ with the uncertainty region $\mathcal{D}$. The last contribution of this thesis is to develop the same robust stability and performance analysis tools for $\mathcal{L}$ as was developed for $\mathcal{D}$ i.e. a necessary and sufficient condition for the stabilization of all plants in $\mathcal{L}$ by a given controller and an LMI-procedure to compute exactly the worst case performance achieved by a given controller over all plants in $\mathcal{L}$. Both tools have been derived from the structural similarities between $\mathcal{D}$ and $\mathcal{L}$.

It is to be noted that a technical problem prevents us from computing

the worst case ν-gap for the uncertainty region $\mathcal{L}$.

1.4 The actors

Before giving the general outline of the thesis, let us present the different "actors" that will intervene in this thesis.

The true system G_0. The true system is the process we want to control. It is assumed to be Single Input Single Output (SISO), Linear Time Invariant (LTI) and finite dimensional.

The uncertainty region. The uncertainty region is deduced from a PE identification procedure on the true system. This is called $\mathcal{D}$ if the model structure is assumed unbiased and $\mathcal{L}$ if the model structure is linearly parametrized and possibly biased. The uncertainty region is a set of systems that contains the true system at a certain probability level.

The model G_{mod}. The model G_{mod} is the model chosen for control design. This model is generally the identified model, center of the uncertainty region $\mathcal{D}$ (or $\mathcal{L}$). However, this is not a requirement: G_{mod} may be given.

The controller C. The controller C is the controller designed from G_{mod} that we want to apply to the unknown true system. In order to apply C to G_0 with confidence, we need to verify if the controller C stabilizes and achieves sufficient performance with all plants in the uncertainty region $\mathcal{D}$ (or $\mathcal{L}$) containing the true system G_0.

1.5 General outline

This thesis is organized as follows:

Chapter 2: Uncertainty region deduced from PE identification with unbiased model structures. This chapter recalls the general results of PE identification with unbiased model structures and presents the procedure that allows one to design uncertainty sets $\mathcal{D}$ using a PE identification procedure with an unbiased model structure.

Chapter 3: A measure of robust stability for the uncertainty region $\mathcal{D}$. This chapter introduces the worst case ν-gap, gives an LMI procedure to compute it and shows why this measure can be considered as a robust stability measure of $\mathcal{D}$.

Chapter 4: A necessary and sufficient robust stability condition for $\mathcal{D}$. This chapter presents the necessary and sufficient condition for the stabilization of all plants in $\mathcal{D}$ by a given controller.

Chapter 5: Worst case performance in $\mathcal{D}$. This chapter defines the notion of worst case performance achieved by a given controller over all the plants in the uncertainty region $\mathcal{D}$ and gives the LMI-based optimization problem that computes it exactly.

Chapter 6: Practical simulation examples. In this chapter, our methodology is applied to two realistic simulation examples: a flexible transmission system and a ferrosilicon production process.

Chapter 7: Frequency domain image of a set of linearly parametrized transfer functions. In this chapter, we analyze the image of the uncertainty region $\mathcal{D}$ in the Nyquist plane in the case where the model structure is chosen linearly parametrized.

Chapter 8: Extension to biased model structures using stochastic embedding. This chapter presents the stochastic embedding assumptions and gives the procedure to design the uncertainty region $\mathcal{L}$ in open-loop and in closed-loop.

Chapter 9: Robustness analysis of $\mathcal{L}$. In this chapter, we give the robust stability and robust performance analysis tools for the uncertainty region $\mathcal{L}$.

Chapter 10: Conclusions. This chapter concludes this thesis and proposes some possible further research topics.

Chapter 2

Uncertainty region deduced from Prediction Error Identification with unbiased model structure

As said in the previous chapter, this work presents a framework that connects Prediction Error (PE) identification and Robust Control Theory. For this purpose, in this chapter, it is shown that PE identification with unbiased model structure allows one to design an uncertainty region containing the true system at a certain probability level, without any further assumptions.

Prediction error identification delivers an estimated model for the true plant G_0. If the parametric structure for the model is sufficiently complex to represent the true system, then this model is asymptotically unbiased, and the covariance matrix of the parameter estimates allows one to construct a parametric uncertainty region U containing the parameters of the true system G_0 at a certain probability level that we can fix at, say, 95 %. The uncertainty region U in the parameter space defines an equivalent uncertainty region $\mathcal{D}$ in the space of transfer functions with the identified model as its center. This uncertainty region $\mathcal{D}$ is thus defined as a set of parametrized transfer functions, whose parameter vector is constrained to lie in an ellipsoidal region in the parameter space.

Chapter outline. In Section 2.1, we first recall the notion of unbiased model structure and the results of PE identification with such model structure. In Section 2.2, we go through the different types of identification (open-loop, closed-loop, Model Error Model approach, ...) and show the procedure to design an uncertainty region with each of these types. In Section 2.3, the general structure of the uncertainty regions delivered by PE identification is presented.

2.1 PE identification with unbiased model structure

In this section, we present the results related to PE identification with unbiased model structure. More details can be e.g. found in [63]. Before proceeding to this, we first recall the classical results of PE identification whatever model structure we choose to perform this identification.

2.1.1 General results of PE identification

PE identification consists of selecting a parametrized model of an unknown system P_0 in a certain model structure using time-domain data collected on this system P_0. The rule by which this selection is performed using the data, is a prediction error criterion i.e. the minimization of the errors between the outputs that are predicted using the parametrized model and the actual outputs collected on the system.

The system P_0 we want to identify can e.g. be a real-life plant or a closed-loop transfer function describing a loop containg the real-life plant. In the sequel, we will always consider systems P_0 having the following properties.

Assumption 2.1 *The system P_0 that we want to identify is stable, single input single output (SISO), finite dimensional and linear time-invariant (LTI), with a discrete-time rational input-output transfer function $P_0(z)$:*

$$y(t) = P_0(z)u(t) + v(t), \tag{2.1}$$

where $u(t)$ is the input signal, $y(t)$ the output signal and $v(t)$ is an additive noise that is assumed to be generated by a white noise $e(t)$ filtered by a discrete-time rational transfer function $\bar{H}_0(z)$:

$$v(t) = \bar{H}_0(z)e(t).$$

The noise $v(t)$ corrupting the output $y(t)$ is thus assumed to be the realization of a zero mean stochastic process.

In order to find a model for the system P_0, we need

1. input and output signals collected on the system P_0
2. a model structure $\mathcal{M}$ for P_0 from which we will select a model for P_0 using the prediction error criterion and the collected data.
3. a model structure for $\bar{H}_0$ from which we will select a model for $\bar{H}_0$ using the same prediction error criterion and the same data.

In order to collect data on P_0, we apply the following procedure:

Definition 2.1 (data collected on P_0) *Let us consider the system P_0 satisfying Assumption 2.1. We apply a known sequence $U_N = \{u(t)|t = 1...N\}$ of N input data to P_0. This input sequence is assumed persistently exciting (see [63]). We collect the corresponding noisy output sequence $Y_N = \{y(t)|t = 1...N\}$ generated by (2.1).*

A model structure is a set of parametrized transfer functions. Let us define the model structure for P_0 as follows:

$$\mathcal{M} = \{P(\theta) \mid \theta \in \mathbf{R}^{k\times 1}\}, \tag{2.2}$$

The vector θ is called the parameter vector. As we will never use the model of $\bar{H}_0$, we will not define the model structure for $\bar{H}_0$ formally. However, we must always keep in mind that a PE identification procedure pertains to the identification of both a model for P_0 and a model of $\bar{H}_0$. Let us now summarize the general results of PE identification in the following proposition.

Proposition 2.1 ([63]) *Let us consider the system P_0 satisfying Assumption 2.1 and the sequences U_N and Y_N collected on P_0 as shown in Definition 2.1. Let us also consider a model structure $\mathcal{M}$ for P_0 as defined in (2.2). A PE identification procedure with U_N, Y_N and $\mathcal{M}$ delivers an identified parameter vector $\hat{\theta}$ defining a model $P(\hat{\theta}) \in \mathcal{M}$. The identified parameter vector $\hat{\theta}$ is the parameter vector that minimizes the sum of the square of the predicted errors i.e. the differences between the*

predicted outputs $\hat{y}(t,\theta)$ [1] *and the actual outputs* $y(t)$*:*

$$\hat{\theta} \stackrel{\Delta}{=} arg \ \min_{\theta} \sum_{t=1}^{N} (\hat{y}(t,\theta) - y(t))^2 \tag{2.3}$$

Moreover, $\hat{\theta}$ *is asymptotically a random vector with gaussian distribution, mean* θ^* *and covariance* C*:*

$$\hat{\theta} \sim As\mathcal{N}(\theta^*, C) \tag{2.4}$$

where $\theta^* \in \mathbf{R}^{k\times 1}$ *is an unknown parameter vector and* $C \in \mathbf{R}^{k\times k}$ *is an unknown symmetric positive definite matrix. Besides an identified parameter vector* $\hat{\theta}$*, the PE identification procedure also delivers an estimate* P_θ *of the covariance matrix* C *of* $\hat{\theta}$*.*

2.1.2 PE identification with unbiased model structure

PE identification with unbiased model structure is the particular case of PE identification where the model structure for P_0 is chosen unbiased. A model structure $\mathcal{M}$ is said unbiased if the system P_0 lies in $\mathcal{M}$:

Definition 2.2 (Unbiased model structure for P_0) *Let us consider a system* P_0 *satisfying Assumption 2.1 and a model structure for* P_0 *as defined in (2.2). The model structure* $\mathcal{M}$ *is said unbiased for* P_0 *if there exists a parameter vector* $\theta_0 \in \mathbf{R}^{k\times 1}$ *such that*

$$P_0 = P(\theta_0) \in \mathcal{M}$$

Definition 2.2 and Proposition 2.1 show that a PE identification procedure with an unbiased model structure delivers a full order model of the true system.

When an unbiased model structure is used, the only error you can obtain on the estimation of P_0 is the covariance error due to the (zero mean) noise $v(t)$ corrupting the output of P_0. The mean of the estimated parameter vector $\hat{\theta}$ is consequently the true parameter vector θ_0. This is summarized in the following proposition.

[1] If we define the model structure for $\bar{H}_0$ as $\mathcal{M}_{\bar{H}} = \{\bar{H}(\theta) \mid \theta \in \mathbf{R}^{k\times 1}\}$, then the predicted outputs $\hat{y}(t,\theta)$ is equal to $\bar{H}^{-1}(\theta)P(\theta)u(t) + (1 - H^{-1}(\theta))y(t)$.

Proposition 2.2 ([63]) *Let us consider that the PE identification procedure described in Proposition 2.1 is performed with an unbiased model structure $\mathcal{M}$ for $P_0 = P(\theta_0)$ as defined in Definition 2.2* [2]*. Then, the identified parameter vector $\hat{\theta}$ defines an unbiased model $P(\hat{\theta}) \in \mathcal{M}$ and has the property of being asymptotically a random vector with gaussian distribution, mean θ_0 and covariance C:*

$$\hat{\theta} \sim As\mathcal{N}(\theta_0, C) \tag{2.5}$$

where $C \in \mathbf{R}^{k \times k}$ is an unknown symmetric positive definite matrix. As for general model structures, the PE identification procedure with unbiased model structure also delivers an estimate P_θ of the covariance matrix C of $\hat{\theta}$.

Although the Gaussian distribution property of the identified parameter vector is an asymptotic property (i.e. a property obtained when $N \to \infty$), we will use this property in the sequel for a finite but sufficiently large number N of data. This widespread approximation in Statistics Theory has been proved accurate in [63]. Using this approximation, the results presented in Proposition 2.2 allows one to define confidence ellipsoids centered at the identified parameter vector $\hat{\theta}$ and containing the unknown parameter vector with a certain probability level.

Proposition 2.3 ([63]) *Let us consider the system $P_0 = P(\theta_0)$ satisfying Assumption 2.1. Let us also consider the identified parameter vector $\hat{\theta}$ and the estimate P_θ of the covariance matrix of $\hat{\theta}$ as delivered by a PE identification procedure performed on P_0 using a sufficiently large number N of input-output data and an unbiased model structure $\mathcal{M}$ (see Proposition 2.2). We have then that the ellipsoid U of size χ i.e.*

$$U = \{\theta \mid (\theta - \hat{\theta})^T P_\theta^{-1} (\theta - \hat{\theta}) < \chi\} \tag{2.6}$$

contains the true parameter vector θ_0 with a probability $\alpha(k, \chi)$:

$$\alpha(k, \chi) = Pr(\theta_0 \in U) = Pr(\chi^2(k) < \chi),$$

where $\chi^2(k)$ is the chi-square probability density function with k degrees of freedom.

[2] The model structure for $\bar{H}_0$ is also assumed unbiased. However, it is not a requirement in the case where the model structures for P_0 and H_0 are independently parametrized and the signals $u(t)$ and $v(t)$ are not correlated.

Proof. This proposition is a direct consequence of the fact that N has been chosen sufficiently large and of Proposition 2.2. □

Remarks.

- The use of the chi-square probability distribution with k degrees of freedom to define the probability density linked to U is in fact an approximation. Indeed, since P_θ is only an estimate of the covariance matrix C obtained with N experimental data, the probability density function linked to U is a function of the F-distribution $F(k, N-k)$: the probability of the presence of θ_0 in U is $Pr(F(k, N-k) < \chi/k)$. Nevertheless, since N will generally be large, we have that $Pr(F(k, N-k) < \chi/k) \approx Pr(\chi^2(k) < \chi)$.
- The probability level $\alpha(k, \chi)$ can be chosen by the designer.
- If you choose a probability level $\alpha(k, \chi) = 0.95$, it actually means that we have a probability of 95 % that the realisation of the noise $v(t)$ in the considered experiment has generated a covariance error on the estimate $\hat{\theta}$ such that the true parameter vector θ_0 lies in the confidence ellipsoid U.

2.1.3 PE identification with unbiased ARX model structures

In the previous subsection, we have briefly presented the general results of PE identification with unbiased model structures. These results are summarized in Proposition 2.2. In order to illustrate these results, we will present, in this subsection, the mathematical details of a PE identification procedure with unbiased model structure when the system P_0 has an ARX structure. A system P_0 is said to have an ARX structure if the relation between its input $u(t)$ and its output $y(t)$ is given by

$$A(\theta_{1,0})y(t) = B(\theta_{2,0})u(t) + e(t). \tag{2.7}$$

The vectors $\theta_{1,0} \in \mathbf{R}^{n_a \times 1}$ and $\theta_{2,0} \in \mathbf{R}^{n_b \times 1}$ are unknown parameter vectors. The signal $e(t)$ is a white noise of variance σ^2. $B(\theta_{2,0})$ is a polynomial in z^{-1} with a certain delay that is here assumed equal to 1:

$$B(\theta_{2,0}) = \begin{pmatrix} z^{-1} & z^{-2} & \dots & z^{-n_b} \end{pmatrix} \theta_{2,0},$$

and $A(\theta_{1,0})$ is a monic polynomial in z^{-1} given by

$$A(\theta_{1,0}) = 1 + \begin{pmatrix} z^{-1} & z^{-2} & \dots & z^{-n_a} \end{pmatrix} \theta_{1,0}.$$

In order to perform a PE identification procedure with unbiased model structure for the system P_0 as defined in (2.7), let us measure N input data $u(t)$ and the corresponding N output data $y(t)$ generated by (2.7) and let us define an unbiased model structure as well for the system $P_0 = B(\theta_{2,0})/A(\theta_{1,0})$ as for the noise model $\bar{H}_0 = 1/A(\theta_{1,0})$:

$$\mathcal{M}_{ARX} = \left\{ P(\theta) = \frac{B(\theta_2)}{A(\theta_1)} \; and \; \bar{H}(\theta) = \frac{1}{A(\theta_1)} \mid \theta = \begin{pmatrix} \theta_1 \\ \theta_2 \end{pmatrix} \in \mathbf{R}^{(n_a+n_b)\times 1} \right\} \tag{2.8}$$

The identification of a model from $\mathcal{M}_{ARX}$ is equivalent to the identification of a parameter vector $\hat{\theta}$ using the criterion presented in (2.3). In order to proceed to the determination of $\hat{\theta}$, let us first introduce the following notations about the actual outputs $y(t)$ and the predicted outputs $\hat{y}(t,\theta)$ that are both used in (2.3):

$$y(t) = \phi(t) \overbrace{\begin{pmatrix} \theta_{1,0} \\ \theta_{2,0} \end{pmatrix}}^{\theta_0} + e(t) \tag{2.9}$$

$$\overbrace{\begin{pmatrix} y(1) \\ y(2) \\ : \\ y(N) \end{pmatrix}}^{Y} = \overbrace{\begin{pmatrix} \phi(1) \\ \phi(2) \\ : \\ \phi(N) \end{pmatrix}}^{\Phi} \theta_0 + \overbrace{\begin{pmatrix} e(1) \\ e(2) \\ : \\ e(N) \end{pmatrix}}^{E}, \tag{2.10}$$

where $\phi(t) = \begin{pmatrix} -y(t-1) & \dots & -y(t-n_a) & u(t-1) & \dots & u(t-n_b) \end{pmatrix}$. The predicted output $\hat{y}(t,\theta)$ for a system in $\mathcal{M}_{ARX}$ is given by $\hat{y}(t,\theta) = \phi(t)\theta$ [63]. As for the actuals outputs, let us construct a vector with the N predicted outputs:

$$\overbrace{\begin{pmatrix} \hat{y}(1,\theta) \\ \hat{y}(2,\theta) \\ : \\ \hat{y}(N,\theta) \end{pmatrix}}^{\hat{Y}(\theta)} = \Phi\theta \tag{2.11}$$

We are now able to find the estimate $\hat{\theta}$ that minimizes the prediction error criterion presented in (2.3). Indeed, using expressions (2.10) and (2.11), we can rewrite that criterion as follows:

$$\hat{\theta} = arg \min_{\theta}[(\Phi\theta - Y)^T(\Phi\theta - Y)].$$

It yields:

$$\hat{\theta} = (\Phi^T\Phi)^{-1}\Phi^T Y = QY \tag{2.12}$$

Let us now analyze the mean and the covariance of the estimate $\hat{\theta}$. The mathematical expectation $\mathcal{E}\hat{\theta}$ of $\hat{\theta}$ can be computed as follows:

$$\begin{aligned} \mathcal{E}\hat{\theta} &= \mathcal{E}[(\Phi^T\Phi)^{-1}\Phi^T \overbrace{(\Phi\theta_0 + E)}^{Y}] \\ &= \theta_0 + (\Phi^T\Phi)^{-1}\Phi^T\mathcal{E}(E) \\ &= \theta_0 \end{aligned} \tag{2.13}$$

We obtain the result of Proposition 2.2 that tells us that the mean of the estimate $\hat{\theta}$ is equal to θ_0 in the case of unbiased model structures. Let us now compute the covariance matrix C of $\hat{\theta}$:

$$\begin{aligned} C = \mathcal{E}[(\hat{\theta} - \theta_0)(\hat{\theta} - \theta_0)^T] &= \mathcal{E}[(QE)(QE)^T] \\ &= \sigma^2 QQ^T \end{aligned} \tag{2.14}$$

The matrix C is unknown since the variance σ^2 of the white noise $e(t)$ is unknown. However, we can obtain an estimate $\hat{\sigma}^2$ of σ^2 by using a maximum likelihood technique [63]. As a consequence, we also obtain an estimate P_θ of C:

$$P_\theta = \hat{\sigma}^2 QQ^T \tag{2.15}$$

Remark. In this subsection, we have analyzed the case of ARX model structures. It is to be noted that, if the chosen model structure is not linear in θ (such as in the ARX model structure), the determination of $\hat{\theta}$ and of P_θ require numerical optimization routines (see e.g. [63]).

2.2 Design of uncertainty regions using PE identification

In the previous section, we have recalled the important results related to PE identification with unbiased model structure. In this section, we will show that we can design an uncertainty region containing the real-life plant G_0, the so-called true system G_0 using a PE identification procedure with unbiased model structure, and this without adding any further assumptions on the true system G_0 than the classical assumptions required by PE identification. We will consider different types of PE identification, namely:

- open-loop identification [63],
- model error model identification [62, 64, 43, 42],
- direct closed-loop identification [78],
- indirect closed-loop identification [78],
- Dual-Youla closed-loop identification [52, 51, 75, 27].

Open-loop identification is the classical way to perform identification. However, in many industrial applications, due to unstable behaviour of the plant, experimental data can only be obtained in closed loop and a closed-loop identification must be performed. Moreover, the recent results on identification for control have promoted the use of closed-loop identification for producing models that are better suited for control design (see e.g. [38, 39]). The properties of the different types of closed-loop identification are compared in e.g. [28]. The model error model approach has been introduced by L. Ljung in order to validate an a-priori given model G_{mod} and consists in the identification of a model for the difference between the true system and the model G_{mod}. Open-loop and closed-loop identification can be considered for this approach.

We will show that all these types of identification lead to uncertainty regions that have the same general structure. Before proceeding to this, we will first present the assumptions we made about the true system G_0. These assumptions are the classical assumptions required by PE identification with unbiased model structure.

2.2.1 Assumptions on the true system G_0

In the sequel, we will assume that the true system G_0 is SISO and LTI. Moreover, we assume that G_0 can be described by a discrete-time rational transfer function $G_0(z)$ having the following general form

$$G_0(z) = G(z, \theta_0) = \frac{z^{-d}(b_0 + b_1 z^{-1} + ... + b_m z^{-m})}{1 + a_1 z^{-1} + ... + a_n z^{-n}} = \frac{Z_2(z)\theta_0}{1 + Z_1(z)\theta_0}, \tag{2.16}$$

where

- d is the delay;
- $\theta_0^T = [a_1 \ ... \ a_n \ b_0 \ ... \ b_m] \in \mathbf{R}^{q \times 1}$, $q \triangleq (n + m + 1)$;
- $Z_1(z) = [z^{-1} \ z^{-2} \ ... \ z^{-n} \ 0 \ ... \ 0]$ is a row vector of size q;
- $Z_2(z) = z^{-d} \ [0 \ ... \ 0 \ 1 \ z^{-1} \ z^{-2} \ ... \ z^{-m}]$ is a row vector of size q.

We will further assume that the input-output relation for G_0 is given by

$$y(t) = G_0 u(t) + v(t), \tag{2.17}$$

where $v(t)$ is additive noise modelled by $v(t) = H_0(z)e(t)$. The transfer function $H_0(z)$ is a discrete-time rational transfer function and $e(t)$ is a white noise of variance σ^2.

These assumptions are equivalent to the assumptions we made about the system P_0 in the previous section. The only difference is that we do not require here that the true system G_0 is stable. Indeed, this stability is not needed for the closed-loop identification procedures. However, the stability of G_0 is required in order to perform an open-loop identification or an identification using the model error model approach in open-loop.

2.2.2 Open-loop PE identification

Let us consider the true system G_0 presented in Section 2.2.1. Here, we further assume that G_0 is stable. The true system G_0 satisfies therefore Assumptions 2.1, and we may therefore perform a PE identification with unbiased model structure with this true system. Using (2.16), an unbiased model structure for G_0 is given by

$$\mathcal{M}_{ol} = \left\{ G(\theta) \mid G(\theta) = \frac{Z_2\theta}{1 + Z_1\theta} \right\}, \tag{2.18}$$

where $\theta \in \mathbf{R}^{q\times 1}$. If we know collect N input data $u(t)$ and output data $y(t)$ on the true system G_0, we have all the elements to perform the identification. As stated in Proposition 2.2, this identification yields a model $G(\hat{\theta}) \in \mathcal{M}_{ol}$ and an estimate of the covariance matrix P_θ of $\hat{\theta}$. Using now Proposition 2.3, the true parameter vector θ_0 lies with probability $\alpha(q,\chi)$ in the ellipsoidal uncertainty region

$$U_{ol} = \{\theta \mid (\theta - \hat{\theta})^T P_\theta^{-1} (\theta - \hat{\theta}) < \chi\} \tag{2.19}$$

This parametric uncertainty region U_{ol} defines a corresponding uncertainty region in the space of transfer functions which we denote $\mathcal{D}_{ol}$:

$$\mathcal{D}_{ol} = \left\{ G(\theta) \mid G(\theta) = \frac{Z_2\theta}{1+Z_1\theta} \; and \; \theta \in U_{ol} \right\} \tag{2.20}$$

Properties of $\mathcal{D}_{ol}$.

$$G_0 \in \mathcal{D}_{ol} \; with \; probability \; \alpha(q,\chi)$$

We have thus defined an uncertainty region $\mathcal{D}_{ol}$ centered at the identified model $G(\hat{\theta})$ and containing the true sytem G_0 with probability $\alpha(q,\chi)$ (e.g. $\alpha = 0.95$).

2.2.3 Model Error Model Approach

In this section, we will show that we can also obtain an uncertainty region containing the true system at a certain probability level using the Model Error Model (MEM) approach. This approach was introduced by Lennart Ljung in [62] for the open-loop case and was extended to the closed-loop case in [43]. We will here only consider the open-loop case in order to remain concise. However, we can also deduce an uncertainty region from MEM in closed-loop as proved in [43, 42]. In the MEM approach, we consider a stable true system G_0 satisfying the assumptions presented in Section 2.2.1 and an a-priori given model G_{mod} for this true system[3]. This approach consists of identifying a model for the error between the given model G_{mod} and the true system G_0. A model for G_0 is then deduced by adding G_{mod} to the identified "error model".

Just as for the open-loop identication case presented in the previous subsection, we collect on the true system G_0 two sequences U_N and Y_N

[3]This model G_{mod} is typically the model we want to use for control design.

containing N inputs $u(t)$ and the corresponding outputs $y(t)$, respectively. Using these data, we compute the N residuals $\varepsilon(t)$:

$$\varepsilon(t) = y(t) - G_{mod}u(t). \tag{2.21}$$

We have then the following relation between the inputs $u(t)$ and the residuals $\varepsilon(t)$:

$$\varepsilon(t) = \overbrace{(G_0 - G_{mod})}^{\delta G_0} u(t) + H_0 e(t) \tag{2.22}$$

As the system δG_0 satisfies Assumptions 2.1, we can perform a PE identification with unbiased model structure for δG_0. An unbiased model structure for δG_0 is a function of the given model G_{mod}. Let us therefore denote it in the following generic form:

$$\mathcal{M}_{mem} = \left\{ \tilde{G}(\eta) \mid \tilde{G}(\eta) = \frac{Z_3\eta}{1 + Z_4\eta} \right\}, \tag{2.23}$$

where we have that η is a real vector of size, say, l and that $Z_3(z)$ and $Z_4(z)$ are row vectors of size l constructed in the same way as Z_1 and Z_2 in (2.16) and therefore containing only delays and zeros. As $\mathcal{M}_{mem}$ is an unbiased model structure for δG_0, there exists a vector η_0 such that $\delta G_0 = \tilde{G}(\eta_0) \in \mathcal{M}_{mem}$. As stated in Proposition 2.2, a PE identification procedure with U_N, $\mathcal{E}_N = \{\varepsilon(t) | t = 1...N\}$ and $\mathcal{M}_{mem}$ yields an unbiased model $\tilde{G}(\hat{\eta})$ of δG_0 and an estimate P_η of the covariance matrix of $\hat{\eta}$. Using now Proposition 2.3, the true parameter vector η_0 lies with probability $\alpha(l, \chi)$ in the ellipsoidal uncertainty region

$$U_{mem} = \{\eta \mid (\eta - \hat{\eta})^T P_\eta^{-1} (\eta - \hat{\eta}) < \chi\} \tag{2.24}$$

From this set U_{mem}, we can deduce the set of corresponding plants $G(\eta)$ defined as:

$$\mathcal{D}_{mem} = \left\{ G(\eta) \mid G(\eta) = G_{mod} + \tilde{G}(\eta) \; and \; \eta \in U_{mem} \right\} \tag{2.25}$$

The notation $G(\eta)$ used in (2.25) denotes the rational transfer function model whose coefficients are uniquely determined from η by the mapping $G(\eta) = G_{mod} + \tilde{G}(\eta)$. The nominal model for the true system G_0 derived from $\tilde{G}(\hat{\eta})$ is $G(\hat{\eta})$. It is important to note that, using the expression of $\tilde{G}(\eta)$ in (2.23), the uncertainty region $\mathcal{D}_{mem}$ can also be rewritten as follows:

$$\mathcal{D}_{mem} = \left\{ G(\eta) \mid G(\eta) = \frac{G_{mod} + Z_5\eta}{1 + Z_6\eta} \; and \; \eta \in U_{mem} \right\} \tag{2.26}$$

with $Z_5 = Z_3 + Z_4 G_{mod}$ and $Z_6 = Z_4$

Properties of U_{mem} and $\mathcal{D}_{mem}$.

$$\eta_0 \in U_{mem} \; with \; probability \; \alpha(l, \chi)$$

$$G_0 = G(\eta_0) \in \mathcal{D}_{mem} \; with \; probability \; \alpha(l, \chi)$$

Just as was done for open-loop identification, we have thus defined an uncertainty region $\mathcal{D}_{mem}$ that is centered at the model $G(\hat{\eta})$ derived from the identified $\tilde{G}(\hat{\eta})$ and that contains the true system G_0 at a certain probability level.

2.2.4 Closed-loop identification

Let us consider again the true system G_0 presented in Section 2.2.1. In order to perform the identification in closed-loop, we connect the true system with a stabilizing controller K as shown in Figure 2.1.

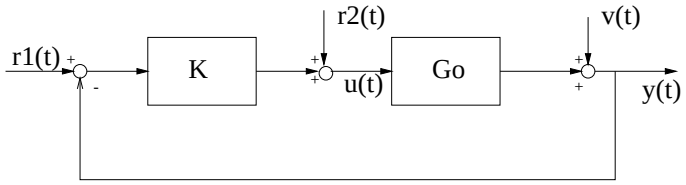

Figure 2.1: Closed-loop connection of G_0 and the controller K

Using Figure 2.1, we can write the following relations between the signals present in the closed loop $[K \; G_0]$:

$$\begin{pmatrix} y(t) \\ u(t) \end{pmatrix} = \overbrace{\begin{pmatrix} \frac{G_0 K}{1+G_0 K} & \frac{G_0}{1+G_0 K} \\ \frac{K}{1+G_0 K} & \frac{1}{1+G_0 K} \end{pmatrix}}^{T(G_0,K)} \begin{pmatrix} r_1(t) \\ r_2(t) \end{pmatrix} + \begin{pmatrix} \frac{1}{1+G_0 K} \\ \frac{-K}{1+G_0 K} \end{pmatrix} v(t) \tag{2.27}$$

$$y(t) = G_0 u(t) + v(t) \tag{2.28}$$

Different types of PE identification can be performed using data collected on the closed loop $[K\ G_0]$. We will here distinguish direct, indirect and Dual-Youla closed-loop identifications and show that uncertainty regions can be deduced from these three types of closed-loop identification.

2.2.4.1 Direct closed-loop identification

The objective of direct closed-loop identification is to identify a model of the true system using input signals $u(t)$ and output signals $y(t)$ collected on the closed loop $[K\ G_0]$. We will therefore apply a sequence of N signals $r_1(t)$ (or $r_2(t)$) to the closed-loop and collect the corresponding sequences of data U_N and Y_N:

$$U_N = \{u(t)|t = 1...N\} \qquad Y_N = \{y(t)|t = 1...N\}$$

The procedure of identification then follows the same procedure as for open-loop identification[4]. The uncertainty region deduced from direct closed-loop identification has therefore the same form as the uncertainty region $\mathcal{D}_{ol}$ given in (2.20).

2.2.4.2 Indirect closed-loop identification

The objective of indirect closed-loop identification is to identify a model of one of the four closed-loop transfer functions describing the loop $[K\ G_0]$. These four "true" closed-loop transfer functions are the entries of the matrix $T(G_0, K)$ defined in (2.27) i.e.

$$T_0^1 = \frac{G_0 K}{1+G_0 K} \quad T_0^2 = \frac{G_0}{1+G_0 K} \quad T_0^3 = \frac{K}{1+G_0 K} \quad T_0^4 = \frac{1}{1+G_0 K} \tag{2.29}$$

The model for G_0 is then computed from the estimate of any one of these four transfer functions by inversion of the mapping (2.29), using knowledge of the controller K. The selection of one of those transfer functions for identification is linked to the available signals and the structure of the controller K. Indeed, it is proved in [21] that the presence of unstable (or unit-circle) poles or zeros in K imposes restrictions

[4]It is nevertheless to be noted that an unbiased model structure for the noise model is here required.

on the subset of these transfer functions that can be identified.

In the sequel, we show how we can construct an uncertainty region $\mathcal{D}_{icl}$ containing the true system in the case where the first closed-loop transfer function T_0^1 is estimated. An uncertainty region $\mathcal{D}_{icl}$ can be derived similarly for the other cases (see e.g. [13] for the identification of T_0^3).

Let us therefore apply a sequence of N data $r_1(t)$ to the closed-loop $[K\ G_0]$ and collect the corresponding sequence of data $y(t)$. We have the following relations between $r_1(t)$ and $y(t)$:

$$y(t) = \overbrace{\frac{G_0 K}{1 + G_0 K}}^{T_0^1} r_1(t) + \frac{1}{1 + G_0 K} v(t) \tag{2.30}$$

Since the transfer function T_0^1 satisfies Assumptions 2.1, the N data $r_1(t)$ and $y(t)$ can be used to identify a full-order model for T_0^1. For this purpose, we need to define an unbiased model structure for T_0^1. Since the structure of T_0^1 is a function of the controller K, let us define it in the following generic way

$$\mathcal{M}_{icl} = \left\{ T(\xi) \mid T(\xi) = \frac{Z_7 \xi}{1 + Z_8 \xi} \right\}, \tag{2.31}$$

where we have that ξ is a real vector of size, say, f and that $Z_3(z)$ and $Z_4(z)$ are row vectors of size f constructed in the same way as Z_1 and Z_2 in (2.16) and therefore containing only delays and zeros. As $\mathcal{M}_{icl}$ is an unbiased model structure for T_0^1, there exists a vector ξ_0 such that $T_0^1 = T(\xi_0) \in \mathcal{M}_{icl}$. As stated in Proposition 2.2, a PE identification procedure with the N data $r_1(t)$, the N corresponding data $y(t)$ and $\mathcal{M}_{icl}$ yields an unbiased model $T(\hat{\xi})$ of T_0^1 and an estimate P_ξ of the covariance matrix of $\hat{\xi}$. Using now Proposition 2.3, we can define an ellipsoidal parametric uncertainty region U_{icl} that contains the true parameter vector ξ_0 at the probability level $\alpha(f, \chi)$:

$$U_{icl} = \{ \xi \mid (\xi - \hat{\xi})^T P_\xi^{-1} (\xi - \hat{\xi}) < \chi \} \tag{2.32}$$

From this set U_{icl}, we can deduce the set of corresponding open-loop plants $G(\xi)$ defined as:

$$\mathcal{D}_{icl} = \left\{ G(\xi) \mid G(\xi) = \frac{T(\xi)}{K(1-T(\xi))} \text{ and } \xi \in U_{icl} \right\} \tag{2.33}$$

The notation $G(\xi)$ used in (2.33) denotes the rational transfer function model whose coefficients are uniquely determined from ξ by the mapping

$$G(\xi) = \frac{T(\xi)}{K(1-T(\xi))}. \tag{2.34}$$

The nominal open-loop model derived from $T(\hat{\xi})$ is $G(\hat{\xi})$. It is important to note that, using the expression of $T(\xi)$ in (2.31), the uncertainty region $\mathcal{D}_{icl}$ can also be rewritten as follows:

$$\mathcal{D}_{icl} = \left\{ G(\xi) \mid G(\xi) = \frac{Z_9 \xi}{1 + Z_{10}\xi} \text{ and } \xi \in U_{icl} \right\} \tag{2.35}$$

with $Z_9 = Z_7/K$ and $Z_{10} = Z_8 - Z_7$

Properties of U_{icl} and $\mathcal{D}_{icl}$.

$$\xi_0 \in U_{icl} \text{ with probability } \alpha(f, \chi)$$

$$G_0 = G(\xi_0) \in \mathcal{D}_{icl} \text{ with probability } \alpha(f, \chi)$$

We have thus defined an uncertainty region $\mathcal{D}_{icl}$ that is centered at the open-loop model $G(\hat{\xi})$ derived from the identifed $T(\hat{\xi})$ and that contains the true system G_0 at a certain probability level.

2.2.4.3 Dual-Youla closed-loop identification

The so-called Youla parametrization gives the parametrization of all controllers stabilizing a plant (see [29]). For identification purpose, this result has been extended to the parametrization of all plants stabilized by a controller [52, 51]. This result is recalled in Proposition 2.4, but beforehand, we give the following definition that is used in Proposition 2.4.

Definition 2.3 ([83]) *Let us consider a transfer function G. The pair $\{N, D\}$ is a coprime factorization of G if*

- *N and D are stable tranfer functions;*
- *$G = \frac{N}{D}$;*
- *there exists stable transfer functions X and Y such that $XN + YD = 1$*

Proposition 2.4 ([83]) *Let us consider a plant G having a coprime factorization $\{N_G, D_G\}$ and a controller C having a coprime factorization $\{N_C, D_C\}$. Let us also assume that C stabilizes G. Then, the set $\mathcal{S}$ of all (LTI and finite dimensional) plants stabilized by C is given by:*

$$\mathcal{S} = \{G_{in} \mid G_{in} = \frac{N_G + D_C R}{D_G - N_C R} \text{ with } R \in \mathcal{R}H_\infty\}$$

The parametrization presented in Proposition 2.4 can be applied to the loop $[K\ G_0]$ presented in Figure 2.1. Indeed, consider a given initial system G_x that is stabilized by K. Using Proposition 2.4, the true system G_0 (also stabilized by K) can be represented in the Youla parametrization for a stable transfer function R_0:

$$G_0 = \frac{N_x + D_K R_0}{D_x - N_K R_0}, \tag{2.36}$$

where $\{N_x, D_x\}$ and $\{N_K, D_K\}$ are coprime factors of G_x and K, respectively [5]. The objective in Dual-Youla closed-loop identification [52, 51] is to identify the Youla parameter R_0 of the true system using data collected on the closed-loop $[K\ G_0]$. A model for the true system is then deduced from the identified Youla parameter.

In order to perform this identification, a sequence of N data $r_1(t)$ is applied to $[K\ G_0]$ and the corresponding data $u(t)$ and $y(t)$ are collected. Using the signals $u(t)$ and $y(t)$, we can compute the following auxiliary signals $x(t)$ and $z(t)$:

$$x(t) = (D_x + KN_x)^{-1}(u(t) + Ky(t)) \tag{2.37}$$

$$z(t) = (D_K + G_x N_K)^{-1}(y(t) - G_x u(t)). \tag{2.38}$$

These auxiliary signals $x(t)$ and $z(t)$ are such that

$$z(t) = R_0 x(t) + H_0(D_K(1 + KG_0))^{-1} v(t). \tag{2.39}$$

[5] It is to be noted that the transfer function R_0 depends on the choice of the pairs $\{N_x, D_x\}$ and $\{N_K, D_K\}$.

Since R_0 satisfies Assumptions 2.1, the sequences of N data $x(t)$ and of N data $z(t)$ can therefore be used to identify a full order model of R_0. For this purpose, we need to define an unbiased model structure for R_0. Since the structure of R_0 is a function of the controller K and of G_x, let us define it in the following generic way:

$$\mathcal{M}_{dy} = \left\{ R(\zeta) \mid R(\zeta) = \frac{Z_{11}\zeta}{1 + Z_{12}\zeta} \right\}, \tag{2.40}$$

where we have that ζ is a real vector of size, say, p and that $Z_{11}(z)$ and $Z_{12}(z)$ are row vectors of size p constructed in the same way as Z_1 and Z_2 in (2.16) and therefore containing only delays and zeros. As $\mathcal{M}_{dy}$ is an unbiased model structure for R_0, there exists a vector ζ_0 such that $R_0 = R(\zeta_0) \in \mathcal{M}_{dy}$. As stated in Proposition 2.2, a PE identification procedure with the N data $x(t)$, the N data $z(t)$ and $\mathcal{M}_{dy}$ yields an unbiased model $R(\hat{\zeta})$ of R_0 and an estimate P_ζ of the covariance matrix of $\hat{\zeta}$. Using now Proposition 2.3, we can define an ellipsoidal parametric uncertainty region U_{dy} that contains the true parameter vector ζ_0 at the probability level $\alpha(p, \chi)$:

$$U_{dy} = \{\zeta \mid (\zeta - \hat{\zeta})^T P_\zeta^{-1} (\zeta - \hat{\zeta}) < \chi\} \tag{2.41}$$

From this set U_{dy}, we can deduce the set of corresponding open loop plants $G(\zeta)$ defined as:

$$\mathcal{D}_{dy} = \left\{ G(\zeta) \mid G(\zeta) = \frac{N_x + D_K R(\zeta)}{D_x - N_K R(\zeta)} \; and \; \zeta \in U_{dy} \right\} \tag{2.42}$$

The nominal open-loop model derived from $R(\hat{\zeta})$ is $G(\hat{\zeta})$. It is important to note that, using the expression of $R(\zeta)$ in (2.40), the uncertainty region $\mathcal{D}_{dy}$ can also be rewritten as follows:

$$\mathcal{D}_{dy} = \left\{ G(\zeta) \mid G(\zeta) = \frac{G_x + Z_{13}\zeta}{1 + Z_{14}\zeta} \; and \; \zeta \in U_{dy} \right\} \tag{2.43}$$

with $Z_{13} = G_x Z_{12} + (D_K Z_{11}/D_x)$ and $Z_{10} = Z_{12} - (N_K Z_{11}/D_x)$

Properties of U_{dy} and $\mathcal{D}_{dy}$.

$$\zeta_0 \in U_{dy} \; with \; probability \; \alpha(p, \chi)$$

$$G_0 = G(\zeta_0) \in \mathcal{D}_{dy} \text{ with probability } \alpha(p, \chi)$$

We have thus defined an uncertainty region $\mathcal{D}_{dy}$ that is centered at the model $G(\hat{\zeta})$ derived from the identifed Youla parameter $R(\hat{\zeta})$ and that contains the true system G_0 at a certain probability level.

2.3 General structure of the uncertainty regions deduced from PE identification

In the previous section, uncertainty regions containing the true system have been obtained as a result of open-loop identification, the model error model identification and direct, indirect and Dual-Youla closed-loop identification. These uncertainty regions take the form of a set of parametrized open-loop transfer functions where the parameter vector lies in an ellipsoid U. This fact can be summarized in the following proposition.

Proposition 2.5 *Consider $G_0 = G(z, \delta_0)$, the true system presented in Section 2.2.1. The uncertainty regions $\mathcal{D}$ resulting from prediction error identification, and which contain the true system G_0 at a prescribed probability level, can all be described in the following generic form:*

$$\mathcal{D} = \left\{ G(z,\delta) \mid G(z,\delta) = \frac{e + Z_N \delta}{1 + Z_D \delta} \text{ and } \delta \in U = \{\delta \mid (\delta - \hat{\delta})^T R (\delta - \hat{\delta}) < 1\} \right\} \tag{2.44}$$

where

- $\delta \in \mathbf{R}^{k \times 1}$ *is a real parameter vector;*
- $\hat{\delta}$ *is the parameter estimate resulting from the identification step;*
- R *is a symmetric positive definite matrix* $\in \mathbf{R}^{k \times k}$ *that is proportional to the inverse of the covariance matrix of* $\hat{\delta}$*;*
- $Z_N(z)$ *and* $Z_D(z)$ *are row vectors of size* k *of known transfer functions;*
- $e(z)$ *is a known transfer function.*

Proof. This proposition is a direct consequence of expressions (2.20), (2.26), (2.35), (2.43). □

Proposition 2.5 defines the uncertainty region $\mathcal{D}$. Let us point out the following characteristics of this uncertainty region.

- The uncertainty region $\mathcal{D}$ is simply and directly the result of a PE identification procedure with unbiased model structure performed on the true system. A PE identification procedure with unbiased model structure leading to an uncertainty region will be called *a validation experiment* in the sequel.
- The true system G_0 lies in $\mathcal{D}$ at a certain probability level that is fixed by the designer.
- The uncertainty region $\mathcal{D}$ is centered at $G(z, \hat{\delta})$ which is a model of the true system G_0. This model is either the identified model (in open-loop identification) or the model of the true system G_0 that is derived from the identified transfer function (in the other cases of identification). This model $G(z, \hat{\delta})$ is generally chosen as *model for control design*. However, it is of course not a requirement.
- Different identification experiments (i.e. open-loop or closed-loop identification, different measured data, ...) lead to different identified parameter vectors, different covariance matrices, and therefore also different sets of systems $\mathcal{D}^{(i)}$.

It has been noted in Chapter 1 that other techniques (i.e. *set membership identification* and the *model invalidation concept*) have been developed to estimate an uncertainty region containing the true system under a variety of assumptions that are often a great distance from the classical assumptions used in PE identification. These techniques generically aim at producing classical frequency domain linear fractional uncertainty regions used in mainstream robust control theory such as additive uncertainty regions (see e.g. [70, 56, 66, 49]) or coprime factor uncertainty regions (see e.g. [16]). The reason for producing such classical uncertainty regions is that a large number of robustness tools have been developed for these particular types of uncertainty regions [92, 91, 86]. Our uncertainty region $\mathcal{D}$ is quite different from these standard uncertainty regions. In order to establish these differences, let us compare the uncertainty region $\mathcal{D}$ with e.g. the additive uncertainty region defined below.

Definition 2.4 (additive uncertainty region) *Let us consider a stable model G_{mod} and a stable transfer function $\Delta(z)$. An additive uncertainty region of size β is then defined as follows:*

$$\mathcal{G}_a = \{G_{in}(z) \mid G_{in}(z) = G_{mod}(z) + \Delta(z) \;\; with \;\; \| \Delta(z) \|_\infty < \beta\}. \quad (2.45)$$

By comparing (2.44) and (2.45), several differences can be noted. However, the major difference is that the uncertainty part δ in $\mathcal{D}$ is a real parameter vector and not a transfer function as in the additive uncertainty region. Our uncertainty region $\mathcal{D}$ is indeed a parametric uncertainty region and not a frequency domain uncertainty region.

Due to the huge developments achieved in robust control theory in the last years, a lot of new robustness results are now also available for uncertainty sets with a parametric (i.e. real) uncertainty part (see e.g. [34, 35, 53, 72, 7, 4, 5]). Some of these results will help us to develop robustness tools adapted to the uncertainty region $\mathcal{D}$ even though manipulations of $\mathcal{D}$ and new results will also be required to obtain these robustness tools.

We have developed a robust stability analyzis tool (see Chapter 4) as well as a robust performance analysis tool (see Chapter 5) for $\mathcal{D}$. The robust analysis tool is a necessary and sufficient condition for the stabilization of all plants in $\mathcal{D}$ by a given controller. This condition is therefore a condition for the stabilization of the true system G_0 by this controller. The robust performance analysis tool is an LMI (Linear Matrix Inequality) procedure computing exactly the worst case performance achieved by a given controller over all plants in $\mathcal{D}$. This worst case performance is therefore a lower bound of the performance achieved by the considered controller with the true system G_0.

We have also developed another type of result for the uncertainty region $\mathcal{D}$ that no more pertains to the validation of one particular controller, but pertains to determining what quality an uncertainty region $\mathcal{D}$ must possess for it to be tuned for robustly stable controller design. Indeed, in Chapter 3, we introduce a measure of size of the uncertainty set $\mathcal{D}$, the worst case ν-gap, that is directly connected to the size of the set of model-based controllers that are guaranteed by the ν-gap theory [84][6] to stabilize all plants in $\mathcal{D}$. More particulary, the smaller is this

[6] This controller set is not guaranteed to contain all stabilizing controllers.

measure, the larger is the set of robustly stabilizing controllers. This robust stability measure can thus be used as a tool to assess the quality (with respect to robustly stable controller design) of an uncertainty region $\mathcal{D}$ obtained by a validation experiment (i.e. a PE identification experiment). This robust stability measure also draws guidelines for the design of the validation experiment: a validation experiment should always aim at producing an uncertainty region $\mathcal{D}$ with a small worst case ν-gap since it implies that the obtained uncertainty region will have a large set of robustly stabilizing controllers.

2.4 Conclusions

In this chapter, we have shown that a validation experiment (i.e. a PE identification procedure with unbiased model structure) allows one to design an uncertainty region containing the true system at a certain probability level, and this without adding any further assumptions. This uncertainty region takes the form of a set of parametrized transfer functions whose parameter vector is constrained to lie in an ellipsoid.

Chapter 3

A measure of robust stability for the uncertainty region $\mathcal{D}$

In the previous chapter, we have presented the design of an uncertainty region using a PE identification procedure performed on the true system using an unbiased model structure. We call this procedure a validation experiment. The uncertainty region $\mathcal{D}$ deduced from such validation experiment takes the form of a set of transfer function parametrized by a real vector which is constrained to lie in an ellipsoid. The uncertainty region $\mathcal{D}$ has the property to contain the true system G_0 at a probability level that can be fixed by the designer. The general structure of $\mathcal{D}$ is given in (2.44). This expression of $\mathcal{D}$ does not inform us about the size of the set of controllers that robustly stabilize all plants in $\mathcal{D}$. In other words, by observing $\mathcal{D}$, we can not say if this controller set is large or small. As, in Chapter 4, we will deduce the stabilization of the true system by a given controller by the verification of the stabilization of all plants in $\mathcal{D}$ by the considered controller, this lack of information is a real drawback. That is why, in this chapter, we introduce a measure of robust stability for the uncertainty region $\mathcal{D}$ that is directly connected to the size of a set of model-based controllers that are guaranteed to robustly stabilize $\mathcal{D}$ (i.e. that stabilize all plants in $\mathcal{D}$).

This robust stability measure for $\mathcal{D}$ is defined as the worst case (i.e. the largest) ν-gap [84, 85] between a model G_{mod} and the plants in $\mathcal{D}$. Here G_{mod} is the model that will be used for control design. This model

G_{mod} is generally the center of the considered uncertainty region $\mathcal{D}$. However, it is not a requirement: this model can be also a reduced order model obtained from this center or an a-priori given model.

Our first contribution is to show that the worst case ν-gap can be computed frequency-wise using an LMI-based optimization problem at each frequency. Our second contribution is to show that the smaller the worst case ν-gap between the model G_{mod} and all plants in some $\mathcal{D}$, the larger is the set of G_{mod}-based controllers [1] that are guaranteed by the ν-gap theory to robustly stabilize $\mathcal{D}$. The worst case ν-gap is thus an indicator of how well an uncertainty set $\mathcal{D}$ is tuned for robustly stable controller design based on the model G_{mod} (chosen for control design). A too large indicator will therefore incite the designer to reject the uncertainty region and to perform a new validation experiment. We also show that the worst case ν-gap can be used as a tool for the selection of the uncertainty region that is best tuned for robust control design, in the case where different validation experiments have delivered different uncertainty regions $\mathcal{D}^{(i)}$. Finally, and it may be the most interesting result, since the worst case ν-gap characterizes what quality an uncertainty region $\mathcal{D}$ (and therefore also the validation experiment that yields this uncertainty set) must possess for it to be tuned for robust control design, our result leads to guidelines for the design of the validation experiment. This result may therefore be considered as the first step in the direction of *PE identification for robust control.*

The ν-gap metric is thus chosen to characterize the amount of uncertainty (i.e. the distance) between the model G_{mod} and the plants in an uncertainty region $\mathcal{D}$. Our approach is thus based on the embedding of the parametric uncertainty region $\mathcal{D}$ into a larger uncertainty set defined by the ν-gap metric. This introduces a conservatism, but allows us to use the ν-gap theory to characterize the size of the controller set that is guaranteed (by this theory) to robustly stabilize $\mathcal{D}$. It is obvious that similar results could have been deduced from the embedding of $\mathcal{D}$ into e.g. an additive or a multiplicative uncertainty region. However, the choice of the ν-gap metric is motivated by the fact that this metric generally leads to the least conservative robust stability results [86].

[1] The G_{mod}-based controllers are the controllers designed from G_{mod}

Chapter outline. We first present, in Section 3.1, the robust stability results linked to the ν-gap metric. In Section 3.2, we then define the worst ν-gap between a model and an uncertainty region $\mathcal{D}$ and a procedure to compute it exactly is given in Section 3.3. In Section 3.4, the worst case ν-gap is then related to the size of the set of model-based controllers that are guaranteed by the ν-gap theory to robustly stabilize an uncertainty region $\mathcal{D}$. After having given different possible uses of the worst case ν-gap , we finish this chapter by presenting a simulation example.

3.1 The ν-gap metric and its robust stability properties

As said in the introduction of this chapter, the robust stability measure for $\mathcal{D}$ is the *worst-case ν-gap* between the model G_{mod} and the uncertainty set $\mathcal{D}$. The worst-case ν-gap is an extension of the ν-gap, introduced by Vinnicombe [84], which is a measure of distance between two transfer functions. For the sake of completeness, we first briefly recall the definition of the ν-gap for scalar transfer functions.

3.1.1 The Vinnicombe ν-gap between two plants

Definition 3.1 *The gap metric between two transfer functions G_1 and G_2, introduced by Vinnicombe [84] and denoted δ_ν, is defined as*

$$\delta_\nu(G_1, G_2) = \begin{cases} \max\limits_{\omega} \kappa\left(G_1(e^{j\omega}), G_2(e^{j\omega})\right) & if\ W(G_1, G_2) = 0 \\ 1 & otherwise \end{cases} \tag{3.1}$$

where

$$\kappa\left(G_1(e^{j\omega}), G_2(e^{j\omega})\right) \triangleq \frac{|G_1(e^{j\omega}) - G_2(e^{j\omega})|}{\sqrt{1+|G_1(e^{j\omega})|^2}\sqrt{1+|G_2(e^{j\omega})|^2}} \tag{3.2}$$

and where $W(G_1, G_2) = wno(1 + G_1^* G_2) + \eta(G_2) - \tilde{\eta}(G_1)$.

Here $G^*(e^{j\omega}) = G(e^{-j\omega})$, $\eta(G)$ (resp. $\tilde{\eta}(G)$) denotes the number of poles of G in the complement of the closed (resp. open) unit disc, while $wno(G)$ denotes the winding number about the origin of $G(z)$ as z follows the unit circle indented into the exterior of the unit disc around

any unit circle pole and zero of $G(z)$.

If the winding number condition $W(G_1, G_2) = 0$ is satisfied, then the ν-gap between two plants has a simple frequency domain interpretation (in the SISO case). Indeed, the quantity $\kappa(G_1(e^{j\omega}), G_2(e^{j\omega}))$ is the chordal distance between the projections of $G_1(e^{j\omega})$ and $G_2(e^{j\omega})$ onto the Riemann sphere of unit diameter with South Pole at the origin of the complex plane [84]. The distance $\delta_\nu(G_1, G_2)$ between G_1 and G_2 is therefore, according to (3.1), the supremum of these chordal distances over all frequencies. Observe that $0 \leqslant \delta_\nu(G_1, G_2) \leqslant 1$.

3.1.2 The generalized stability margin of a closed loop system

Consider now a closed loop system made up of the feedback interconnection of a system G and a controller C: see Figure 3.1. The closed loop transfer function matrix between $[r_1 \;\; r_2]^T$ and $[y \;\; u]^T$ can be written as

$$T(G,C) = \begin{pmatrix} T_{11} & T_{12} \\ T_{21} & T_{22} \end{pmatrix} = \begin{pmatrix} \frac{GC}{1+GC} & \frac{G}{1+GC} \\ \frac{C}{1+GC} & \frac{1}{1+GC} \end{pmatrix}. \tag{3.3}$$

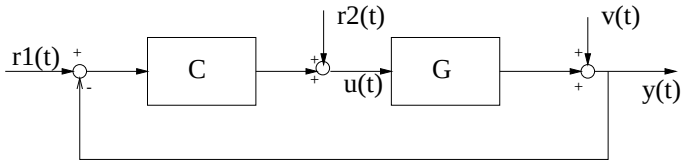

Figure 3.1: Closed-loop connection of a system G and a controller C

Definition 3.2 *The* **generalized stability margin** *of the closed loop system is defined as*

$$b_{GC} = \begin{cases} \|T(G,C)\|_\infty^{-1} & \text{if } [C \;\; G] \text{ is stable} \\ 0 & \text{otherwise} \end{cases} \tag{3.4}$$

It can be shown [84] that an alternative definition is

$$b_{GC} = \begin{cases} \min\limits_{\omega} \ \kappa\left(G(e^{j\omega}), -\frac{1}{C(e^{j\omega})}\right) & \text{if } [C\ G] \text{ is stable} \\ \\ 0 \ \text{otherwise} \end{cases} \tag{3.5}$$

Thus, the generalized stability margin of a closed loop system $[C\ G]$ is measured by the least chordal distance between the projections on the Riemann sphere of G and of the inverse of $-C$. It is to be noted that, for a given plant G, the generalized stability margin has a maximum $b_{opt}(G)$ (see e.g. [91]) given by

$$b_{opt}(G) = \max_{C} b_{GC} = \sqrt{1 - \| \begin{pmatrix} N & M \end{pmatrix} \|_H^2}, \tag{3.6}$$

where $\| A \|_H$ is the Hankel norm of the operator A (see e.g. [92]) and $\{N, M\}$ is the normalized coprime factorization of G i.e. the coprime factorization (see Definition 2.3) such that $N^*N + M^*M = 1$

3.1.3 Robust stability and the ν-gap

The main interest of the ν-gap metric is its use in a range of robust stability results. One of this result relates the size of the set of robustly stabilizing controllers of a ν-gap uncertainty set (i.e. an uncertainty set defined with the ν-gap) to the size of this uncertainty set [84, 85].

Proposition 3.1 ([84, 85]) *Let us consider an ν-gap uncertainty set $\mathcal{G}_\nu$ of size β and centered at a model G_{mod}:*

$$\mathcal{G}_\nu = \{G \mid \delta_\nu(G_{mod}, G) \leq \beta\}.$$

Then, a controller C stabilizing G_{mod} stabilizes all plants in the uncertainty region $\mathcal{G}_\nu$ if and only if it lies in the controller set:

$$\{C(z) \mid b_{G_{mod}C} > \beta\}$$

The size β of a ν-gap uncertainty set $\mathcal{G}_\nu$ is thus directly connected to the size of the set of all controllers that robustly stabilize $\mathcal{G}_\nu$. Moreover, the smaller is this size β, the larger is the set of controllers that robustly stabilize the uncertainty set $\mathcal{G}_\nu$. Let us now present a direct consequence of Proposition 3.1 which relates the size of the set of controllers that are guaranteed to stabilize two plants G_1 and G_2 to $\delta_\nu(G_1, G_2)$ [84].

Corollary 3.1 ([84]) *Let us consider a nominal plant G_1 and a perturbed plant G_2 and denote $\delta_\nu(G_1, G_2)$ the ν-gap between these two plants. Then, a controller C stabilizing G_1 also stabilizes G_2 if this controller lies in the controller set*

$$\{\ C \mid b_{G_1,C} > \delta_\nu(G_1, G_2)\}$$

3.2 The worst case ν-gap between a model and $\mathcal{D}$

The nice stability properties presented in the previous section show that the G_{mod}-based controller set that is guaranteed (by Proposition 3.1) to robustly stabilize $\mathcal{D}$ will be large, if the largest ν-gap between G_{mod} and any plant in $\mathcal{D}$ remains small. We call this "largest ν-gap" the worst case ν-gap $\delta_{WC}(G_{mod}, \mathcal{D})$ between G_{mod} and the set $\mathcal{D}$.

Definition 3.3 *Consider an uncertainty region $\mathcal{D}$ having the structure given in (2.44) and a model G_{mod}. The worst case Vinnicombe distance $\delta_{WC}(G_{mod}, \mathcal{D})$ is given by*[2] *:*

$$\delta_{WC}(G_{mod}, \mathcal{D}) = \max_{G_{in} \in \mathcal{D}} \delta_\nu(G_{mod}, G_{in}) \tag{3.7}$$

Another important quantity is now defined: the worst case chordal distance. This quantity, whose computation is the result of a convex optimization problem involving LMI constraints as will be shown in Section 3.3, will allow us to give an alternative expression for $\delta_{WC}(G_{mod}, \mathcal{D})$.

Definition 3.4 *At a particular frequency ω, we define $\kappa_{WC}(G_{mod}(e^{j\omega}), \mathcal{D})$ as the maximum chordal distance between $G_{mod}(e^{j\omega})$ and the frequency responses of all plants in $\mathcal{D}$ at this frequency:*

$$\kappa_{WC}(G_{mod}(e^{j\omega}), \mathcal{D}) = \max_{G_{in} \in \mathcal{D}} \kappa(G_{mod}(e^{j\omega}), G_{in}(e^{j\omega})) \tag{3.8}$$

This last quantity can now be used to give an alternative expression of the worst case Vinnicombe distance. This is done in the following lemma, which is an extension of a property presented in [85, page 66].

[2]Note that, with some abuse, even though it could happen that the term "supremum" should be used instead of "maximum", we will always use the term "maximum" in the sequel.

Lemma 3.1 *If $W(G_{mod}, G_{in}) = 0$ for one plant $G_{in} \in \mathcal{D}$, then the worst case Vinnicombe distance $\delta_{WC}(G_{mod}, \mathcal{D})$ defined in (3.7) can also be expressed in the following way using the worst case chordal distance:*

$$\delta_{WC}(G_{mod}, \mathcal{D}) = \max_{\omega} \kappa_{WC}(G_{mod}(e^{j\omega}), \mathcal{D}) \tag{3.9}$$

where $\kappa_{WC}(G_{mod}(e^{j\omega}), \mathcal{D})$ is defined in (3.8).

Proof. The winding number condition may be omitted in (3.9). Indeed, assume there exists one $G_1 \in \mathcal{D}$ for which $W(G_{mod}, G_1) \neq 0$, i.e. $\delta_\nu(G_{mod}, G_1) = 1$. Since the ellipsoid U in the expression (2.44) of $\mathcal{D}$ is a connected set, then there always exists a piecewize continuous application ϕ of [0 1] to plants in $\mathcal{D}$ such that $\phi(0) = G_{in}$ and $\phi(1) = G_1$. As $W(G_{mod}, G_{in}) = 0$ and $W(G_{mod}, G_1) \neq 0$, there exists a $G_2 = \phi(\lambda) \in \mathcal{D}$ such that $(1 + G^*_{mod}(e^{j\omega_0})G_2(e^{j\omega_0}) = 0)$ and therefore such that $\kappa(G_{mod}(e^{j\omega_0}), G_2(e^{j\omega_0})) = 1$ for some frequency ω_0. So, $\delta_{WC}(G_{mod}, \mathcal{D}) = 1$ □

Remark. If $G_{mod} \in \mathcal{D}$, we always have $W(G_{mod}, G_{mod}) = 0$ and therefore (3.9) is always valid.

3.3 Computation of the worst case chordal distance and worst case ν-gap

In the previous subsection, we have defined the worst case ν-gap between the model G_{mod} and all plants in an uncertainty region $\mathcal{D}$ having the general structure (2.44). Now we give a procedure to compute this worst case ν-gap $\delta_{WC}(G_{mod}, \mathcal{D})$. According to Lemma 3.1, this is equivalent to finding a procedure to compute the worst case chordal distance $\kappa_{WC}(G_{mod}(e^{j\omega}), \mathcal{D})$ defined in (3.8), since $\delta_{WC}(G_{mod}, \mathcal{D})$ is the maximum over all frequencies of the worst case chordal distance. In the following theorem, we show that the computation of the worst case chordal distance $\kappa_{WC}(G_{mod}(e^{j\omega}), \mathcal{D})$ at a particular frequency ω can be formulated as a convex optimization problem involving Linear Matrix Inequality (LMI) constraints [17]. An LMI is a matrix inequality of the form $F(\zeta) \triangleq F_0 + \sum_{i=1}^{q} \zeta_i F_i \leq 0$, where $\zeta \in \mathbf{R}^q$ is the variable, and $F_i = F_i^T \in \mathbf{R}^{t \times t}$, $i = 0, \ldots, q$ are given. Several algorithms that have practical efficiency have been devised for solving these problems, see [82]. The LMI problems can be solved using the free ware code SP [82]

and its Matlab/Scilab interface `LMITOOL` [32] or the available commercial Matlab Toolbox, LMI Control Toolbox [36].

Theorem 3.1 *Consider a model G_{mod} and an uncertainty region $\mathcal{D}$ given in (2.44). Then $\kappa_{WC}(G_{mod}(e^{j\omega}), \mathcal{D}) = \sqrt{\gamma_{opt}}$, where γ_{opt} is the optimal value of γ in the following standard convex optimization problem involving LMI constraints evaluated at ω:*

$$\begin{array}{ll} minimize & \gamma \\ over & \gamma,\ \tau \\ subject\ to & \tau \geq 0\ and \end{array}$$

$$\begin{pmatrix} Re(a_{11}) & Re(a_{12}) \\ Re(a_{12}^*) & Re(a_{22}) \end{pmatrix} - \tau \begin{pmatrix} R & -R\hat{\delta} \\ (-R\hat{\delta})^T & \hat{\delta}^T R\hat{\delta} - 1 \end{pmatrix} < 0 \qquad (3.10)$$

where

- $a_{11} = (Z_N^* Z_N - Z_N^* x Z_D - Z_D^* x^* Z_N + Z_D^* x^* x Z_D) - \gamma(Z_N^* Q Z_N + Z_D^* Q Z_D)$,
- $a_{12} = Z_N^* e - Z_N^* x - Z_D^* e x^* + Z_D^* x x^* - \gamma(Z_N^* e Q + Z_D^* Q)$,
- $a_{22} = e e^* - e^* x - e x^* + x x^* - \gamma(e e^* Q + Q)$,
- $Q = 1 + x^* x$ *and* $x = G_{mod}(e^{j\omega})$.

The worst case ν-gap is then obtained as

$$\delta_{WC}(G_{mod}, \mathcal{D}) = \max_{\omega} \kappa_{WC}(G_{mod}(e^{j\omega}), \mathcal{D})$$

Proof. We prove that the square root of the solution of the LMI optimization problem gives the worst case chordal distance $\kappa_{WC}(G_{mod}(e^{j\omega}), \mathcal{D})$ at some frequency ω. The derivation of the worst case ν-gap is a direct consequence of Lemma 3.1.

If we denote the frequency response of the model $G_{mod}(e^{j\omega})$ by x, and that of any plant $G(e^{j\omega}, \delta) \in \mathcal{D}$ by $y(\delta)$, then a convenient way to state the problem of computing the worst case chordal distance at some frequency ω is as follows:

$$minimize\ \gamma\ such\ that\ \kappa(x, y(\delta))^2 < \gamma\ for\ all\ y(\delta) \in \mathcal{D}$$

The expression $\kappa(x, y(\delta))^2 < \gamma$ has to be transformed into an LMI constraint. This can easily be done as proved in the following expressions.

$$\left(\frac{|x - y(\delta)|}{\sqrt{1+|x|^2}\sqrt{1+|y(\delta)|^2}} \right)^2 < \gamma \Longleftrightarrow$$

$$x^*x + y(\delta)^*y(\delta) - y(\delta)^*x - x^*y(\delta) - \gamma(1+x^*x)(1+y(\delta)^*y(\delta)) < 0 \Longleftrightarrow$$

$$\begin{pmatrix} y(\delta) \\ 1 \end{pmatrix}^* \begin{pmatrix} 1-\gamma(1+x^*x) & -x \\ -x^* & x^*x - \gamma(1+x^*x) \end{pmatrix} \begin{pmatrix} y(\delta) \\ 1 \end{pmatrix} < 0 \tag{3.11}$$

By pre-multiplying (3.11) by $(1 + Z_D\delta)^*$ and post-multiplying the same expression by $(1 + Z_D\delta)$, we obtain:

$$\begin{pmatrix} e + Z_N\delta \\ 1 + Z_D\delta \end{pmatrix}^* \begin{pmatrix} 1-\gamma(1+x^*x) & -x \\ -x^* & x^*x - \gamma(1+x^*x) \end{pmatrix} \begin{pmatrix} e + Z_N\delta \\ 1 + Z_D\delta \end{pmatrix} < 0 \tag{3.12}$$

which is equivalent with the following constraint on δ with variable γ:

$$\begin{pmatrix} \delta \\ 1 \end{pmatrix}^* \begin{pmatrix} a_{11} & a_{12} \\ a_{12}^* & a_{22} \end{pmatrix} \begin{pmatrix} \delta \\ 1 \end{pmatrix} < 0 \tag{3.13}$$

with a_{11}, a_{12} and a_{22} as defined in the statement of Theorem (3.1). Since δ is real, it can be shown that (3.13) is equivalent with

$$\overbrace{\begin{pmatrix} \delta \\ 1 \end{pmatrix}^T \begin{pmatrix} Re(a_{11}) & Re(a_{12}) \\ Re(a_{12}^*) & Re(a_{22}) \end{pmatrix} \begin{pmatrix} \delta \\ 1 \end{pmatrix}}^{\psi(\delta)} < 0 \tag{3.14}$$

This last expression is equivalent to stating that $\kappa(G_{mod}(e^{j\omega}), G(e^{j\omega}, \delta))^2 < \gamma$ for a particular $\delta \in U$. However, this must be true for all $\delta \in U$. Therefore, (3.14) must be true for all δ such that:

$$\overbrace{\begin{pmatrix} \delta \\ 1 \end{pmatrix}^T \begin{pmatrix} R & -R\hat{\delta} \\ (-R\hat{\delta})^T & \hat{\delta}^T R\hat{\delta} - 1 \end{pmatrix} \begin{pmatrix} \delta \\ 1 \end{pmatrix}}^{\rho(\delta)} < 0 \tag{3.15}$$

which is equivalent to the statement "$\delta \in U$".

Let us now recapitulate. Computing $\kappa_{WC}(G_{mod}(e^{j\omega}), \mathcal{D})^2$ is equivalent to finding the smallest γ such that $\psi(\delta) < 0$ for all δ for which $\rho(\delta) < 0$. By the $\mathcal{S}$ procedure [55, 17], this problem is equivalent to finding the smallest γ and a positive scalar τ such that $\psi(\delta) - \tau\rho(\delta) < 0$, for all $\delta \in \mathbf{R}^{k\times 1}$ which is precisely (3.10). To complete this proof, note that the worst case chordal distance at ω is thus equal to $\sqrt{\gamma_{opt}}$ where γ_{opt} is the optimal value of γ. □

Remark. Our computation of the worst case ν-gap requires thus the computation of the worst case chordal distance over a frequency grid.

3.4 A robust stability measure for $\mathcal{D}$

In the previous section, the notion of worst case ν-gap between a model G_{mod} and an uncertainty region $\mathcal{D}$ has been introduced and a procedure has been given to compute this distance. This worst case ν-gap can be considered as a robustness measure of $\mathcal{D}$ with respect to robustly stable controller design based on the model G_{mod}. We have indeed the following result.

Proposition 3.2 *Consider an uncertainty region $\mathcal{D}$ having the structure given by (2.44) and a model G_{mod}. All controllers C that stabilize G_{mod} and that lie in the set*

$$\mathcal{C}(G_{mod}, \mathcal{D}) = \{C \mid b_{G_{mod},C} > \delta_{WC}(G_{mod}, \mathcal{D})\} \tag{3.16}$$

are guaranteed to stabilize all plants in the uncertainty region $\mathcal{D}$. It is to be noted that the stability margin $b_{G_{mod},C}$ achievable by a controller C with G_{mod} is bounded by $b_{opt}(G_{mod})$ defined in (3.6).

Proof. Using the definition of the worst case ν-gap given in (3.7), we see that $\mathcal{D}$ is embedded in the uncertainty region $\{G|\delta_\nu(G_{mod}, G) \leq \delta_{WC}(G_{mod}, \mathcal{D})\}$. This theorem is thus a direct consequence of Proposition 3.1. □

Proposition 3.2 tells us that the worst case ν-gap between the model G_{mod} and an uncertainty set $\mathcal{D}$ is a measure of size of the set $\mathcal{D}$ that is

directly connected to the size of the set $\mathcal{C}(G_{mod}, \mathcal{D})$ of G_{mod}-based controllers that are guaranteed to stabilize all plants in $\mathcal{D}$. Proposition 3.2 shows also that *the smaller $\delta_{WC}(G_{mod}, \mathcal{D})$, the larger is this robustly stabilizing controller set.* Thus, the worst case ν-gap is a nice and compact measure of the ability of an uncertainty set $\mathcal{D}$ to be robustly stabilized by a large set of controllers designed from G_{mod} and therefore of how well the uncertainty region $\mathcal{D}$ is tuned for robustly stable controller design based on G_{mod}.

It is to be noted that there may be additional controllers outside the set $\mathcal{C}(G_{mod}, \mathcal{D})$ that stabilize all models in $\mathcal{D}$. Indeed, according to Proposition 3.1, the set $\mathcal{C}(G_{mod}, \mathcal{D})$ contains all controllers that stabilize all systems in the uncertainty set $\{G | \delta_\nu(G_{mod}, G) \leq \delta_{WC}(G_{mod}, \mathcal{D})\}$ that embeds $\mathcal{D}$. However, the advantage of this description is that the size of the set $\mathcal{C}(G_{mod}, \mathcal{D})$ (i.e. $\delta_{WC}(G_{mod}, \mathcal{D})$) is only a function of G_{mod} and $\mathcal{D}$. In Chapter 4, a necessary and sufficient condition will be given for the stabilization of all plants in $\mathcal{D}$ by a given controller. However, this necessary and sufficient condition may not be used as a measure of robust stability for $\mathcal{D}$, as will be shown in the next chapter.

3.4.1 Practical uses of the worst case ν-gap

As said above, the worst case ν-gap is a nice and compact measure of how well the uncertainty region $\mathcal{D}$ is tuned for robust control design with respect to G_{mod}. In order to present practical uses of this measure, let us consider the two following situations:

1. We have performed one validation experiment leading to one uncertainty region $\mathcal{D}$. No model is given for control design.

2. We have performed different validation experiments leading to different uncertainty regions $\mathcal{D}^{(i)}$ and somebody has given us a model G_{mod} for control design.

First situation

In the first situation, a model has to be chosen for control design. This model G_{mod} is typically chosen equal to the center $G(z, \hat{\delta})$ of the uncertainty region $\mathcal{D}$ deduced from the validation experiment. The worst case ν-gap $\delta_{WC}(G(z, \hat{\delta}), \mathcal{D})$ can then be used as a tool to "validate the

validation experiment". Indeed, if the worst case ν-gap is small with respect to the optimal stability margin $b_{opt}(G(z,\hat{\delta}))$ (see (3.6)), then the set $\mathcal{C}(G(z,\hat{\delta}),\mathcal{D})$ of $G(z,\hat{\delta})$-based controllers that are guaranteed to robustly stabilize $\mathcal{D}$ is large and the designer will be therefore generally incited to keep the uncertainty region $\mathcal{D}$: a controller can be designed from G_{mod} and the results of the next chapters can be used to validate the controller for stability and performance with respect to the "validated" uncertainty region $\mathcal{D}$. On the contrary, if the worst case ν-gap is large with respect to the optimal stability margin $b_{opt}(G(z,\hat{\delta}))$, then the set $\mathcal{C}(G(z,\hat{\delta}),\mathcal{D})$ of $G(z,\hat{\delta})$-based controllers that are guaranteed to robustly stabilize $\mathcal{D}$ is small. Therefore, even though the set $\mathcal{C}(G(z,\hat{\delta}),\mathcal{D})$ is not guaranteed to contain all robustly stabilizing controllers, the designer will be nevertheless generally incited to reject the uncertainty region $\mathcal{D}$ and to perform a new validation experiment in order to obtain a new uncertainty region $\mathcal{D}_{bis}$ with a larger set of stabilizing controllers. For this purpose, the designer could e.g. use the guidelines that will be presented in Section 3.4.2.

Second situation

In the second situation, the worst case ν-gap can be used as a tool to select one uncertainty region among the different uncertainty regions obtained from the different validation experiments, using a robust stability criterion. In order to compare these uncertainty regions, we have indeed this first result:

Theorem 3.2 *Consider two uncertainty regions $\mathcal{D}^{(1)}$ and $\mathcal{D}^{(2)}$ obtained from two different validation experiments. If we have that $\delta_{WC}(G_{mod},\mathcal{D}^{(1)}) < \delta_{WC}(G_{mod},\mathcal{D}^{(2)})$, then $\mathcal{C}(G_{mod},\mathcal{D}^{(2)}) \subset \mathcal{C}(G_{mod},\mathcal{D}^{(1)})$.*

Theorem 3.2, which directly results from Proposition 3.2, gives us guidelines to choose the uncertainty region that is best tuned to robustly stable controller design with respect to G_{mod}. These guidelines are summarized in the following proposition.

Proposition 3.3 *Consider t uncertainty regions $\mathcal{D}^{(i)}$ obtained from t different validation experiments and a model G_{mod}. Then the uncertainty region $\mathcal{D}^*$ that generates the largest set $\mathcal{C}(G_{mod},\mathcal{D}^{(i)})$ $(i = 1...t)$ of robustly stabilizing controllers is the uncertainty region:*

$$\mathcal{D}^* = arg \min_{\mathcal{D}^{(i)}} \delta_{WC}(G_{mod},\mathcal{D}^{(i)}) \tag{3.17}$$

Remarks concerning the second situation.

- The choice of the model G_{mod} for the control design is an important feature. Indeed, we analyze the robustness properties of the uncertainty regions $\mathcal{D}^{(i)}$ with respect to controllers designed from G_{mod} (and stabilizing it). If the smallest worst case ν-gap between G_{mod} and the different $\mathcal{D}^{(i)}$ remains "large", then the chosen model G_{mod} is not appropriate for a control design procedure for G_0 because the actual $\delta_\nu(G_{mod}, G_0)$ may be too large. A better model G_{mod} must then be chosen: for example, the center of one of the uncertainty regions $\mathcal{D}^{(i)}$. This important matter will be further discussed in Section 3.4.3.

- As already said earlier, the set $\mathcal{C}(G_{mod}, \mathcal{D}^{(i)})$ contains all controllers that stabilize all systems in the uncertainty set $\{G|\delta_\nu(G_{mod}, G) \leq \delta_{WC}(G_{mod}, \mathcal{D}^{(i)})\}$ that embeds $\mathcal{D}^{(i)}$. Thus, there may be additional controllers outside the set $\mathcal{C}(G_{mod}, \mathcal{D}^{(i)})$ that stabilize all models in $\mathcal{D}^{(i)}$, in that sense, our analysis is conservative. However, since G_{mod} lies typically within all $\mathcal{D}^{(i)}$, we essentially introduce the same conservatism for each $\mathcal{D}^{(i)}$ and therefore our procedure remains valid for the selection of the best $\mathcal{D}^{(i)}$.

3.4.2 Consequences for the design of the validation experiment

In the previous subsections, we have shown that the worst case ν-gap between the model G_{mod} and an uncertainty region $\mathcal{D}$ deduced from an identification experiment is a good measure to determine if the uncertainty region $\mathcal{D}$ is well tuned for robustly stable controller design based on the model G_{mod}. Our result therefore gives a meaning to the concept of *identification for robust control*: a validation experiment (i.e. an identification experiment) is "tuned for robust control design" if the worst case ν-gap for the uncertainty set delivered by this validation experiment is small, because it implies that, for that uncertainty set, the set $\mathcal{C}(G_{mod}, \mathcal{D})$ of robustly stabilizing controllers is large.

Our result gives us also guidelines to design the validation experiment: we should always aim to design a validation experiment leading to an identified model G_{mod} and an uncertainty region $\mathcal{D}$ such that the worst case ν-gap between G_{mod} and $\mathcal{D}$ is the smallest possible. In order

to achieve this, the uncertainty distribution delivered by the validation experiment has to be small in the frequency range where the resolution of the ν-gap metric is the largest i.e. around the cut-off frequency [86]. The validation experiment should therefore be designed such that the input signal has a large power spectrum around the cut-off frequency of the true system. Indeed, the uncertainty distribution in the frequency range is asymptotically inversely proportional to the spectrum of the input signal in open-loop identification [63] and inversely proportional to the spectrum of the input signal due to the reference signal in closed-loop identification [44].

It is to be noted that, in [24], such an idea of minimizing a quality measure of an uncertainty region to find the best possible uncertainty region is also proposed in the framework of an iterative scheme. However, the measure presented in [24] is a function of the controller present in the loop and is therefore only a measure of quality of the uncertainty region with respect to that particular controller as opposed to our measure (the worst case ν-gap) which is controller-independent.

3.4.3 Validation of an a-priori given model G_{mod}

As already stated earlier, the worst-case ν-gap $\delta_{WC}(G_{mod}, \mathcal{D})$ is an indicator of how well the uncertainty set $\mathcal{D}$ is tuned for robustly stable controller design with a model G_{mod}. Therefore, this worst case ν-gap gives not only information about $\mathcal{D}$, but it gives also information about the model G_{mod}. In fact, it is an indicator of the quality of the pair $\{G_{mod}\, \mathcal{D}\}$ for robust control design. This has the following consequences for the case where the model G_{mod} that will be used for control design is given.

The model G_{mod} for control design can indeed either be chosen equal to the identified model $G(z, \hat{\delta})$, center of the considered uncertainty region $\mathcal{D}$ or be given. In the second case (i.e. the model G_{mod} is given), we have really no idea if that model is reliable or not for control design with respect to the true system G_0. A validation experiment on G_0 leading to a set $\mathcal{D}$ and the computation of the corresponding worst case ν-gap $\delta_{WC}(G_{mod}, \mathcal{D})$ will help us to assess the quality of G_{mod} for (robust) control purpose. Indeed, if the obtained worst case ν-gap is relatively small (with respect to $b_{opt}(G_{mod})$), we then know that the set $\mathcal{C}(G_{mod}, \mathcal{D})$ of G_{mod}-based controllers that robustly stabilize $\mathcal{D}$ (and

therefore also the true system G_0) is relatively large. Such result validates the model G_{mod}. We can see this result from an other point of view : if $\delta_{WC}(G_{mod}, \mathcal{D})$ is small, then $\delta_\nu(G_{mod}, G_0)$ is also small, since we have that

$$\delta_\nu(G_{mod}, G_0) \leq \delta_{WC}(G_{mod}, \mathcal{D}).$$

Using Corollary 3.1, we can therefore conclude that a small $\delta_{WC}(G_{mod}, \mathcal{D})$ implies a large set of controllers that stabilizes both G_{mod} and G_0.

3.5 A simulation example

In this section, we give an example of the use of the worst case ν-gap as a selection tool for uncertainty regions delivered by validation experiments (see Section 3.4.1, second situation). For this purpose, let us consider the following true system G_0 and the following model G_{mod} of this true system.

$$y = G_0 u + e = \frac{0.1047z^{-1} + 0.0872z^{-2}}{1 - 1.5578z^{-1} + 0.5769z^{-2}}u + e$$

$$G_{mod} = \frac{0.1060z^{-1} + 0.0928z^{-2}}{1 - 1.5308z^{-1} + 0.5467z^{-2}}$$

where e is a white noise of variance 0.1. The actual ν-gap between G_0 and G_{mod} is $\delta_\nu(G_0, G_{mod}) = 0.0193$. We perform one validation experiment in open loop and one in closed loop (with the controller $K = (1.27 - 1.04z^{-1})/(1 - 0.6z^{-1})$ in the loop) leading to two different uncertainty regions, each of which contains G_0 with probability 0.95. We call these two uncertainty regions $\mathcal{D}_{ol}$ and $\mathcal{D}_{cl}$, respectively. In order to decide which of these uncertainty regions is best tuned for robustly stable control design based on the model G_{mod}, we compute the measure of robustness of these two uncertainty regions with respect to G_{mod}, i.e. $\delta_{WC}(G_{mod}, \mathcal{D}_{ol})$ and $\delta_{WC}(G_{mod}, \mathcal{D}_{cl})$. For this purpose, we first compute the worst case chordal distances at each frequency for $\mathcal{D}_{ol}$ and $\mathcal{D}_{cl}$ using the LMI tools developed in Section 3.3. The worst case chordal distances at each frequency $\kappa_{WC}(G_{mod}(e^{j\omega}), \mathcal{D}_{ol})$ and $\kappa_{WC}(G_{mod}(e^{j\omega}), \mathcal{D}_{cl})$ are represented in Figure 3.2 where they are compared with the actual chordal distance $\kappa(G_{mod}(e^{j\omega}), G_0(e^{j\omega}))$ between G_{mod} and G_0. According to Lemma 3.1 and since $W(G_{mod}, \hat{G}_{ol}) =$

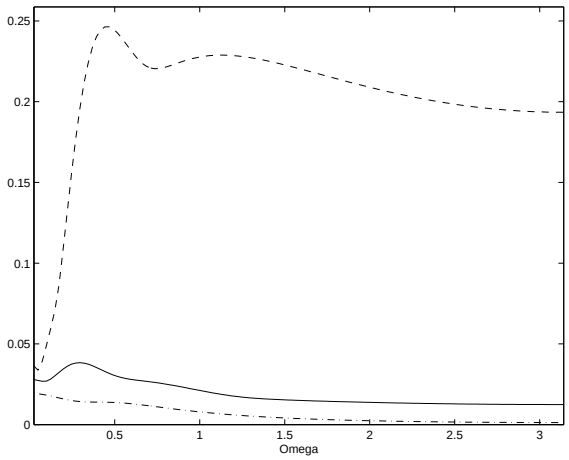

Figure 3.2: $\kappa_{WC}(G_{mod}(e^{j\omega}), \mathcal{D}_{ol})$ (dashed), $\kappa_{WC}(G_{mod}(e^{j\omega}), \mathcal{D}_{cl})$ (solid) and $\kappa(G_{mod}(e^{j\omega}), G_0(e^{j\omega}))$ (dashdot) at each frequency

$W(G_{mod}, \hat{G}_{cl}) = 0$ ($\hat{G}_{ol}$ and $\hat{G}_{cl}$ are the centers of $\mathcal{D}_{ol}$ and $\mathcal{D}_{cl}$, respectively), we can derive the worst case Vinnicombe distances from the worst chordal distances as follows:

$$\delta_{WC}(G_{mod}, \mathcal{D}_{ol}) = \max_{\omega} \kappa_{WC}(G_{mod}(e^{j\omega}), \mathcal{D}_{ol}) = 0.2464$$

$$\delta_{WC}(G_{mod}, \mathcal{D}_{cl}) = \max_{\omega} \kappa_{WC}(G_{mod}(e^{j\omega}), \mathcal{D}_{cl}) = 0.0384$$

Therefore, by Proposition 3.3, the set $\mathcal{C}(G_{mod}, \mathcal{D}_{cl})$ of controllers stabilizing G_{mod} that robustly stabilizes $\mathcal{D}_{cl}$ is much larger than the set $\mathcal{C}(G_{mod}, \mathcal{D}_{ol})$ that robustly stabilizes $\mathcal{D}_{ol}$. To illustrate this statement, let us design two controllers from the model G_{mod}. These two controllers are given below with the achieved generalized stability margins:

$$C_1 = \frac{1.8464 - 1.3647z^{-1}}{1 - 0.4545z^{-1}} \quad b_{G_{mod},C_1} = 0.2861$$

$$C_2 = 3 \quad b_{G_{mod},C_2} = 0.0653$$

We directly see that the controller C_1 is guaranteed to stabilize the plants in the two uncertainty regions since it belongs to both guaranteed

sets of stabilizing controllers $\mathcal{C}(G_{mod}, \mathcal{D}_{ol})$ and $\mathcal{C}(G_{mod}, \mathcal{D}_{cl})$ defined in Proposition 3.2. Indeed:

$$b_{G_{mod},C_1} > \delta_{WC}(G_{mod}, \mathcal{D}_{ol}) > \delta_{WC}(G_{mod}, \mathcal{D}_{cl}).$$

However, the controller C_2 belongs to $\mathcal{C}(G_{mod}, \mathcal{D}_{cl})$ only : C_2 therefore stabilizes all the plants in $\mathcal{D}_{cl}$. As $C_2 \notin \mathcal{C}(G_{mod}, \mathcal{D}_{ol})$, it is not guaranteed, by Proposition 3.2, to stabilize all plants in $\mathcal{D}_{ol}$. Proposition 3.2 only gives a sufficient condition. To check whether C_2 actually stabilizes all plants in $\mathcal{D}_{ol}$, we use the "necessary and sufficient" test that will be developed in Chapter 4. This test fails, and therefore C_2 does not stabilize all plants in $\mathcal{D}_{ol}$ whereas it does stabilize all plants in $\mathcal{D}_{cl}$ by Proposition 3.2.

3.6 Conclusions

We have proposed a measure of robust stability for the uncertainty region $\mathcal{D}$ as delivered by prediction error identification. This measure is the largest ν-gap between the nominal model and all plants in the uncertainty region. We have shown that this measure is computable frequency-wise using an LMI based optimization problem at each frequency. We have also shown that the smaller the worst case ν-gap between the model and an uncertainty region, the larger is the set of model-based controllers that are guaranteed by the ν-gap theory to robustly stabilize all plants in the uncertainty region. This measure is thus an indicator of how well the uncertainty region is tuned for robust control design with the chosen model. This measure therefore also gives us guidelines to select the uncertainty region that is best tuned for robust stability analysis among all available ones. To illustrate the impact of our results in terms of the connection between identification and robust control, we return to the example above. With our robust stability measure for uncertainty sets, we were able to conclude that the G_{mod}-based controller set that is guaranteed to robustly stabilize $\mathcal{D}_{cl}$ is much larger than the set that is guaranteed to robustly stabilize $\mathcal{D}_{ol}$. Hence, the closed-loop identification design that led to the uncertainty set $\mathcal{D}_{cl}$ is a much better experiment design than the open-loop design that led to $\mathcal{D}_{ol}$. The results of this chapter have thus allowed us to establish a connection between identification design and stability robustness of the controllers resulting from such design. We have therefore paved the way to a new research field i.e. *PE identification for robust control.*

Chapter 4

A necessary and sufficient robust stability condition for $\mathcal{D}$

In the previous chapters, it has been shown that a PE identification procedure allows one to design an uncertainty region $\mathcal{D}$ containing the true system at a certain probability level. This uncertainty region takes the form of a set of parametrized transfer functions where the parameter vector is constrained to lie in an ellipsoid. We have introduced a measure of this uncertainty region that is connected to the size of the model-based controllers that are guaranteed (by the ν-gap theory) to stabilize all plants in $\mathcal{D}$. This measure has been proved to be an indicator of how well the uncertainty set $\mathcal{D}$ is tuned for robust control design with respect to G_{mod}.

In this chapter, we consider that the tools presented in the previous chapter has allowed us to select an uncertainty region $\mathcal{D}$ and a model G_{mod} and that a controller C for the true system has been designed from the model G_{mod}. The problem solved in this chapter is the problem of finding a necessary and sufficient condition for the stabilization of all plants in the uncertainty region $\mathcal{D}$ by the controller C. If the controller C stabilizes all plants in $\mathcal{D}$, we will say that this controller is *validated for stability*. The result of this chapter pertains thus to the validation of one specific controller. It is also important to note that this robust stability condition is also a condition guaranteeing the stabilization of the true system G_0 by the controller C.

Robust stability theory developed in e.g. [34, 31, 92, 68, 53] provides some necessary and sufficient conditions for the stabilization, by a given controller C, of all plants in an uncertainty region, provided this uncertainty region is defined in the general LFT (linear fractional transformation) framework for robust stability analysis. Our contribution in the proposed stability validation procedure is to show that one can rewrite the closed-loop connection of the controller C and all plants in the uncertainty region $\mathcal{D}$ obtained from a validation experiment into a particular LFT that takes into account the parametric description of $\mathcal{D}$ (i.e. the uncertainty part of the obtained LFT is a real vector) and whose (real) stability radius is exactly computable, using the result presented in [53, 72]. The proposed approach has the complementary advantage of being easily extensible to the design of a controller that is assured to stabilize all plants in $\mathcal{D}$ using the result in [73] extended in [6]. Indeed, [73] and [6] show that several robust synthesis problems for rank-ones LFT's (that is the type of LFT's we here obtain) can be stated in terms of convex or quasi-convex optimization. It is also to be noted that, since the uncertainty region has been rewitten as an LFT, μ-synthesis (see e.g. [92]) may also be considered in order to design a controller that is guaranteed to achieve a certain level of performance with all plants in $\mathcal{D}$. However, the drawback of this technique is that it is not guaranteed to converge.

In the previous chapter, we have already given a condition for the stabilization of all plants in $\mathcal{D}$ by a controller. Indeed, we presented there a set $\mathcal{C}(G_{mod}, \mathcal{D})$ of G_{mod}-based controllers that are guaranteed to stabilize all plants in $\mathcal{D}$. If the controller C designed from G_{mod} lies in $\mathcal{C}(G_{mod}, \mathcal{D})$, then, it stabilizes all plants in $\mathcal{D}$. However, as already said in Chapter 3, the set $\mathcal{C}(G_{mod}, \mathcal{D})$ is not assured to contain all controllers that robustly stabilize $\mathcal{D}$. Indeed, this controller set only contains all controllers robustly stabilizing all plants in a larger set [1] that embeds $\mathcal{D}$. The advantage in the present approach is that the obtained robust stability condition is necessary and sufficient. This is a consequence of the fact that our new stability results apply directly to the parametrized set $\mathcal{D}$ resulting from the identification step, thereby avoiding the conservativeness resulting from the overbounding of $\mathcal{D}$ by a larger ν-gap uncertainty set.

[1] i.e. $\{G | \delta_\nu(G_{mod}, G) \leq \delta_{WC}(G_{mod}, \mathcal{D})\}$

In [72, 57], the authors consider a similar but much simpler structure than $\mathcal{D}$ and show that this simpler structure can be expressed as an LFT. In this paper, we give a general formulation of this LFT for general expression of the uncertainty region $\mathcal{D}$.

Other authors have tackled the robust stability problem in the presence of an uncertainty region defined by a real (parameter) vector from another point of view (see e.g. [7, 23, 4, 5] and references therein). In this literature, the stability of an uncertain polynomial is analyzed. For control purposes, the analyzed polynomial is the denominator of the closed-loop transfer function. In this approach, the parameters of the open-loop system are generally assumed to vary in a hypercube (i.e. each parameter varies in an interval) and not in an ellipsoid like in $\mathcal{D}$. However, in [7], the treated problem is closer to our problem: the authors present a procedure that gives, for a given controller, the largest *ellipsoid* in the space of the system parameters for which the stabilization of the closed-loop transfer function denominator is guaranteed. Their approach uses Euclidean space geometry to project the parameters of the open-loop system into those of the common denominator of the closed-loop transfer functions and conversely. This result could have been used in order to find a procedure to validate a controller for stability. Our choice for the procedure based on the computation of the stability radius is motivated by the fact that this procedure uses the general framework of the robustness theory which allows one to easily extend our robust analysis approach to robust synthesis using μ-synthesis or the results of [73].

Chapter outline. In Section 4.1, we present a robust stability theorem for a real vector uncertainty. In Section 4.2, we design the LFT framework of all closed-loop connections made up of a plant in an uncertainty set $\mathcal{D}$ and a controller. In Section 4.3, using this LFT framework and the robust stability theorem, we deduce a necessary and sufficient condition for the robust stabilization of all plants in $\mathcal{D}$ by the controller C. We finish this chapter by an example (Section 4.4) and some conclusions (Section 4.5).

4.1 Robust stability for a real vector uncertainty

As said in the introduction, the aim of this chapter is to find a necessary and sufficient condition for the stabilization of all plants in an uncertainty region $\mathcal{D}$ by a given controller. Robust stability theory provides such necessary and sufficient conditions [34, 31, 92, 68, 53]. But for the application of robust stability results, it is required that the closed loop connections of this controller to all plants in the uncertainty region be rewritten as a set of loops that connect a known fixed dynamic matrix $M(z)$ to an uncertainty part $\Delta(z)$ of known structure that belongs to a prescribed uncertainty domain. In this section, we recall an important result of robust stability analysis [72, 53] in the case when the uncertainty part $\Delta(z)$ is assumed to be a real vector.

Let us consider a set of loops $[M(z)\ \beta]$ that obey the following system of equations (see Figure 4.1).

$$\begin{cases} p = \beta q \\ q = M(z)p \end{cases} \tag{4.1}$$

In this set of loops, it is assumed that $M(z) \in \mathcal{R}H_\infty$ is a known *fixed* row vector of size b and that the uncertainty part β is a real vector $\in \mathbf{R}^{b\times 1}$ that varies in the following uncertainty domain: $|\beta|_2 < 1$. $|\beta|_2$ represents the 2-norm of the vector β i.e. $|\beta|_2 = \sqrt{\beta^T\beta}$.

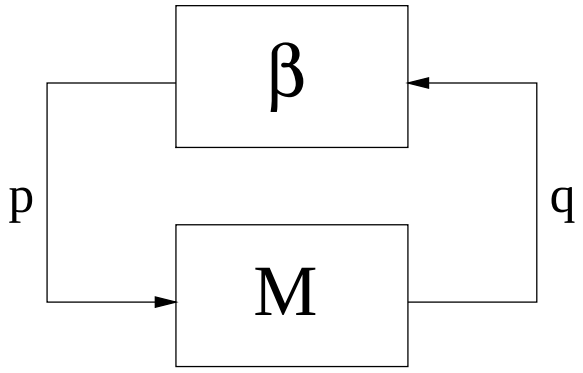

Figure 4.1: set of loops $[M(z)\ \beta]$

The robust stability theorem linked to the set of loops $[M(z)\ \beta]$ is

now summarized in the following proposition.

Proposition 4.1 *If $M(z) \in \mathcal{R}H_\infty$ and $\beta \in \mathbf{R}^{b\times 1}$, then the loops $[M(z)\ \beta]$ given in (4.1) are internally stable for all $\beta \in \mathbf{R}^{b\times 1}$ such that $|\beta|_2 < 1$ if and only if*

$$\max_\omega \mu(M(e^{j\omega})) \leq 1 \tag{4.2}$$

The value $\mu(M(e^{j\omega}))$ is called the stability radius of the loop $[M(z)\ \beta]$ at the frequency ω and is defined below.

Definition 4.1 (stability radius [72, 53]) *For $M(e^{j\omega})$ a known complex matrix $\in \mathbf{C}^{1\times b}$ and $\beta \in \mathbf{R}^{b\times 1}$, the stability radius $\mu(M(e^{j\omega}))$ is defined as follows if $Im(M(e^{j\omega})) \neq 0$:*

$$\mu(M(e^{j\omega})) = \sqrt{|Re(M)|_2^2 - \frac{(Re(M)Im(M)^T)^2}{|Im(M)|_2^2}} \tag{4.3}$$

and $\mu(M(e^{j\omega})) = |M|_2$, if $Im(M) = 0$. The stability radius is in fact the structured singular value linked to the loop $[M(z)\ \beta]$: $\mu(M(e^{j\omega}))$ is the inverse of the smallest value of $|\beta|_2$ such that $1 - M(e^{j\omega})\beta = 0$.

Remarks. In [72], the stability radius at a given frequency is defined for a real uncertainty that is a row vector. The case of a column vector is similar and yields Definition 4.1. Note also that the stability radius is discontinuous only at the frequencies where M is real [71].

4.2 LFT framework for the uncertainty region $\mathcal{D}$ and a controller C

In order to apply Proposition 4.1 to check the stabilization of all plants in the uncertainty region $\mathcal{D}$ described in Proposition 2.5 by some model-based controller C, the first step is to find the particular set of loops $[M(z)\ \beta]$ that correspond to the closed-loop connections of all plants in $\mathcal{D}$ with C. This first step can be achieved using the following theorem.

Theorem 4.1 (LFT framework for $\mathcal{D}$) *Consider an uncertainty region $\mathcal{D}$ of plant transfer functions given by (2.44) and a controller $C(z)$ whose numerator and denominator are denoted $X(z)$ and $Y(z)$, respectively ($C(z) = X(z)/Y(z)$). The set of closed-loop connections*

$[G(z,\delta)\ C]$ for all $G(z,\delta) \in \mathcal{D}$ can be rewritten into the set of loops $[M_{\mathcal{D}}\ \phi]$ which obey the following system of equations

$$\begin{cases} p = \phi q \\ q = M_{\mathcal{D}}(z)p \end{cases}$$

where the uncertainty part ϕ is a real column vector of size k that varies in the uncertainty domain: $|\phi|_2 < 1$, and where the part $M_{\mathcal{D}}(z)$ is a row vector of size k defined as :

$$M_{\mathcal{D}}(z) = \frac{-(Z_D + \frac{X(Z_N - eZ_D)}{Y+eX})T^{-1}}{1 + (Z_D + \frac{X(Z_N - eZ_D)}{Y+eX})\hat{\delta}}, \tag{4.4}$$

with T a square root of the matrix R defining U in (2.44) : $R = T^T T$.

Proof. The closed-loop connection of C and a particular plant $G(z,\delta) = (e + Z_N\delta)/(1 + Z_D\delta)$ in $\mathcal{D}$ (see (2.44)) is given by

$$\begin{cases} y = \frac{e+Z_N\delta}{1+Z_D\delta}u \\ u = -Cy \end{cases} \tag{4.5}$$

Let us rewrite (4.5) in a convenient way for the LFT formulation:

$$\begin{cases} y = (e + \frac{(Z_N - eZ_D)\delta}{1+Z_D\delta})u \\ u = -Cy \end{cases} \tag{4.6}$$

By introducing two new signals q and p_1, we can restate (4.6) as

$$\begin{cases} \begin{pmatrix} q \\ y \end{pmatrix} = \overbrace{\begin{pmatrix} -Z_D & 1 \\ Z_N - eZ_D & e \end{pmatrix}}^{H(z)} \begin{pmatrix} p_1 \\ u \end{pmatrix} \\ p_1 = \delta q \\ u = -Cy \end{cases} \tag{4.7}$$

By doing so, we have isolated the uncertainty vector δ from the known transfer matrix $H(z)$ and the controller $C(z)$, as is shown in Figure 4.2.

The variables y and u are now eliminated from (4.7), yielding the following system of equations representing a loop which is of the type (4.1) required by Proposition 4.1.

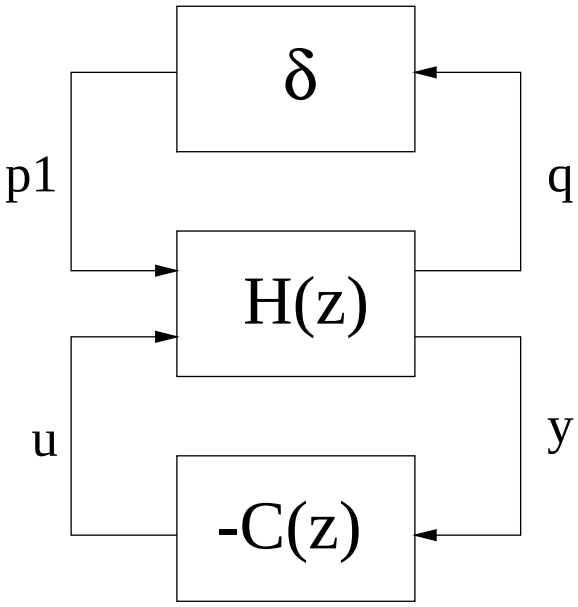

Figure 4.2: Equivalent loop for $[G(z,\delta)\ C]$

$$\begin{cases} p_1 = \delta q \\ q = \overbrace{(-Z_D - \frac{C(Z_N - eZ_D)}{1+eC})}^{M_1(z)} p_1 \end{cases} \tag{4.8}$$

The system (4.8) is equivalent to the closed-loop connection of a particular $G(z,\delta)$ in $\mathcal{D}$ with the controller C. In order to consider the closed-loop connections for all plants in $\mathcal{D}$, we have to consider all $\delta \in \mathbf{R}^{k\times 1}$ lying in the ellipsoid U given by:

$$U = \{\delta \mid (\delta - \hat{\delta})^T R(\delta - \hat{\delta}) < 1\}. \tag{4.9}$$

This last expression is the uncertainty domain of the real uncertainty vector δ. This uncertainty domain is not quite standard. Therefore, the set of loops $[M_1(z)\ \delta]$ with $\delta \in U$ can not be immediatly used in this form in Proposition 4.1. A last step is then to normalize the uncertainty domain using a method presented e.g. in [72, 57] . Using $R = T^T T$, we now define the real vector $\phi \in \mathbf{R}^{k\times 1}$ as follows:

$$\phi \stackrel{\Delta}{=} T(\delta - \hat{\delta}). \tag{4.10}$$

Using now (4.9) and (4.10), we have

$$\delta \in U \Leftrightarrow \phi^T \phi < 1 \Longleftrightarrow |\phi|_2 < 1 \tag{4.11}$$

ϕ is therefore an uncertainty vector with same structure as δ (i.e. $\phi \in \mathbf{R}^{k\times 1}$) but with an uncertainty domain as required by Proposition 4.1. The uncertainty vector δ is therefore replaced by ϕ in (4.8). For this purpose, we first denote $p \stackrel{\Delta}{=} \phi q$. Since $\delta = \hat{\delta} + T^{-1}\phi$, we have

$$\left\{ \begin{array}{l} p_1 = \delta q \\ q = M_1(z) p_1 \end{array} \right. \Leftrightarrow \left\{ \begin{array}{l} p = \phi q \\ \\ q = \frac{M_1 T^{-1}}{1 - M_1 \hat{\delta}} p = \overbrace{\frac{-(Z_D + \frac{X(Z_N - eZ_D)}{Y + eX}) T^{-1}}{1 + (Z_D + \frac{X(Z_N - eZ_D)}{Y + eX})\hat{\delta}}}^{M_{\mathcal{D}}(z)} p \end{array} \right. \tag{4.12}$$

The set of loops $[M_{\mathcal{D}}(z)\ \phi]$ for $\phi \in \mathbf{R}^{k\times 1}$ and $|\phi|_2 < 1$ is therefore equivalent to the set of closed-loop connections $[G(z,\delta)\ C]$ for all plants $G(z,\delta)$ in $\mathcal{D}$. This completes the proof. □

4.3 Robust stability condition for the uncertainty region $\mathcal{D}$

Theorem 4.1 allows us to "transform" our problem of testing if the controller C stabilizes all the plants in the uncertainty region $\mathcal{D}$ into the *equivalent* problem of testing if the set of loops $[M_{\mathcal{D}}\ \phi]$ are stable for all real vector $\phi \in \mathbf{R}^{k\times 1}$ such that $|\phi|_2 < 1$. This equivalent problem is the one which is treated by Proposition 4.1. Therefore, using Proposition 4.1 and Theorem 4.1, we can now formulate our main stability theorem.

Theorem 4.2 (robust stability condition) *Consider an uncertainty region $\mathcal{D}$ of plant transfer functions having the general form given in (2.44) and let C be a controller that stabilizes the center $G(z,\hat{\delta})$ of $\mathcal{D}$. All the plants in the uncertainty region $\mathcal{D}$ are stabilized by the controller C if and only if*

$$\max_{\omega} \mu(M_{\mathcal{D}}(e^{j\omega})) \leq 1 \tag{4.13}$$

where the stability radius μ and $M_{\mathcal{D}}(z)$ are defined in Definition 4.1 and in (4.4), respectively.

Proof. $M_{\mathcal{D}}(z)$ lies in $\mathcal{R}H_\infty$ since its denominator is the denominator of the sensitivity function of the closed loop $[G(z,\hat{\delta})\ C]$ which is stable by assumption. Therefore, this theorem is a direct consequence of Proposition 4.1 and Theorem 4.1. □

This theorem gives a necessary and sufficient condition for the stabilization of all plants in $\mathcal{D}$ by a controller that has been designed from the chosen model G_{mod}. This necessary and sufficient condition involves the computation at each frequency of the stability radius $\mu(M_{\mathcal{D}}(e^{j\omega}))$. This computation is achieved using Definition 4.1.

Important remark. We now discuss why this necessary and sufficient robust stability result is not used to compute a robust stability measure for the set $\mathcal{D}$ and why we have used the worst case ν-gap for this purpose (see Chapter 3). Let us define the following quantity:

$$\mu_{min}(\mathcal{D}) = \min_{C\ stabilizing\ G(z,\hat{\delta})} \left(\max_{\omega} \mu(M_{\mathcal{D}}(e^{j\omega})) \right) \tag{4.14}$$

Recall that $M_{\mathcal{D}}(z)$ is a function of C and of $\mathcal{D}$. Using the definition of $\mu_{min}(\mathcal{D})$ and Theorem 4.2, we can state that all controllers stabilizing $G(z,\hat{\delta})$ that lie in

$$\{C \mid \mu_{min}(\mathcal{D}) \leq \max_{\omega} \mu(M_{\mathcal{D}}(e^{j\omega})) \leq 1\}, \tag{4.15}$$

stabilize all plants in $\mathcal{D}$. Moreover the set (4.15) is the set that contains **all** these robustly stabilizing controllers. As a consequence, the quantity $\mu_{min}(\mathcal{D})$ is thus an indicator of how well the uncertainty region $\mathcal{D}$ is tuned for robustly stable controller design. Indeed, the smaller is $\mu_{min}(\mathcal{D})$, the larger is the set of robustly stabilizing controllers. Moreover, it is a better indicator than the worst case ν-gap since the set (4.15) contains all robustly stabilizing controllers as opposed to the set (3.16). However, to our knowledge, this indicator $\mu_{min}(\mathcal{D})$ has not been proved computable in polynomial time in the case of an uncertainty region like $\mathcal{D}$. That is why we have opted for the worst case ν-gap as measure of robust stability for the set $\mathcal{D}$. It is nevertheless to be noted that our current research aims at applying the results of [73] to compute $\mu_{min}(\mathcal{D})$.

4.4 Simulation Example

To illustrate our results, we present an example of controller validation for a model identified in closed-loop. Let us consider the following true system G_0 with an Output Error structure:

$$y = \overbrace{\frac{0.1047z^{-1} + 0.0872z^{-2}}{1 - 1.5578z^{-1} + 0.5769z^{-2}}}^{G_0} u + e(t),$$

where $e(t)$ is a unit-variance white noise. The sampling time is 0.05 second.

Validation experiment. Let us perform a validation experiment in closed-loop using the indirect approach (see Section 2.2.4). Let us thus identify an unbiased model $T(\hat{\xi})$ of the true closed-loop transfer function T_0^1 (defined in (2.29)) by collecting 1000 reference data $r_1(t)$ and output data $y(t)$ on the closed loop made up of G_0 and the controller $K = 3$: $u = 3(r - y)$. This controller stabilizes G_0. It yields:

$$T(\hat{\xi}) = \frac{0.3179z^{-1} + 0.2783z^{-2}}{1 - 1.2129z^{-1} + 0.8251z^{-2}}$$

The open-loop model $G(\hat{\xi})$ corresponding to $T(\hat{\xi})$ is equal to

$$G(\hat{\xi}) = \frac{1}{K} \times \frac{T(\hat{\xi})}{1 - T(\hat{\xi})} = \frac{0.1060z^{-1} + 0.0928z^{-2}}{1 - 1.5308z^{-1} + 0.5467z^{-2}}$$

Following the procedure presented in Section 2.2.4.2, we can design an uncertainty region $\mathcal{D}_{icl}$ from the estimated covariance matrix P_ξ of the parameters of the closed-loop model $T(\hat{\xi})$. The region containing the true system G_0 with probability 0.98 is given by

$$\mathcal{D}_{icl} = \{G(\xi) \mid G(\xi) = \frac{T(\xi)}{K(1 - T(\xi))} \; and \; \xi \in U_{icl}\}$$

where $U_{icl} = \{\xi \mid (\xi - \hat{\xi})^T P_\xi^{-1} (\xi - \hat{\xi}) < 12.6\}$. It has been shown in Chapter 2 that $\mathcal{D}_{icl}$ can be expressed in the general structure (2.44) of the uncertainty regions delivered by PE identification.

The worst case ν-gap $\delta_{WC}(G(\hat{\xi}), \mathcal{D}_{icl})$ between the identified model $G(\hat{\xi})$ and the set $\mathcal{D}_{icl}$ is here equal to 0.1015 which is relatively small

with respect to the optimal stability margin $b_{opt}(G(\hat{\xi})) = 0.5719$. The set $\mathcal{C}(G(\hat{\xi}), \mathcal{D}_{icl})$ of $G(\hat{\xi})$-based controllers that are guaranteed to robustly stabilize $\mathcal{D}_{icl}$ is thus large and we therefore decide to use $G(\hat{\xi})$ as model for control design and $\mathcal{D}_{icl}$ for the validation of the controller C that will be designed from $G(\hat{\xi})$.

Control design. The model $G(\hat{\xi})$ deduced from the identified closed-loop transfer function is used to design a controller with a lead-lag filter:

$$C(z) = \frac{1.8464 - 1.3647z^{-1}}{1 - 0.4545z^{-1}}$$

With this controller, the designed closed-loop $[G(\hat{\xi})\ C]$ has a stability margin of 57 degrees and a gain margin of 10dB. The cut-off frequency ω_c is equal to 0.5 which corresponds to a *real* frequency of 11 rad/s.

Before applying this controller $C(z)$ to the true system, we verify whether it stabilizes all plants in the uncertainty region $\mathcal{D}_{icl}$ deduced from the validation experiment, using the results presented in this chapter.

Validation of C for stability. For this purpose, we construct the row vector $M_{\mathcal{D}_{icl}}(z)$ defined in Theorem 4.1 and we compute the corresponding stability radius $\mu(M_{\mathcal{D}_{icl}}(e^{j\omega}))$ at all frequencies. According to Definition 4.1, we know that $\mu(M_{\mathcal{D}_{icl}}(e^{j\omega}))$ has a different expression at the frequencies where $M_{\mathcal{D}_{icl}}(e^{j\omega})$ is real. It occurs here at $\omega = 0$ and $\omega = \pi$. The stability radii at these two frequencies are:

$$\mu(M_{\mathcal{D}_{icl}}(e^{j0})) = 0.0962 \ \textit{and}\ \mu(M_{\mathcal{D}_{icl}}(e^{j\pi})) = 0.0340$$

The stability radii at the other frequencies (i.e. in $(0\ \pi)$) are plotted in Figure 4.3.

The maximum over all frequencies in $[0\ \pi]$ is 0.1313. Since this maximum is smaller than 1, we conclude that $C(z)$ stabilizes all plants in $\mathcal{D}_{icl}$ and therefore also the true system G_0. In other words, the controller $C(z)$ is validated for stability.

4.5 Conclusions

In the previous chapter, an uncertainty region $\mathcal{D}$ has been deduced from a validation experiment (i.e. a PE identification procedure with unbi-

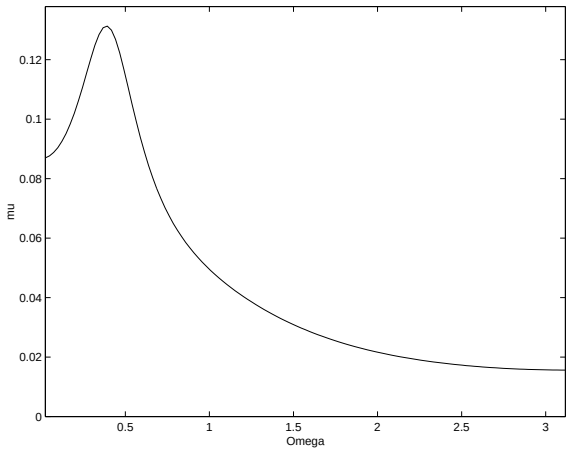

Figure 4.3: $\mu(M_{\mathcal{D}_{icl}}(e^{j\omega}))$ in $(0\ \pi)$

ased model structure). In this chapter, we have developed a tool for the robust stability analysis for the uncertainty region $\mathcal{D}$. This tool is a necessary and sufficient condition for the validation of a controller for stability that is to say a necessary and sufficient condition for the stabilization of all plants in $\mathcal{D}$ by this controller. This tool gives therefore a condition for the stabilisation of the true system G_0 by this controller (modulo the chosen probability level for the presence of G_0 in $\mathcal{D}$).

The necessary and sufficient condition has been deduced by recasting the general structure of the uncertainty region $\mathcal{D}$ in an LFT framework taking into account the parametric description of $\mathcal{D}$ and for which the stability radius is exactly computable.

Chapter 5

Worst case performance in $\mathcal{D}$

In the previous chapter, we have developed a robust stability analysis tool for the uncertainty region $\mathcal{D}$ as delivered by a validation experiment. This tool takes the form of a necessary and sufficient condition for the stabilization of all plants in $\mathcal{D}$ by a given controller. In this chapter, we will develop a robust performance analysis tool. For this purpose, we will again consider an uncertainty region $\mathcal{D}$ and a model G_{mod} from which we have designed a controller C and we will propose an LMI-based optimization problem that computes exactly the worst case performance achieved by the considered controller C over all plants in the uncertainty region $\mathcal{D}$. The controller C is then said *validated for performance* if the worst case performance is better than some threshold value. As in the previous chapter, the result presented in this chapter pertains to the validation of one specific controller. It is also important to note that the worst case performance is of course a lower bound of the performance achieved by C over the true system G_0, since G_0 lies in $\mathcal{D}$.

Our robust performance analysis tool is thus based on the computation of the worst case performance of a closed-loop made up of the considered controller and a system in the uncertainty region $\mathcal{D}$. The performance of a particular loop made up of the controller C and a plant in $\mathcal{D}$ is here defined as the largest singular value of a weighted version of the matrix containing the four closed-loop transfer functions of this loop. Our definition of the worst case performance is thus very

general and, by an appropriate choice of the weights, allows one to derive most of the commonly used worst case performance measures such as e.g. the largest modulus of the sensitivity function. Our contribution is to show that the computation of the worst case performance can be formulated as an LMI-based optimization problem. The LMI formulation of the problem uses the fact that the uncertainty part (i.e. the real parameter vector) of the uncertainty region $\mathcal{D}$ appears linearly in the expression of both the numerator and the denominator of the systems in the uncertainty region $\mathcal{D}$ and, as a consequence, also appears linearly in the expression of the different closed-loop transfer functions.

Our approach to compute the worst case performance differs significantly from the usual approach proposed in e.g. [33, 35]. In these papers, the computation of the worst case performance in an uncertainty region described by an LFT is performed using the computation of a quantity ν. The quantity ν is an extension of the structured singular value μ. However, [33] and [35] only give a way to compute this quantity ν for a limited amount of parametric uncertainties. The case of an uncertainty given by a real vector (such as in our uncertainty region $\mathcal{D}$) is not tackled. This case is nevertheless tackled in e.g. [5, page 402]. In [5], the authors give a procedure to compute the worst case performance in uncertainty regions defined by a real vector that is constrained to lie in a hypercube. Their procedure, which is an extension of a theorem presented in [18], is based on the fact that the difficult computation of the worst case performance in such uncertainty region can be achieved with a fixed number of simple optimization problems with one parameter. However, this procedure can not be used for the computation of the worst case performance in $\mathcal{D}$ since the real vector in $\mathcal{D}$ is constrained to lie in an ellipsoid and not in a hypercube. The contribution of our approach is therefore to give a solution for the computation of the worst case performance in the case of an uncertainty region defined by a real vector that is constrained to lie in an ellipsoid (and that appears linearly both in the numerator and the denominator of the systems in the uncertainty region).

Chapter outline. In Section 5.1, we present the general criterion measuring the worst case performance achieved by a controller over all plants in an uncertainty region $\mathcal{D}$. In Section 5.2, we show that more particular worst case performance levels can be deduced from this general

criterion. In Section 5.3, the LMI-based optimization problem allowing one to compute the worst case performance is presented. We finish by a simulation example (Section 5.4) and some conclusions (Section 5.5).

5.1 The general criterion measuring the worst case performance

As said in the introduction, the aim of this chapter is to find a procedure to compute the worst case performance achieved by a given controller C over all plants in an uncertainty region $\mathcal{D}$ having the general structure given in (2.44). In this section, we will define the criterion measuring the worst case performance. In order to define this criterion, let us first define the performance of a loop $[C\ G]$.

There is no unique way of defining the performance of a closed-loop system. However, most commonly used performance criteria can be derived from some norm of a frequency weighted version of the matrix $T(G,C)$ of the closed-loop system $[C\ G]$ made up of G in feedback with the controller C.

Definition 5.1 *Given a plant $G(z)$ and a stabilizing controller $C(z)$, the performance of a closed-loop system $[C\ G]$ is defined as the following frequency function*

$$J(G,C,W_l,W_r,\omega) = \sigma_1\left(W_l T(G(e^{j\omega}),C(e^{j\omega}))W_r\right) \tag{5.1}$$

where $W_l(z) = diag(W_{l1},W_{l2})$ and $W_r(z) = diag(W_{r1},W_{r2})$ are diagonal weights, $\sigma_1(A)$ denotes the largest singular value of A, and $T(G,C)$ is the transfer matrix of the closed-loop system defined in (3.3).

The worst case performance criterion over all plants in an uncertainty region $\mathcal{D}$ is then defined as follows.

Definition 5.2 *Consider an uncertainty region $\mathcal{D}$ of systems $G(z,\delta)$ with $\delta \in U$ whose general structure is given in (2.44). Consider also a controller $C(z)$. The worst case performance achieved by this controller at a frequency ω over all systems in $\mathcal{D}$ is defined as:*

$$J_{WC}(\mathcal{D},C,W_l,W_r,\omega) = \max_{G(z,\delta)\in\mathcal{D}} \sigma_1\left(W_l T(G(e^{j\omega},\delta),C(e^{j\omega}))W_r\right). \tag{5.2}$$

Note that J_{WC} is a frequency function : it defines a template. J_{WC} has thus to be computed at each frequency.

5.2 More specific worst case performance levels derived from the general criterion

In the previous section, we have defined the performance of a closed loop and the worst case performance achieved by a controller C over all plants in $\mathcal{D}$ in a very general way. In this section, we will show that the criterion (5.2) allows one to define more specific worst case performance levels.

In [25], the performance of a loop $[C\ G]$ is defined as $\| W_l T(G,C) W_r \|_\infty$. In this framework, the nominal performance of the designed loop $[C\ G_{mod}]$[1] is therefore $\| W_l T(G_{mod},C) W_r \|_\infty$ and the worst case performance for an uncertainty region $\mathcal{D}$ is the maximum over all frequencies of the general criterion $J_{WC}(\mathcal{D}, C, W_l, W_r, \omega)$.

A more fundamental way of defining the performance of a closed loop $[C\ G]$ is that proposed for the first time in [89]. The performance can be "measured" by the shape of the modulus of the frequency response of the different closed-loop transfer functions (i.e. $T_{11}(G,C)$, $T_{12}(G,C)$, $T_{21}(G,C)$ and $T_{22}(G,C)$ defined in (3.3)). Let us take the example of the sensitivity function $T_{22}(G,C)$ to motivate this choice. The modulus of the frequency response of $T_{22}(G,C)$ at a particular frequency ω gives the rejection rate of an output disturbance at the frequency ω. Furthermore, the bandwidth of this frequency response gives an idea of the rejection time for constant disturbance rejection. The importance of the resonance peak is also an indication of the overshoot in constant disturbance rejection.

If the performance is defined as the modulus of the frequency response of one of the transfer functions T_{ij} $(i,j{=}1{,}2)$, the worst case performance in the uncertainty region $\mathcal{D}$ is defined as the largest modulus, over all $G(z,\delta) \in \mathcal{D}$, of the corresponding closed-loop transfer function T_{ij}. Let us now define this worst case performance related to T_{ij} $(i,j{=}1{,}2)$ more formally.

Definition 5.3 (The worst case performance for T_{ij}) *Consider an uncertainty region $\mathcal{D}$ given by (2.44) and containing all systems $G(z,\delta)$ with $\delta \in U$. Consider also a controller $C(z)$ and the closed-loop transfer*

[1] Recall that G_{mod} is the model from which we have designed C.

function T_{ij} (i, j=1,2) defined in (3.3). The worst case performance for T_{ij} is the following frequency function :

$$t_{\mathcal{D}}(\omega, T_{ij}) = \max_{G(z,\delta)\in\mathcal{D}} \left| T_{ij}(e^{j\omega}, \delta) \right|, \tag{5.3}$$

where $T_{ij}(z,\delta) \triangleq T_{ij}(G(z,\delta), C(z))$ and $|A|$ denotes the modulus of A.

For instance, if we choose the sensitivity function T_{22}, $t_{\mathcal{D}}(\omega, T_{22})$ provides the lowest rejection rate of a perodic output disturbance at ω, the minimal bandwidth and the maximal resonance peak over the set of closed-loop systems composed of the controller C and all plants in $\mathcal{D}$. These worst case values must be compared with the static error, the bandwidth and the resonance peak of the sensitivity function of the designed closed loop $[C\ G_{mod}]$.

The worst case performance for T_{ij} can be derived from the computation of the general criterion defined in (5.2). This property is summarized in the following proposition whose proof is trivial.

Proposition 5.1 *The worst case performance for the closed-loop transfer function T_{ij} i.e. $t_{\mathcal{D}}(\omega, T_{ij})$ is equal to the general criterion J_{WC} when the following weights are used.*

$$W_l = \begin{pmatrix} f(i) & 0 \\ 0 & 1-f(i) \end{pmatrix} \quad W_r = \begin{pmatrix} f(j) & 0 \\ 0 & 1-f(j) \end{pmatrix} \tag{5.4}$$

where $f(x) = 1$ if $x = 1$ and $f(x) = 0$ if $x = 2$.

5.3 Computation of the general criterion

The general criterion measuring the worst case performance level has been defined in Section 5.1. In Section 5.2, more specific worst case performance levels have been shown to be derivable from this general criterion by appropriately choosing the diagonal weights W_r and W_l. We now present a procedure for the computation of the general criterion $J_{WC}(\mathcal{D}, C, W_l, W_r, \omega)$ at a given frequency ω. This computation boils down to an optimization problem involving Linear Matrix Inequality (LMI) constraints [17], as shown in the following theorem.

Theorem 5.1 *Consider an uncertainty region $\mathcal{D}$ defined in (2.44) and a controller $C(z) = X(z)/Y(z)$ [2]. Then, at frequency ω, the criterion function $J_{WC}(\mathcal{D}, C, W_l, W_r, \omega)$ is obtained as*

$$J_{WC}(\mathcal{D}, C, W_l, W_r, \omega) = \sqrt{\gamma_{opt}}, \tag{5.5}$$

where γ_{opt} is the optimal value of γ for the following standard convex optimization problem involving LMI constraints evaluated at ω:

$$\begin{array}{ll} \textit{minimize} & \gamma \\ \textit{over} & \gamma,\ \tau \\ \textit{subject to} & \tau \geq 0 \quad \textit{and} \end{array}$$
$$\begin{pmatrix} Re(a_{11}) & Re(a_{12}) \\ Re(a_{12}^*) & Re(a_{22}) \end{pmatrix} - \tau \begin{pmatrix} R & -R\hat{\delta} \\ (-R\hat{\delta})^T & \hat{\delta}^T R\hat{\delta} - 1 \end{pmatrix} < 0 \tag{5.6}$$

where

- $a_{11} = (Z_N^* W_{l1}^* W_{l1} Z_N + Z_D^* W_{l2}^* W_{l2} Z_D) - \gamma(Q Z_1^* Z_1)$
- $a_{12} = Z_N^* W_{l1}^* W_{l1} e + W_{l2}^* W_{l2} Z_D^* - \gamma(Q Z_1^* (Y + eX))$
- $a_{22} = e^* W_{l1}^* W_{l1} e + W_{l2}^* W_{l2} - \gamma(Q(Y + eX)^*(Y + eX))$
- $Q = 1/(X^* W_{r1}^* W_{r1} X + Y^* W_{r2}^* W_{r2} Y)$
- $Z_1 = X Z_N + Y Z_D$.

Proof. In order to ease the establishment of the proof, we rewrite the weighted matrix $T_w(z, \delta) \stackrel{\Delta}{=} W_l T(G(z, \delta), C(z)) W_r$, using the definition of the closed-loop transfer matrix T in (3.3) and the expression of $G(z, \delta)$ in (2.44):

$$T_w(z, \delta) = \frac{\begin{pmatrix} W_{l1} X(e + Z_N \delta) W_{r1} & W_{l1} Y(e + Z_N \delta) W_{r2} \\ W_{l2} X(1 + Z_D \delta) W_{r1} & W_{l2} Y(1 + Z_D \delta) W_{r2} \end{pmatrix}}{Y + eX + (X Z_N + Y Z_D)\delta} \tag{5.7}$$

It is important to note that $T_w(z, \delta)$ is of rank one. As a result (5.7) can be written as follows:

[2] $X(z)$ and $Y(z)$ are the polynomials corresponding to the numerator and to the denominator of $C(z)$, respectively

$$T_w(z,\delta) = \begin{pmatrix} \frac{W_{l1}(e+Z_N\delta)}{Y+eX+Z_1\delta} \\ \frac{W_{l2}(1+Z_D\delta)}{Y+eX+Z_1\delta} \end{pmatrix} \begin{pmatrix} XW_{r1} & YW_{r2} \end{pmatrix} \tag{5.8}$$

with $Z_1 = XZ_N + YZ_D$. Using the above introduced notations, we can now state that proving Theorem 5.1 is equivalent to proving that the solution γ_{opt} of the LMI problem (5.6), evaluated at ω, is such that:

$$\sqrt{\gamma_{opt}} = \max_{\delta\in U} \sigma_1(T_w(e^{j\omega},\delta)) \Longleftrightarrow \gamma_{opt} = \max_{\delta\in U} \lambda_1(T_w(e^{j\omega},\delta)^* T_w(e^{j\omega},\delta))$$

where $U = \{\delta \mid (\delta-\hat{\delta})^T R(\delta-\hat{\delta}) < 1\}$, and where $\sigma_1(A)$ and $\lambda_1(A)$ denote the largest singular value and the largest eigenvalue of A, respectively.

An equivalent and convenient way of restating the problem of computing $\max_{\delta\in U} \lambda_1(T_w(e^{j\omega},\delta)^* T_w(e^{j\omega},\delta))$ is as follows:

$$\textit{minimize } \gamma \textit{ such that } \lambda_1(T_w(e^{j\omega},\delta)^* T_w(e^{j\omega},\delta)) - \gamma < 0 \qquad \forall \delta \in U.$$

Since $T_w(e^{j\omega},\delta)$ has rank one, we have:

$$\lambda_1(T_w(e^{j\omega},\delta)^* T_w(e^{j\omega},\delta)) - \gamma < 0 \Longleftrightarrow$$

$$\begin{pmatrix} \frac{W_{l1}(e+Z_N\delta)}{Y+eX+Z_1\delta} \\ \frac{W_{l2}(1+Z_D\delta)}{Y+eX+Z_1\delta} \end{pmatrix}^* \begin{pmatrix} \frac{W_{l1}(e+Z_N\delta)}{Y+eX+Z_1\delta} \\ \frac{W_{l2}(1+Z_D\delta)}{Y+eX+Z_1\delta} \end{pmatrix} (X^*W_{r1}^*W_{r1}X + Y^*W_{r2}^*W_{r2}Y) - \gamma < 0 \Longleftrightarrow$$

$$\begin{pmatrix} \frac{W_{l1}(e+Z_N\delta)}{Y+eX+Z_1\delta} \\ \frac{W_{l2}(1+Z_D\delta)}{Y+eX+Z_1\delta} \\ 1 \end{pmatrix}^* \begin{pmatrix} I_2 & 0 \\ 0 & -\gamma Q \end{pmatrix} \begin{pmatrix} \frac{W_{l1}(e+Z_N\delta)}{Y+eX+Z_1\delta} \\ \frac{W_{l2}(1+Z_D\delta)}{Y+eX+Z_1\delta} \\ 1 \end{pmatrix} < 0 \tag{5.9}$$

where $Q = 1/(X^*W_{r1}^*W_{r1}X + Y^*W_{r2}^*W_{r2}Y)$. By pre-multiplying (5.9) by $(Y + eX + Z_1\delta)^*$ and post-multiplying the same expression by $(Y + eX + Z_1\delta)$, we obtain:

$$\begin{pmatrix} W_{l1}(e+Z_N\delta) \\ W_{l2}(1+Z_D\delta) \\ Y+eX+Z_1\delta \end{pmatrix}^* \begin{pmatrix} I_2 & 0 \\ 0 & -\gamma Q \end{pmatrix} \begin{pmatrix} W_{l1}(e+Z_N\delta) \\ W_{l2}(1+Z_D\delta) \\ Y+eX+Z_1\delta \end{pmatrix} < 0, \tag{5.10}$$

which is equivalent to the following constraint on δ with variable γ :

$$\begin{pmatrix} \delta \\ 1 \end{pmatrix}^* \begin{pmatrix} a_{11} & a_{12} \\ a_{12}^* & a_{22} \end{pmatrix} \begin{pmatrix} \delta \\ 1 \end{pmatrix} < 0, \tag{5.11}$$

where

$$\begin{aligned} a_{11} &= (Z_N^* W_{l1}^* W_{l1} Z_N + Z_D^* W_{l2}^* W_{l2} Z_D) - \gamma(Q Z_1^* Z_1) \\ a_{12} &= Z_N^* W_{l1}^* W_{l1} e + W_{l2}^* W_{l2} Z_D^* - \gamma(Q Z_1^* (Y + eX)) \\ a_{22} &= e^* W_{l1}^* W_{l1} e + W_{l2}^* W_{l2} - \gamma(Q(Y + eX)^*(Y + eX)). \end{aligned}$$

Since δ is real, it can be shown that (5.11) is equivalent with

$$\overbrace{\begin{pmatrix} \delta \\ 1 \end{pmatrix}^T \begin{pmatrix} Re(a_{11}) & Re(a_{12}) \\ Re(a_{12}^*) & Re(a_{22}) \end{pmatrix} \begin{pmatrix} \delta \\ 1 \end{pmatrix}}^{\psi(\delta)} < 0 \tag{5.12}$$

This last expression is equivalent to stating that $\lambda_1(T_w(e^{j\omega}, \delta)^* T_w(e^{j\omega}, \delta)) - \gamma < 0$ for a particular δ in U. However, this must be true for all $\delta \in U$. Therefore (5.12) must be true for all δ such that

$$\overbrace{\begin{pmatrix} \delta \\ 1 \end{pmatrix}^T \begin{pmatrix} R & -R\hat{\delta} \\ (-R\hat{\delta})^T & \hat{\delta}^T R \hat{\delta} - 1 \end{pmatrix} \begin{pmatrix} \delta \\ 1 \end{pmatrix}}^{\rho(\delta)} < 0 \tag{5.13}$$

which is equivalent to the statement "$\delta \in U$".

Let us now recapitulate. Computing $\max_{\delta \in U} \lambda_1(T_w(e^{j\omega}, \delta)^* T_w(e^{j\omega}, \delta))$ is equivalent to finding the smallest γ such that $\psi(\delta) < 0$ for all δ for which $\rho(\delta) < 0$. By the $\mathcal{S}$ procedure [55, 17], this problem is equivalent to finding the smallest γ and a positive scalar τ such that $\psi(\delta) - \tau\rho(\delta) < 0$, for all $\delta \in \mathbf{R}^{k \times 1}$, which is precisely (5.6). To complete this proof, note that since $\lambda_1(T_w(e^{j\omega}, \delta)^* T_w(e^{j\omega}, \delta)) = \sigma_1^2(T_w(e^{j\omega}, \delta))$, the value $\max_{\delta \in U} \sigma_1(T_w(e^{j\omega}, \delta))$ at ω is equal to $\sqrt{\gamma_{opt}}$, where γ_{opt} is the optimal value of γ. □

5.4 Simulation example

In order to illustrate the results of this chapter, let us reconsider the example presented in Section 4.4 of the previous chapter. Recall that the controller C designed from the identified model $G(\hat{\xi})$ has already been validated for stability. Indeed, we have checked that it stabilizes

all systems in the uncertainty region $\mathcal{D}_{icl}$ deduced from the validation experiment. Let us now validate this controller C for performance. Stabilization does indeed not imply good performance with all plants in $\mathcal{D}_{icl}$ (including the true system).

In order to verify that C gives satisfactory performance with all plants in $\mathcal{D}_{icl}$, we choose the sensitivity function T_{22} as performance indicator and we compute the worst case performance level $t_{\mathcal{D}_{icl}}(\omega, T_{22})$ for T_{22} at each frequency. This can be done by computing $J_{WC}(\mathcal{D}_{icl}, C, W_l, W_r, \omega)$ using Theorem 5.1 with the particular weights $W_l = W_r = diag(0,1)$. The worst case modulus of all sensitivity functions over $\mathcal{D}_{icl}$ is represented in Figure 5.1. In this figure, the worst case performance level $t_{\mathcal{D}_{icl}}(\omega, T_{22})$ is compared with the sensitivity functions of the designed closed loop $[C\ G(\hat{\xi})]$ and of the achieved closed loop $[C\ G_0]$. From $t_{\mathcal{D}_{icl}}(\omega, T_{22})$, we can find that the worst case static error $(=t_{\mathcal{D}_{icl}}(0, T_{22}))$ resulting from a constant disturbance of unit amplitude is equal to 0.1692, whereas this static error is 0.0834 in the designed closed-loop. The achieved static error is 0.1017. Using $t_{\mathcal{D}_{icl}}(\omega, T_{22})$, we can also see that the bandwidth of $\omega_c = 0.5$ in the designed closed-loop is preserved for all closed loops with a plant in $\mathcal{D}_{icl}$ since $t_{\mathcal{D}_{icl}}(\omega, T_{22})$ is equal to 1 at $\omega_c \simeq 0.5$. The difference between the resonance peak of the designed sensitivity function (i.e. $\max_\omega \parallel T_{22}(G(\hat{\xi}), C) \parallel = 1.6184$) and the worst case reasonance peak achieved by a plant in $\mathcal{D}_{icl}$ (i.e. $\max_\omega t_{\mathcal{D}_{icl}}(\omega, T_{22}) = 1.7075$) also remains small. Note that the actually achieved resonance peak (i.e. $\max_\omega \parallel T_{22}(G_0, C) \parallel$) is equal to 1.6229.

We may therefore conclude that the controller C is validated for performance since the difference between the nominal and worst case performance level remains very small at every frequency. Since the controller C has now been validated for stability and for performance, one would confidently apply the controller to the true system G_0, assuming that the nominal performance is judged to be satisfactory.

5.5 Conclusions

In this chapter, we have developed a robust performance analysis tool for the uncertainty region $\mathcal{D}$ as delivered by a PE identification procedure. Our tool is based on the computation of the worst case performance

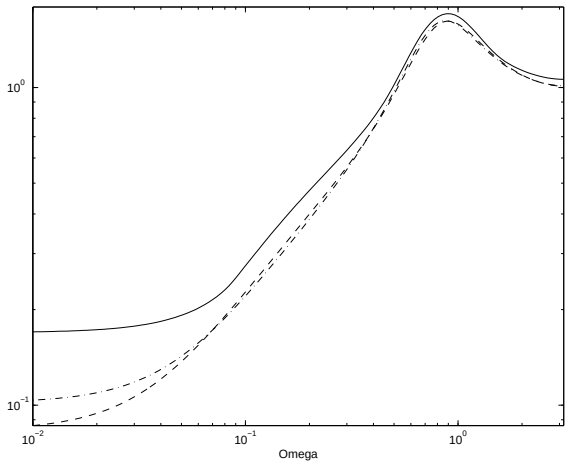

Figure 5.1: $t_{\mathcal{D}_{icl}}(\omega, T_{22})$ (solid) and modulus of the designed sensitivity function $T_{22}(G(\hat{\xi}), C)$ (dashed) and actually achieved sensitivity function $T_{22}(G_0, C)$ (dashdot)

achieved by a given controller over all plants in such uncertainty region. We have defined this worst case performance in a very general way and have shown that its computation at each frequency boils down to an LMI-based optimization problem.

This worst case performance is a lower bound for the performance achieved by the considered controller over the true system G_0 (modulo the chosen probability level for the presence of G_0 in $\mathcal{D}$).

Chapter 6

Practical simulation examples

Let us summarize what we have achieved until now. In Chapter 2, we have deduced an uncertainty set $\mathcal{D}$ containing the true system at a certain probability level from a validation experiment i.e. a classical PE identification procedure. In Chapter 3, we have introduced a robust stability measure of that uncertainty set. This measure is connected to the size of the controller set that is guaranteed by the ν-gap theory to robustly stabilize $\mathcal{D}$ and is therefore an indicator of how well the uncertainty region $\mathcal{D}$ is tuned for robust control design. In Chapter 4 and Chapter 5, we have presented a procedure to validate a controller for stability and for performance with respect to such uncertainty region $\mathcal{D}$. We have indeed given a necessary and sufficient condition for the stabilization of all plants in $\mathcal{D}$ by a given controller and we have established an optimization problem in order to compute exactly the worst case performance achieved by this controller over all plants in $\mathcal{D}$.

In this chapter, we present two illustrations of the practical use that could be made of our results. As opposed to the examples presented in the previous chapters, these are more realistic in the sense that they represent real-life systems and the methodology is applied to these systems "from the beginning to the end". The first illustration is performed on the widely publicized Landau benchmark transmission system [59]. This benchmark represents only one facet of a control application, namely a tracking problem with a step disturbance rejection objective in an essentially noise-free environment. To make our presentation complete, we

have also applied our methodology to a typical industrial process control application, in which the main objective is stochastic disturbance rejection. In the first illustration , we choose the identified model as model G_{mod} for control design. In the second illustration, the model for control design is given a-priori.

6.1 Flexible transmission system

6.1.1 Problem setting

We consider as *unknown true system* the half-load model of the flexible transmission system used as a benchmark in a special issue of the European Journal of Control: see [59].

$$\begin{aligned} G_0(z) &= z^{-3}\frac{0.10276 + 0.18123z^{-1}}{1 - 1.99185z^{-1} + 2.20265z^{-2} - 1.84083z^{-3} + 0.89413z^{-4}} \\ &\triangleq z^{-3}\frac{B_0(z)}{A_0(z)}. \end{aligned}$$

The sampling period is $0.05s$. The output of the system is subject to step disturbances filtered through $H_0(z) = \frac{1}{A_0(z)}$. This means that the plant can be seen as a nonstandard ARX system described by

$$A_0(z)y(t) = z^{-3}B_0(z)u(t) + p(t) \tag{6.1}$$

where $u(t)$ is the input of the plant, $y(t)$ its output and $p(t)$ a sequence of step disturbances with zero mean and variance σ_p^2. From a stochastic point of view, $p(t)$ is equivalent, up to second order moments, with $\frac{1}{\Delta(z)}e(t)$ where $\Delta(z) = 1 - z^{-1}$ and $e(t)$ is a sequence of Gaussian white noise with zero mean and appropriate variance. Hence, a standard ARX description of the plant is given by

$$A_0(z)\Delta(z)y(t) = z^{-3}B_0(z)\Delta(z)u(t) + e(t), \tag{6.2}$$

and the standard prediction error identification algorithm for ARX models can be used to identify the system, provided the data are prefiltered by $\Delta(z)$.

Objective. Our objective is to apply our methodology to the true flexible transmission system G_0 in order to verify that a controller C, satisfying a number of specifications with an identified model, satisfies also these specifications with the unknown G_0. These requirements are:

- stability of the loop $[C\ G_0]$
- a maximum value of less than 6 dB for the sensitivity function $T_{22}(G_0, C) = 1/(1 + G_0C)$.
- rejection of the step output disturbances $p(t)$ filtered by $1/A_0$ within 1.2s (for 90% rejection of the measured peak values).

These specifications are some of the specifications of the benchmark [59].

6.1.2 Validation experiment

Since the true system is unknown, a first step in our methodology is to perform a validation experiment on the true system G_0 in order to identify a model G_{mod} for the true system G_0 and in order to construct an uncertainty region containing the true system G_0 at a certain probability level, say 95%. We will here perform the validation experiment in closed loop using a direct approach (see Section 2.2.4.1).

In order to perform a validation in closed loop, we need to connect a controller K in feedback with G_0. The controller K is here chosen as the one obtained by Landau et al. using a combined pole placement/sensitivity function shaping method [58]. Its feedback part is described by

$$\begin{aligned} K(z) \quad = \quad & \frac{0.401602 - 1.079378z^{-1} + 0.284895z^{-2} + 1.358224z^{-3}}{1 - 1.031142z^{-1} - 0.995182z^{-2} + 0.752086z^{-3}} \\ & \frac{-0.986549z^{-4} - 0.271961z^{-5} + 0.306937z^{-6}}{+0.710744z^{-4} - 0.242297z^{-5} - 0.194209z^{-6}}. \end{aligned} \tag{6.3}$$

It also has a feedforward part that we shall not consider here (since we will excite the closed-loop system with the signal $r_2(t)$ in Figure 2.1).

The closed-loop system $[K\ G_0]$ is excited by means of a reference signal $r_2(t)$ injected at the input of G_0 (see Figure 2.1). The signal $r_2(t)$ is chosen as a PRBS with variance $\sigma_{r_2}^2 = 0.5541$, while the output step disturbances $p(t)$ are simulated as a random binary sequence with variance $\sigma_p^2 = 0.01$ and cut-off frequency at $\omega = 0.1\pi$ (normalized frequency). A realization of $r_2(t)$ and $p(t)$ are shown in Figure 6.1. The disturbance $p(t)$ is filtered by $1/A_0(z)$ and added to the output of the system. 256 data samples $y(t)$ and $u(t)$ $(t = 1...256)$ are measured, and

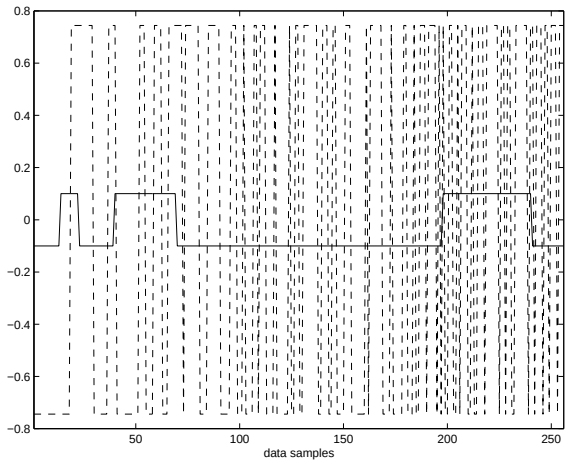

Figure 6.1: A realization of $r_2(t)$ (dashed) and $p(t)$ (solid)

a model $G(z,\hat{\delta})$ with the same ARX(4,2,3) structure as G_0 is identified after prefiltering these data by $\Delta(z)$:

$$G_{mod} = G(z,\hat{\delta}) = z^{-3}\frac{0.1016 + 0.1782z^{-1}}{1 - 1.986z^{-1} + 2.187z^{-2} - 1.824z^{-3} + 0.8897z^{-4}}. \tag{6.4}$$

This identified model G_{mod} will be used in the sequel as nominal model in order to find a controller C that satisfies the specifications presented at the end of Section 6.1.1 when C is applied to G_{mod}.

The estimated covariance matrix of the parameter vector $\hat{\delta} = \begin{pmatrix} -1.986 & 2.187 & -1.824 & 0.8897 & 0.1016 & 0.1782 \end{pmatrix}^T$ is given by:

$$P_\delta = 10^{-3}\times \begin{pmatrix} 0.0840 & -0.1166 & 0.1024 & -0.0532 & -0.0062 & -0.0027 \\ -0.1166 & 0.2145 & -0.1966 & 0.1009 & 0.0057 & 0.0008 \\ 0.1024 & -0.1966 & 0.2184 & -0.1197 & -0.0074 & -0.0041 \\ -0.0532 & 0.1009 & -0.1197 & 0.0853 & 0.0063 & 0.0037 \\ -0.0062 & 0.0057 & -0.0074 & 0.0063 & 0.0064 & 0.0021 \\ -0.0027 & 0.0008 & -0.0041 & 0.0037 & 0.0021 & 0.0061 \end{pmatrix}. \tag{6.5}$$

The 95% uncertainty region $\mathcal{D}_{cl}$ around $G_{mod} = G(z,\hat{\delta})$ can be ex-

pressed as follows:

$$\mathcal{D}_{cl} = \{G(z,\delta) \mid G(z,\delta) = \frac{Z_N \delta}{1 + Z_D \delta} \; with \; \delta \in U_{cl}\} \tag{6.6}$$

$$U_{cl} = \{\delta \in \mathbf{R}^{6\times 1} \mid (\delta - \hat{\delta})^T P_\delta^{-1} (\delta - \hat{\delta}) < 12.6\}, \tag{6.7}$$

where

$$Z_N(z) = \begin{pmatrix} 0 & 0 & 0 & 0 & z^{-3} & z^{-4} \end{pmatrix}$$
$$Z_D(z) = \begin{pmatrix} z^{-1} & z^{-2} & z^{-3} & z^{-4} & 0 & 0 \end{pmatrix}.$$

The size χ of the ellipsoid U_{cl} is here equal to 12.6 since $Pr(\chi^2(6) < 12.6) = 0.95$. This uncertainty region $\mathcal{D}_{cl}$ contains the true system[1] since we have that

$$\left(\delta_0 - \hat{\delta}\right)^T P_\delta^{-1} \left(\delta_0 - \hat{\delta}\right) = 4.7050 < 12.6$$

where $\delta_0 = \begin{pmatrix} -1.99185 & 2.20265 & -1.84083 & 0.89413 & 0.10276 & 0.18123 \end{pmatrix}^T$ denotes the parameter vector of the true system:

$$G_0 = \frac{Z_N \delta_0}{1 + Z_D \delta_0}. \tag{6.8}$$

6.1.3 Robust stability measure of $\mathcal{D}_{cl}$

The results of Chapter 3 are now used in order to verify if $\mathcal{D}_{cl}$ is stabilized by a large set of controllers stabilizing the identified model $G_{mod} = G(z,\hat{\delta})$. This can be achieved by computing the worst case ν-gap $\delta_{WC}(G_{mod}, \mathcal{D}_{cl})$ between the identified model G_{mod} and the plants in the set $\mathcal{D}_{cl}$. For this purpose, we first compute the worst case chordal distances $\kappa_{WC}(G_{mod}(e^{j\omega}), \mathcal{D}_{cl})$ at each frequency using the LMI tools developed in Section 3.3. The worst case chordal distances are represented in Figure 6.2 where they are compared with the actual chordal distances $\kappa(G_{mod}(e^{j\omega}), G_0(e^{j\omega}))$ between the identified model G_{mod} and the true system G_0.

According to Lemma 3.1, since G_{mod} is the center of $\mathcal{D}_{cl}$, we can derive the worst case ν-gap $\delta_{WC}(G_{mod}, \mathcal{D}_{cl})$ from the worst chordal distances as follows:

$$\delta_{WC}(G_{mod}, \mathcal{D}_{cl}) = \max_\omega \kappa_{WC}(G_{mod}(e^{j\omega}), \mathcal{D}_{cl}) = 0.1085.$$

[1] In practice, G_0 is unknown.

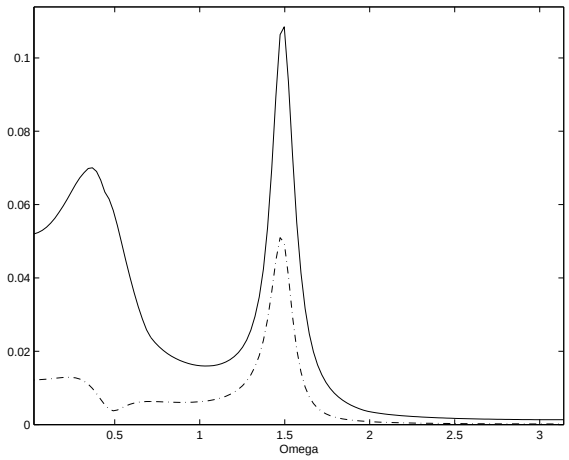

Figure 6.2: $\kappa_{WC}(G_{mod}(e^{j\omega}), \mathcal{D}_{cl})$ (solid) and $\kappa(G_{mod}(e^{j\omega}), G_0(e^{j\omega}))$ (dashdot) at each frequency

The optimal stability margin $b_{opt}(G_{mod})$ can also be computed using (3.6) and is here equal to 0.4650. We may therefore conclude that the set $\mathcal{C}(G_{mod}, \mathcal{D}_{cl})$ of G_{mod}-based controllers that are guaranteed by the ν-gap theory to robustly stabilize $\mathcal{D}_{cl}$, is relatively large. We are therefore incited to keep the pair $\{G_{mod}\ \mathcal{D}_{cl}\}$ in order to make the design of the controller C and to validate this controller for stability and for performance.

6.1.4 Control design based on G_{mod}

We will now use the identified model G_{mod} in order to find a controller C that satisfies the specifications presented at the end of Section 6.1.1 when C is applied to G_{mod}. For this purpose, we can e.g. use the robust controller for flexible transmission systems obtained by Nordin and Gutman using QFT design [67]:

$$\begin{aligned} C(z) \quad = \quad & \frac{0.0355 + 0.0181z^{-1}}{1 - z^{-1}} \times \frac{18.8379 - 43.4538z^{-1} + 26.4126z^{-2}}{1 + 0.6489z^{-1} + 0.1478z^{-2}} \\ & \times \frac{0.5626 - 0.7492z^{-1} + 0.3248z^{-2}}{1 - 1.4998z^{-1} + 0.6379z^{-2}} \times \frac{1.0461 + 0.5633z^{-2}}{1 + 0.4564z^{-1} + 0.1530z^{-2}} \\ & \times \frac{1.3571 - 1.0741z^{-1} + 0.4702z^{-2}}{1 - 0.6308z^{-1} + 0.3840z^{-2}}. \end{aligned}$$

The controller C has thus not really been designed from the identified model G_{mod}, but this controller satisfies nevertheless all specifications with the model G_{mod}.

We will now verify whether this controller satisfies these specifications with all plants in $\mathcal{D}_{cl}$ (and therefore also with the true system G_0)[2]. Let us begin by the validation of C for stability.

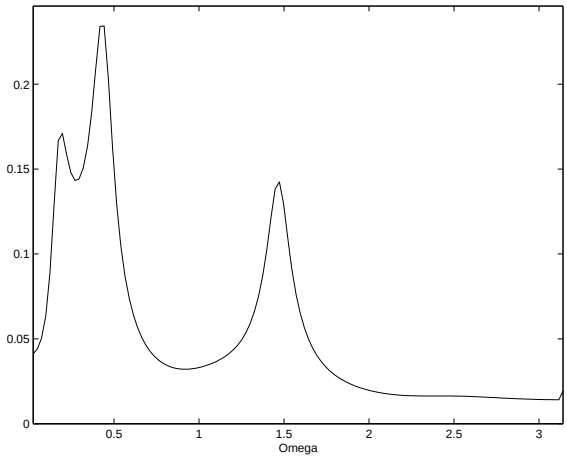

Figure 6.3: $\mu(M_{\mathcal{D}_{cl}}(e^{j\omega}))$ at each frequency

6.1.5 Controller validation for stability

Following the procedure of Chapter 4, we build the dynamic vector $M_{\mathcal{D}_{cl}}\left(e^{j\omega}\right)$ corresponding to the candidate controller C, and we compute its stability radius at each frequency according to Theorem 4.2. These stability radii are represented in Figure 6.3. The maximum value of the stability radius is

$$\max_{\omega} \mu(M_{\mathcal{D}_{cl}}(e^{j\omega})) = 0.2384$$

[2]Since we have chosen a controller C that satisfies the specification of the benchmark [59], we know that the specifications will be satisfied with G_0. However, this fact does not imply that C will satisfy these specifications with all plants in $\mathcal{D}_{cl}$, and our objective in this illustration is not to design a robust controller from G_{mod}, but to show that our methodology allows one to verify the specifications about the loop $[C\ G_0]$ using controller validation procedures based on the uncertainty set $\mathcal{D}_{cl}$.

Since this maximum value is smaller than one, we may conclude that the controller C stabilizes all plants in the uncertainty set $\mathcal{D}_{cl}$. Consequently, we can also guarantee that the "to-be-validated" controller $C(z)$ stabilizes the true flexible transmission system G_0. The first requirement presented at the end of Section 6.1.1 (i.e. the stability of the achieved loop $[C\ G_0]$) is thus satisfied.

6.1.6 Controller validation for performance

The second requirement presented at the end of Section 6.1.1 was that the designed controller should ensure *a maximum value of less than* 6 *dB for the sensitivity function.* The third requirement was that *the step disturbances* $p(t)$ *should be removed within 1.2s.* The third requirement is thus a time-domain specification. In order to may verify this last specification within our frequency domain framework, let us translate the time-domain specification into a frequency domain specification. Using the approximation of the second order system, we can assume that the rejection time of a step disturbance is inversely proportional to the cut-off frequency of the transfer function between the considered disturbance and the output of the system. In this case, this transfer function $T_{py}(G_0, C)$ is given by:

$$T_{py}(G_0, C) = \frac{1}{A_0} \times \frac{1}{1 + G_0 C} = \frac{1}{1 + (Z_D + Z_N C)\delta_0}$$

where we have used the fact that $G_0 = B_0/A_0 = (Z_N\delta_0)/(1 + Z_D\delta_0)$ (see (6.8)). Since we know that the nominal transfer function $T_{py}(G_{mod}, C)$ satisfies the specification of a rejection time of 1.2s, the third requirement can be stated as follows: *the cut-off frequency of* $T_{py}(G_0, C)$ *must be close to the cut-off frequency of* $T_{py}(G_{mod}, C)$.

Since the true system is unknown, we will verify whether the controller C achieves these requirements with all systems in $\mathcal{D}_{cl}$. For this purpose, we choose two different worst case performance criteria. The first one is the largest modulus of the sensitivity function T_{22} defined in (5.3) i.e. $t_{\mathcal{D}_{cl}}(\omega, T_{22})$. This worst case performance criterion can be computed using the LMI procedure presented in Theorem 5.1. The second worst case performance criterion $t_{\mathcal{D}_{cl}}(\omega, T_{py})$ is the largest modulus of the transfer function T_{py}:

$$t_{\mathcal{D}_{cl}}(\omega, T_{py}) = \max_{G(e^{j\omega},\delta)\in\mathcal{D}} \left| \frac{1}{1 + (Z_D(e^{j\omega}) + Z_N(e^{j\omega})C(e^{j\omega}))\delta} \right|$$

This quantity can not be computed by the LMI procedure of Theorem 5.1. However, it is easy to develop a similar LMI procedure in order to compute $t_{\mathcal{D}_{cl}}(\omega, T_{py})$ exactly. Using these worst case performance criteria, the controller C is termed validated for performance if

- $\max_\omega t_{\mathcal{D}_{cl}}(\omega, T_{22}) < 6\ dB$
- the minimal cut-off frequency of $T_{py}(G(z,\delta), C)$ for a plant $G(z,\delta)$ in $\mathcal{D}_{cl}$ that can be deduced from $t_{\mathcal{D}_{cl}}(\omega, T_{py})$, is close to the cut-off frequency of $T_{py}(G_{mod}, C)$.

Let us now compute these criteria. Figure 6.4 presents $t_{\mathcal{D}_{cl}}(\omega, T_{22})$, and compares it with the nominal sensitivity $|T_{22}(G_{mod}, C)|$ and the achieved sensitivity $|T_{22}(G_0, C)|$. Figure 6.5 does the same for the transfer function T_{py}. In Figure 6.4, we observe that

$$\max_\omega t_{\mathcal{D}_{cl}}(\omega, T_{22}) = 5\ dB < 6\ dB.$$

In Figure 6.5, we observe that the minimal cut-off frequency of $T_{py}(G(z,\delta), C)$ for a plant $G(z,\delta)$ in $\mathcal{D}_{cl}$ is equal to 0.014 ($t_{\mathcal{D}_{cl}}(\omega, T_{py}) = 0\ dB$ in $\omega = 0.014$) and that the cut-off frequency of $T_{py}(G_{mod}, C)$ is equal to 0.0153. The minimal cut-off frequency is thus very close to the cut-off frequency of $T_{py}(G_{mod}, C)$. The controller C is thus validated for performance. In other words, the controller C satisfies both performance specifications with all plants in $\mathcal{D}_{cl}$. As a consequence, the controller C is also guaranteed to achieve these performance requirements with the true flexible transmission system G_0.

With the controller validation procedures for stability and for performance, we have thus been able to prove that the controller C "designed from G_{mod}", achieves the specifications presented at the end of Section 6.1.1 with the true system G_0. Our objective is thus reached.

6.1.7 Conclusions

Let us summarize what we have achieved in this section. Our objective was to apply our methodology to the true flexible transmission system G_0 in order to verify that a controller C, satisfying a number of specifications with the identified model, satisfies also these specifications with the unknown G_0. For this purpose, we have performed a validation experiment on the true system yielding a model G_{mod} and an uncertainty

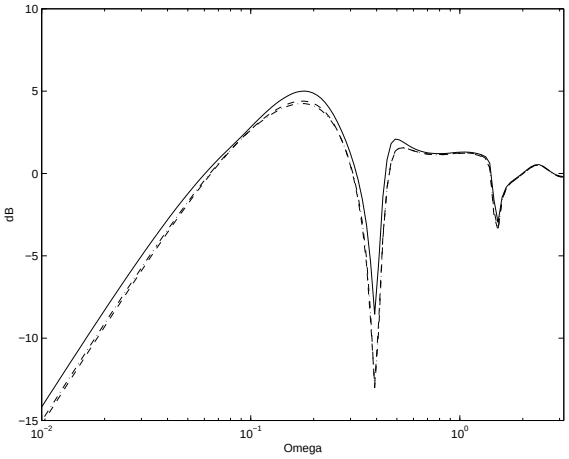

Figure 6.4: $t_{\mathcal{D}_{cl}}(\omega, T_{22})$ (solid), $|T_{22}(G_0, C)|$ (dashed), $|T_{22}(G_{mod}, C)|$ (dashdot) at each frequency

region $\mathcal{D}_{cl}$ containing the true system (with a probability of 95%). The relatively small worst case ν-gap between the model and the plants in $\mathcal{D}_{cl}$ has incited us to keep the pair $\{G_{mod}\ \mathcal{D}_{cl}\}$ in order to design a controller and to validate this controller for stability and performance. Then, a robust controller C that satisfies the performance specifications with the model G_{mod}, has been chosen. Using our controller validation procedures, we have been able to prove that the chosen controller C also achieves the desired level of performance with all plants in the uncertainty set $\mathcal{D}_{cl}$. As a consequence, the controller C can be applied to the true flexible transmission system since we are assured that the achieved performance will be satisfactory (modulo the probability level of 95% for the presence of G_0 in $\mathcal{D}_{cl}$).

6.2 Ferrosilicon production process

The first illustration was representative of a mechanical engineering control problem, in which there was no stochastic noise, and where the control objective was one of tracking and rejection of step disturbances. In order to illustrate the generality of our validation theory, we now present an application that is representative of industrial process control applications, in which the control objective is one of rejection of stochastic

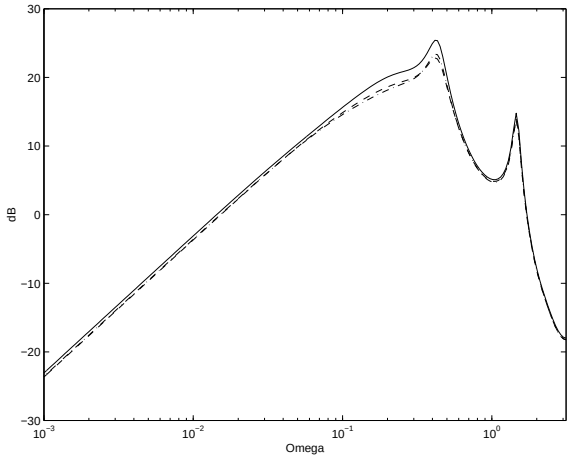

Figure 6.5: $t_{\mathcal{D}_{cl}}(\omega, T_{py})$ (solid), $|T_{py}(G_0, C)|$ (dashed), $|T_{py}(G_{mod}, C)|$ (dashdot) at each frequency

disturbances. In this second illustration, we will assume that the model G_{mod} for control design has been given a-priori.

6.2.1 Problem setting

The plant model and the controllers used in this simulation example are taken from a paper by Ingason and Jonsson [54]. Ferrosilicon is a two-phase mixture of the chemical compound $FeSi_2$ and the element silicon. The balance between silicon and iron is regulated around 76% of the total weight in silicon, 22% in iron and 2% in aluminium by adjusting the input of raw materials to the furnace. Those are charged batchwize to the top of the furnace, each batch consisting of a fixed amount of quartz (SiO_2) and a variable quantity of coal/coke (C) and iron oxyde (Fe_2O_3). The quantity of coal/coke which is burned in the furnace does not influence the silicon ratio in the mixture, hence the control input is the amount of iron oxyde.

The authors of [54] have obtained the following ARX model for the process:

$$y(t) + ay(t-1) = bu(t-1) + d + e(t) \tag{6.9}$$

where the sampling period is one day, $y(t)$ is the percentage of silicon in the mixture that must be regulated around 76%, $u(t)$ is the quantity

of iron oxyde in the raw materials (expressed in kilogrammes), d is a constant and $e(t)$ is a stochastic disturbance. The nominal values of the parameters and their standard deviations are:

$$\begin{array}{lll} a = -0.44, & b = -0.0028, & d = 46.1, \\ \sigma_a = 0.07, & \sigma_b = 0.001, & \sigma_d = 5.6. \end{array} \tag{6.10}$$

Here, for the sake of illustrating our theory, we make the assumption that the true system is

$$G_0(z) = \frac{b_0 z^{-1}}{1 + a_0 z^{-1}} = \frac{-0.0032 z^{-1}}{1 - 0.34 z^{-1}},$$

$$H_0(z) = \frac{1}{1 + a_0 z^{-1}} = \frac{1}{1 - 0.34 z^{-1}}, \qquad d_0 = 44.$$

The nominal model chosen for control design is the one obtained by Ingason and Jonsson [54]:

$$G_{mod}(z) = \frac{b z^{-1}}{1 + a z^{-1}} = \frac{-0.0028 z^{-1}}{1 - 0.44 z^{-1}},$$

$$H_{mod}(z) = \frac{1}{1 + a z^{-1}} = \frac{1}{1 - 0.44 z^{-1}}, \qquad d = 46.1,$$

This model G_{mod} was used by the authors of [54] to compute a GPC controller. The control law that minimizes the cost function

$$J_u = E\left[\sum_{j=1}^{2} \left(y(t+j) - r(t+j)\right)^2 + \sum_{j=1}^{2} \lambda \left(\Delta u(t+j-1)\right)^2\right]$$

where $\Delta(z) = 1 - z^{-1}$, is given by

$$u(t) = \begin{bmatrix} 1 & 0 \end{bmatrix} \left(H^T H + F^T \Lambda F\right)^{-1} \left(H^T \left(w(t) - v(t)\right) - F^T \Lambda g(t)\right) \tag{6.11}$$

where

$$\begin{aligned} H &= \begin{bmatrix} b & 0 \\ -ab & b \end{bmatrix}, \\ F &= \begin{bmatrix} 1 & 0 \\ -1 & 1 \end{bmatrix}, \\ v(t) &= \begin{bmatrix} -ay(t) + d \\ a^2 y(t) - ad + d \end{bmatrix}, \\ w(t) &= \begin{bmatrix} r(t) & r(t) \end{bmatrix}^T, \\ g(t) &= \begin{bmatrix} -u(t-1) & 0 \end{bmatrix}^T, \\ \Lambda &= \lambda I. \end{aligned}$$

λ is a tuning parameter. The resulting controller is a controller $C_\lambda(z)$ made up of three parts:

$$u(t) = C_\lambda(z) \begin{pmatrix} r(t) \\ -y(t) \\ 1 \end{pmatrix} = \begin{pmatrix} C_\lambda^r(z) & C_\lambda^y(z) & C_\lambda^d(z) \end{pmatrix} \begin{pmatrix} r(t) \\ -y(t) \\ 1 \end{pmatrix} \tag{6.12}$$

where

$$\begin{aligned} C_\lambda^r(z) &= \frac{b^3 + 2b\lambda - ab\lambda}{(b^4 + 3b^2\lambda + a^2b^2\lambda + \lambda^2 - 2ab^2\lambda) - (b^2\lambda + \lambda^2)z^{-1}}, \\ C_\lambda^y(z) &= -\frac{ab^3 + ab\lambda - a^2b\lambda + a^3b\lambda}{(b^4 + 3b^2\lambda + a^2b^2\lambda + \lambda^2 - 2ab^2\lambda) - (b^2\lambda + \lambda^2)z^{-1}}, \\ C_\lambda^d(z) &= -\frac{b^3 + b\lambda + b\lambda(1-a)^2}{(b^4 + 3b^2\lambda + a^2b^2\lambda + \lambda^2 - 2ab^2\lambda) - (b^2\lambda + \lambda^2)z^{-1}} d \end{aligned}$$

The part $C_\lambda^d(z)$ is the part of the controller whose objective is to reject the constant perturbation d_0 and the part $C_\lambda^y(z)$ is the only part which is important for stability analysis. The reference signal $r(t)$ is generally constant and given by $r(t) = 76$.

Objective. Our objective is to analyze the robustness properties of the GPC controller $C_\lambda(z)$ with $\lambda = 0.0007$ in order to may apply this controller to the true system G_0 *with confidence* that is to say with the assurance that the behaviour of the loop $[C_{\lambda=0.0007}\ G_0]$ will be satisfactory with respect to the following requirements i.e.

- stability of the loop $[C_{\lambda=0.0007}\ G_0]$
- rejection of the stochastic noise $v(t) = H_0 e(t)$.

The controller C achieves of course these specifications with the model G_{mod}.

6.2.2 Validation experiments

Since the true system G_0 is unknown, we need to perform a validation experiment in order to design an uncertainty region containing the true system. In fact, we will here perform two validation experiments: one in open-loop and the other one using direct closed-loop identification.

Open-loop validation experiment

The "true plant" model (G_0, H_0) was excited with $u(t)$ chosen as a PRBS with variance $\sigma^2_{u_{ol}} = 20$, which is the maximum input variance admissible for this process [54]. The noise $e(t)$ was chosen as a Gaussian white noise sequence with variance $\sigma^2_e = 0.078$, which corresponds to the noise acting on the real process as shown by experiments made by the authors of [54]. The variance of the output was then $\sigma^2_{y_{ol}} = 0.0884$. Recall that the validation experiment, i.e. the construction of an uncertainty set $\mathcal{D}_{ol}$, consists of performing a PE identification using an unbiased model structure. Therefore, 300 input-output data samples were collected, corresponding approximately to one year of measurements. These data were used to identify an ARX model with exact structure

$$G(z,\,\delta_{ol}) = \frac{\delta_2 z^{-1}}{1+\delta_1 z^{-1}}, \qquad H(z,\,\delta_{ol}) = \frac{1}{1+\delta_1 z^{-1}}. \tag{6.13}$$

We found

$$\hat{\delta}_{ol} = \begin{pmatrix} \hat{\delta}_1 \\ \hat{\delta}_2 \end{pmatrix} = \begin{pmatrix} -0.3763 \\ -0.0073 \end{pmatrix}, \quad P_{\delta_{ol}} = \begin{pmatrix} 2.8131\times 10^{-3} & -1.2784\times 10^{-5} \\ -1.2784\times 10^{-5} & 1.4887\times 10^{-5} \end{pmatrix}, \tag{6.14}$$

We then design the 95% uncertainty region $\mathcal{D}_{ol}$ around $G(z,\,\hat{\delta}_{ol})$ following the procedure of Section 2.2.2:

$$\mathcal{D}_{ol} = \{G(z,\delta) \mid G(z,\delta) = \frac{Z_N\delta}{1+Z_D\delta} \; with \; \delta \in U_{ol}\}$$

$$U_{ol} = \{\delta \in \mathbf{R}^{2\times 1} \mid (\delta-\hat{\delta}_{ol})^T P^{-1}_{\delta_{ol}} (\delta-\hat{\delta}_{ol}) < 5.99\},$$

where

$$Z_N(z) = \begin{pmatrix} 0 & z^{-1} \end{pmatrix} \quad and \quad Z_D(z) = \begin{pmatrix} z^{-1} & 0 \end{pmatrix}.$$

The size χ of the ellipsoid U_{ol} is here equal to 5.99 since $Pr(\chi^2(2) < 5.99) = 0.95$. The obtained uncertainty region $\mathcal{D}_{ol}$ contains as well the in practice unknown true system G_0 as the chosen model G_{mod}.

Closed-loop validation experiment

The closed-loop validation was performed with a sub-optimal GPC controller obtained by setting $\lambda = 0.001$ in (6.12). We added a PRBS signal to the constant reference $r(t) = 76$ such that we obtained $\sigma^2_{u_{cl}} = 20$.

The variance of $r(t)$ was then $\sigma_r^2 = 0.014$, the noise $e(t)$ having the same properties as in open-loop validation. With these settings, the output variance was $\sigma_{y_{cl}}^2 = 0.0880$. Observe that the input variance is the same as in open loop, and that the output variance is very close to that of the open-loop experiment. Again, 300 input-output data samples were collected and used to identify an ARX model with the same structure as in open-loop validation (6.13), using a direct prediction error method. We found

$$\hat{\delta}_{cl} = \begin{pmatrix} \hat{\delta}_1 \\ \hat{\delta}_2 \end{pmatrix} = \begin{pmatrix} -0.3575 \\ -0.0067 \end{pmatrix}, \quad P_{\delta_{cl}} = \begin{pmatrix} 2.8323 \times 10^{-3} & -8.7845 \times 10^{-6} \\ -8.7845 \times 10^{-6} & 6.2416 \times 10^{-6} \end{pmatrix}. \tag{6.15}$$

We then design the 95% uncertainty region $\mathcal{D}_{cl}$ around $G(z, \hat{\delta}_{cl})$ following the procedure for direct closed-loop identification of Section 2.2.4.1:

$$\mathcal{D}_{cl} = \{G(z,\delta) \mid G(z,\delta) = \frac{Z_N \delta}{1 + Z_D \delta} \; with \; \delta \in U_{cl}\}$$

$$U_{cl} = \{\delta \in \mathbf{R}^{2\times 1} \mid (\delta - \hat{\delta}_{cl})^T P_{\delta_{cl}}^{-1} (\delta - \hat{\delta}_{cl}) < 5.99\},$$

whith the same Z_N and Z_D as in $\mathcal{D}_{ol}$. As $\mathcal{D}_{ol}$, this uncertainty region $\mathcal{D}_{cl}$ contains as well the in practice unknown true system G_0 as the model G_{mod}.

6.2.3 Comparison of $\mathcal{D}_{ol}$ and $\mathcal{D}_{cl}$

The worst case ν-gap is now used to compare the two uncertainty sets deduced from the two validation experiments. For this purpose, we first compute the worst case chordal distances at each frequency for $\mathcal{D}_{ol}$ and $\mathcal{D}_{cl}$ using the LMI tools developed in Section 3.3. According to Lemma 3.1 and since G_{mod} lies in both uncertainty sets, we can derive the worst case Vinnicombe distances from the worst chordal distances as follows:

$$\delta_{WC}(G_{mod}, \mathcal{D}_{ol}) = \max_{\omega} \kappa_{WC}(G_{mod}(e^{j\omega}), \mathcal{D}_{ol}) = 0.0225$$

$$\delta_{WC}(G_{mod}, \mathcal{D}_{cl}) = \max_{\omega} \kappa_{WC}(G_{mod}(e^{j\omega}), \mathcal{D}_{cl}) = 0.0156$$

Since the optimal stability margin $b_{opt}(G_{mod})$ is equal to 0.99, the sets $\mathcal{C}(G_{mod}, \mathcal{D}_{ol})$ and $\mathcal{C}(G_{mod}, \mathcal{D}_{cl})$ of controllers stabilizing G_{mod} that are guaranteed to robustly stabilize $\mathcal{D}_{ol}$ and $\mathcal{D}_{cl}$, respectively, are relatively

large. Indeed, the worst case ν-gaps $\delta_{WC}(G_{mod}, \mathcal{D}_{ol})$ and $\delta_{WC}(G_{mod}, \mathcal{D}_{cl})$ are very small with respect to $b_{opt}(G_{mod})$. Consequently, both uncertainty sets are relatively well tuned for robustly stable controller design based on G_{mod}. We therefore decide to keep and to apply the controller validation procedures to both uncertainty sets.

6.2.4 Controller validation for stability

Sufficient test

In this illustration, we also consider the sufficient robust stability condition that can be deduced from the worst case ν-gap in order to show that this condition can be conservative with respect to the necessary and sufficient condition developed in Chapter 4.

The controller $C_{\lambda=0.0007}$ achieves a very small stability margin $b_{G_{mod}C^y_{\lambda=0.0007}}$ with G_{mod} equal to 0.0169. The controller $C_{\lambda=0.0007}$ lies thus in $\mathcal{C}(G_{mod}, \mathcal{D}_{cl})$ but not in $\mathcal{C}(G_{mod}, \mathcal{D}_{ol})$ since we have that

$$\delta_{WC}\left(G_{mod},\, \mathcal{D}_{ol}\right) > b_{G_{mod}\, C_{\lambda=0.0007}} = 0.0169 > \delta_{WC}\left(G_{mod},\, \mathcal{D}_{cl}\right). \quad (6.16)$$

Therefore, from this sufficient test, we can conclude that $C_{\lambda=0.0007}$ stabilizes all plants in the set $\mathcal{D}_{cl}$. To make an undoubted statement about the set $\mathcal{D}_{ol}$, we will need to use the necessary and sufficient test developed in Chapter 4.

Necessary and sufficient test

We first verify if $C_{\lambda=0.0007}$ stabilizes the centers of $\mathcal{D}_{ol}$ and $\mathcal{D}_{cl}$. Since it is the case, we build the dynamic vectors $M_{\mathcal{D}_{ol}}\left(e^{j\omega}\right)$ and $M_{\mathcal{D}_{cl}}\left(e^{j\omega}\right)$ corresponding to the candidate controller $C_{\lambda=0.0007}$, and we compute their stability radii according to Theorem 4.2. Their respective maximum values are

$$\max_{\omega}\ \mu\left(M_{\mathcal{D}_{ol}}\left(e^{j\omega}\right)\right) = 0.6572 < 1, \quad (6.17)$$

$$\max_{\omega}\ \mu\left(M_{\mathcal{D}_{cl}}\left(e^{j\omega}\right)\right) = 0.2111 < 1, \quad (6.18)$$

Since these two values are smaller than one, Theorem 4.2 confirms that $C_{\lambda=0.0007}$ stabilizes all systems in the uncertainty set $\mathcal{D}_{cl}$, but also shows that $C_{\lambda=0.0007}$ also stabilizes all systems in $\mathcal{D}_{ol}$. Such *quantitative* result

for a controller with a so small stability margin as $C_{\lambda=0.0007}$ confirms our first *qualitative* observation that was that both uncertainty sets are well tuned for robustly stable controller design based on G_{mod} (and this even though that qualitative observation is based on a sufficient condition that would have invalidated the particular controller $C_{\lambda=0.0007}$ when $\mathcal{D}_{ol}$ is considered (see (6.16))).

Beside these considerations, the main conclusion we can derive from these stability tests is that the "to-be-validated" controller $C_{\lambda=0.0007}$ is guaranteed to stabilize the true ferrosilicon production process G_0. Therefore, the first of the requirements presented at the end of Section 6.2.1 (i.e. the stability of the achieved loop $[C_{\lambda=0.0007}\ G_0]$) is satisfied.

6.2.5 Controller validation for performance

The second requirement presented at the end of Section 6.2.1 was to reject the noise $v(t) = H_0(z)e(t)$, which is essentially located at low frequencies ($H_0(e^{j\omega})$ is a first order low-pass filter; see Figure 6.6). A performance specification in the frequency domain is therefore that the sensitivity function $T_{22}(G_0, C^y_{\lambda=0.0007}(z)) = 1/(1 + G_0 C^y_{\lambda=0.0007}(z))$ be low at low frequencies in order to attenuate $v(t)$. We thus define the worst-case performance criterion as the largest modulus of the sensitivity function T_{22} defined in (5.3) i.e. $t_{\mathcal{D}}(\omega, T_{22})$. This worst case performance criterion can be computed using the LMI procedure presented in Theorem 5.1. We will call the controller $C_{\lambda=0.0007}(z)$ validated if $t_{\mathcal{D}}(\omega, T_{22})$ is high-pass with $\max_\omega t_{\mathcal{D}}(\omega, T_{22})$ reasonably small. The Bode diagrams of the worst-case and achieved sensitivity functions are depicted in Figure 6.6.

Clearly, the controller is validated by the closed-loop validation experiment yielding $\mathcal{D}_{cl}$ but not by the open-loop experiment yielding $\mathcal{D}_{ol}$.

The main conclusion we can derive from this performance test is that the controller $C_{\lambda=0.0007}$ will sufficiently decrease the output variance when it will be applied to G_0. We have indeed proved that, for one of the two uncertainty sets containing G_0 (i.e. $\mathcal{D}_{cl}$), the worst case modulus of the sensitivity function is a high pass filter with a reasonably small reasonance peak allowing rejection of the noise $v(t)$.

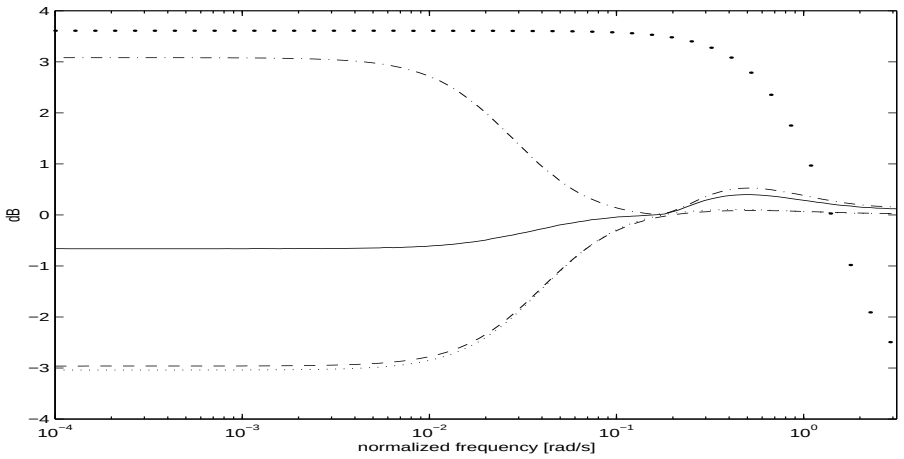

Figure 6.6: Open-loop and closed-loop controller validation for performance: $t_{\mathcal{D}_{ol}}(\omega, T_{22})$ $(-\cdot)$, $t_{\mathcal{D}_{cl}}(\omega, T_{22})$ (—), $|T_{22}(G_0, C_{\lambda=0.0007})|$ $(--)$, $|T_{22}(G_{mod}, C_{\lambda=0.0007})|$ $(\cdots)$ and $|H_0|$ $(\cdot)$

Remark. Even if $\mathcal{D}_{ol}$ is a "good" uncertainty region with respect to robustly stable controller design with G_{mod} (i.e. it has a large set of stabilizing controllers), it appears that the worst case performance achieved by $C_{\lambda=0.0007}$ with the plants in $\mathcal{D}_{ol}$ is really bad. This is a consequence of the fact that the worst case ν-gap is only an indicator of robust stability and not an indicator of robust performance.

6.2.6 Conclusions

Let us summarize what we have achieved in this second illustration. We have applied our methodology to the case of a chemical process where the control objective is the rejection of stochastic disturbances. We have chosen a model G_{mod} for the true ferrosilicon production process G_0. From the model G_{mod}, a GPC controller has been designed. We have performed validation experiments on the true system leading to two uncertainty sets containing the true system (with a probability of 95%). The results of Chapter 3 have then shown that both uncertainty sets have a large robustly stabilizing controller set. After that, using our controller validation procedures, we have been able to prove that the considered controller stabilizes and achieves sufficient performance with all plants in one of the uncertainty set. As a consequence, the

controller can be applied to the true system since we are assured that the achieved performance will be satisfactory (modulo the probability level of 95% for the presence of G_0 in the uncertainty set).

Chapter 7

Frequency domain image of a set of linearly parametrized transfer functions

In the previous chapters, we have analyzed the set $\mathcal{D}$ of parametrized transfer functions containing the true system at a certain probability level and we have given some robustness tools for such a set. In this chapter, we will do something rather different : we will analyze the image of such a set in the Nyquist plane. The description of the image of $\mathcal{D}$ in its general structure is quite complicated. Therefore, we will limit us to uncertainty sets $\mathcal{D}$ where the plants are linearly parametrized. It is to be noted that such structure will be used in the next chapter in order to extend our result to the case of biased model structures.

For model structures that are linear in the parameter vector θ, we show that the image in the Nyquist plane of a parametric confidence region $\mathcal{D}$ defined by an ellipsoid U_θ in the parameter space is a frequency domain confidence region $\mathcal{L}$ made up of ellipses $U(\omega)$ at each frequency in the Nyquist plane. The properties of the inverse image of this frequency domain confidence region in parameter space are also analyzed. We establish that the inverse image $C_\theta(U(\omega))$ of each ellipse $U(\omega)$ in the parameter space is a much larger volume than the initial ellipsoid U_θ, since the mapping between the parametric and frequency domains is not bijective. We also show that this inverse image $C_\theta(U(\omega))$ is different at

each frequency. Consequently, the inverse image of the whole frequency domain confidence region $\mathcal{L}$ is the intersection of these different volumes $C_\theta(U(\omega))$ over the whole frequency range. We show by an example that this intersection may be a strict subset of the initial ellipsoid U_θ in parameter space. The confidence region $\mathcal{L}$ in the Nyquist plane is thus generally the image of more parameter vectors θ than those in U_θ. Consequently, the probability level linked to the confidence region $\mathcal{L}$ is larger than the probability level linked to the confidence region U_θ in parameter space.

Our definition of the image of the parametric confidence region $\mathcal{D}$ in the Nyquist plane is very close to the concept of *value set* of a family of parametrized polynomials (see e.g. [4] and references therein). These value sets have been analyzed for a large amount of constraints on the parameters (e.g. polytope, sphere, ...). The general use of these value sets is to verify whether a family of polynomials is different from zero at each frequency and is therefore stable. The results presented in this chapter are nevertheless broader than those in [4]. Indeed, our results determine not only the image $\mathcal{L}$ of $\mathcal{D}$ in the Nyquist plane, but also determine the inverse image of $\mathcal{L}$ in the parameter space. Moreover, since we consider here a probabilistic framework as opposed to the deterministic framework in [4], our results give in addition the probability level linked to the image $\mathcal{L}$ of the confidence region $\mathcal{D}$ in the Nyquist plane.

Chapter outline. In Section 7.1, we present, in a very general way, the linearly parametrized systems we will consider and we define a set $\mathcal{D}$ that contains the linearly parametrized systems whose parameter vector is constrained to lie in an ellipsoid. We show in Section 7.2 that this general problem applies to the case of uncertainty sets deduced from prediction error identification. In Section 7.3, we present two theorems that describe the image of an ellipsoid by a nonbijective mapping, as well as the inverse image defined by such mapping. In Section 7.4, we present the frequency domain set $\mathcal{L}$, image of the set $\mathcal{D}$ in the Nyquist plane. In Section 7.5, we analyze the inverse image of the set $\mathcal{L}$. In Section 7.6, we define the probability level linked to $\mathcal{L}$ and give the value of this probability level. In the last sections, we give some comments about the case of model structures that are not linearly parametrized and we finish by an illustration and some conclusions.

7.1 Problem statement

As stated in the introduction, we consider linearly parametrized transfer functions. The case of nonlinearly parametrized transfer functions will be briefly discussed in Section 7.8. Let us thus consider the following system description:

$$G(z,\theta) = \bar{G}(z) + \Lambda(z)\theta \tag{7.1}$$

with $\theta \in \mathbf{R}^{k\times 1}$ the parameter vector, $\bar{G}(z)$ a known transfer function and $\Lambda(z)$ a known row vector of transfer functions. Let us further assume that θ has a Gaussian probability density function with zero mean and covariance $P_\theta \in \mathbf{R}^{k\times k}$ i.e.

$$\theta \sim \mathcal{N}(0, P_\theta) \tag{7.2}$$

We have therefore:

$$\theta^T P_\theta^{-1} \theta \sim \chi^2(k) \tag{7.3}$$

where $\chi^2(k)$ is the chi-square probability density function with k degrees of freedom.

Let us now write the frequency response $g(e^{j\omega},\theta)$ of $G(z,\theta)$ at the frequency ω in the following form:

$$\begin{aligned} g(e^{j\omega},\theta) &\triangleq \begin{pmatrix} Re(G(e^{j\omega},\theta)) \\ Im(G(e^{j\omega},\theta)) \end{pmatrix} \\ &= \overbrace{\begin{pmatrix} Re(\bar{G}(e^{j\omega})) \\ Im(\bar{G}(e^{j\omega})) \end{pmatrix}}^{\bar{g}(e^{j\omega})} + \overbrace{\begin{pmatrix} Re(\Lambda(e^{j\omega})) \\ Im(\Lambda(e^{j\omega})) \end{pmatrix}}^{T(e^{j\omega})}\theta \end{aligned} \tag{7.4}$$

The frequency response vector $g(e^{j\omega},\theta)$ has thus a Gaussian probability density function with mean $\bar{g}(e^{j\omega})$ and covariance $P_g(\omega) = cov((g(e^{j\omega},\theta)-\bar{g}(e^{j\omega}))(g(e^{j\omega},\theta)-\bar{g}(e^{j\omega}))^T) = T(e^{j\omega})P_\theta T(e^{j\omega})^T \in \mathbf{R}^{2\times 2}$. We have thus

$$\begin{gathered} g(e^{j\omega},\theta) \sim \mathcal{N}(\bar{g}(e^{j\omega}), P_g(\omega)) \\ (g(e^{j\omega},\theta) - \bar{g}(e^{j\omega}))^T P_g(\omega)^{-1} (g(e^{j\omega},\theta) - \bar{g}(e^{j\omega})) \sim \chi^2(2) \end{gathered} \tag{7.5}$$

The results presented in (7.5) are very common and can e.g. be found in [47]. However, these results do not give a response to some important

questions. If we design a confidence ellipsoid in the parameter space using (7.3), is the image of such confidence ellipsoid in the Nyquist plane a confidence region with the same probability level? How can we relate this image with the known probability density function of the frequency response (7.5)? If we design a confidence ellipse at each frequency using (7.5) and define a set by connecting all these ellipses, what is the inverse image of that set in parameter space? In order to answer these questions, we will consider throughout this paper the following confidence ellipsoid in parameter space and the corresponding region in transfer function space. We will choose a probability level of 0.95 for these confidence regions.

Definition 7.1 *Let us consider the parametrized model structure given in (7.1) and the probability density function of the parameter vector θ given in (7.2). The ellipsoid U_θ of size χ:*

$$U_\theta = \{\theta \mid \theta^T P_\theta^{-1} \theta < \chi\}, \tag{7.6}$$

with χ such that $Pr(\chi^2(k) < \chi) = 0.95$, is a confidence ellipsoid of probability 0.95 in the parameter space. We define the set $\mathcal{D}$ of transfer functions that correspond to the parameters $\theta \in U_\theta$:

$$\mathcal{D} = \{G(z,\theta) \mid \theta \in U_\theta\} \tag{7.7}$$

The probability level $\alpha(\mathcal{D})$ linked to $\mathcal{D}$ is thus given by $\alpha(\mathcal{D}) \stackrel{\Delta}{=} Pr(G(z,\theta) \in \mathcal{D}) = 0.95$.

In the next sections, we describe the image in the Nyquist plane of the uncertainty region $\mathcal{D}$ and we analyze the properties of such image, as well as its inverse image, with respect to the probability level. But beforehand, we relate the general problem presented in this section to the particular case of the uncertainty sets that can be derived from PE identification.

7.2 Link with the uncertainty set deduced from PE identification

For this purpose, let us consider the following linearly parametrized model structure.

$$\mathcal{M} = \{G(z,\delta) \mid G(z,\delta) = Z(z)\delta\}, \tag{7.8}$$

where $\delta \in \mathbf{R}^{k\times 1}$ is the parameter vector and $Z(z)$ is a transfer vector containing known transfer functions (such as Laguerre or Legendre basis functions). According to Proposition 2.2, if the true system can be described as a plant $G(z,\delta_0)$ in $\mathcal{M}$, then a PE identification procedure with the model structure $\mathcal{M}$ and N input-output data delivers an unbiased estimate $\hat{\delta}$ of the true parameter vector and an estimate P_δ of the covariance matrix C of $\hat{\delta}$. The estimate $\hat{\delta}$ can be considered as the realization of a Gaussian distribution with mean δ_0 and covariance C. In order to design confidence ellipsoids containing the true system at a certain probability level, we can then consider the following distribution:

$$(\delta - \hat{\delta})^T P_\delta^{-1} (\delta - \hat{\delta}) \sim \chi^2(k) \tag{7.9}$$

Using the last expression and the procedure described in Chapter 2, we can design an uncertainty set $\mathcal{D}_{pei}$ containing the true system $G(z,\delta_0)$ at a certain probability level, say 95 %. This uncertainty set $\mathcal{D}_{pei}$ has the following structure:

$$\mathcal{D}_{pei} = \{G(z,\delta) \mid G(z,\delta) = Z(z)\delta \ with \ \delta \in U_{pei}\} \tag{7.10}$$

$$U_{pei} = \{\delta \mid (\delta - \hat{\delta})^T P_\delta^{-1} (\delta - \hat{\delta}) < \chi\}, \tag{7.11}$$

where χ is such that $Pr(\chi^2(k) < \chi) = 0.95$. The uncertainty set $\mathcal{D}_{pei}$ can be rewritten in the formalism of Section 7.1. Indeed, let us denote $\theta \stackrel{\Delta}{=} \delta - \hat{\delta}$, $\bar{G} \stackrel{\Delta}{=} Z(z)\hat{\delta}$ and $P_\theta \stackrel{\Delta}{=} P_\delta$. Then, (7.10) and (7.11) are, respectively, equivalent with:

$$\mathcal{D}_{pei} = \{G(z,\theta) \mid G(z,\theta) = \bar{G}(z) + Z(z)\theta \ with \ \theta \in U_{pei}\}$$

$$U_{pei} = \{\theta \mid \theta^T P_\theta^{-1} \theta < \chi\},$$

By comparing these last expressions with (7.7) and (7.6), we see that the problem of finding the image in the Nyquist plane of the uncertainty set $\mathcal{D}_{pei}$ deduced from PE identification and containing the true system with probability 95 %, in the case where that true system is linearly parametrized, can be solved by solving the general problem presented in the previous section.

7.3 Linear algebra preliminaries

The general problem presented in Section 7.1 consists of finding (and of analysing) the image in the Nyquist plane of the set of plants $\mathcal{D}$ defined

in (7.7). We first present two theorems that describe properties of a mapping T between a real vector y and another real vector x of lower dimension. This mapping has the following expression

$$x = Ty \tag{7.12}$$

where $y \in \mathbf{R}^{k\times 1}$, $x \in \mathbf{R}^{n\times 1}$ $(n < k)$ are real vectors, and $T \in \mathbf{R}^{n\times k}$ is a real matrix of rank n.

Let us first recall a well-known lemma that will be useful to prove the first theorem.

Lemma 7.1 *Let us consider the partitioned symmetric positive definite matrix* $P \in \mathbf{R}^{k\times k}$*:*

$$P = \begin{pmatrix} P_{11} & P_{12} \\ P_{12}^T & P_{22} \end{pmatrix}$$

with $P_{11} \in \mathbf{R}^{n\times n}$*,* $P_{12} \in \mathbf{R}^{n\times(k-n)}$ *and* $P_{22} \in \mathbf{R}^{(k-n)\times(k-n)}$*. Let us also consider two real vectors* $x \in \mathbf{R}^{n\times 1}$ *and* $\bar{x} \in \mathbf{R}^{(k-n)\times 1}$ *and an ellipsoid* $U_{x\bar{x}}$ *defined as:*

$$U_{x\bar{x}} = \left\{ \begin{pmatrix} x \\ \bar{x} \end{pmatrix} \mid \begin{pmatrix} x \\ \bar{x} \end{pmatrix}^T P^{-1} \begin{pmatrix} x \\ \bar{x} \end{pmatrix} < 1 \right\}.$$

Then the set U_x

$$U_x \stackrel{\Delta}{=} \{x \mid \begin{pmatrix} x \\ \bar{x} \end{pmatrix} \in U_{x\bar{x}}\} \tag{7.13}$$

is also an ellipsoid given by

$$U_x = \{x \mid x^T P_{11}^{-1} x < 1\} \tag{7.14}$$

Proof. see Appendix A.1. □

Note that U_x is not the intersection of $U_{x\bar{x}}$ with the subspace $\bar{x} = 0$; it is a larger set. Let us now present our two theorems about the mapping T defined in (7.12).

Theorem 7.1 *Let us consider the mapping* T *defined in (7.12) and the ellipsoid* U_y *of size* χ *in the y-space:*

$$U_y = \{y \mid y^T P_y^{-1} y < \chi\}, \tag{7.15}$$

with $P_y \in \mathbf{R}^{k\times k}$ a positive definite matrix. The image U_x of U_y by the mapping T i.e. $U_x \stackrel{\Delta}{=} \{x \mid x = Ty \text{ with } y \in U_y\}$ is an ellipsoid in the x-space given by

$$U_x = \{x \mid x^T P_x^{-1} x < \chi\}, \tag{7.16}$$

with $P_x = TP_yT^T \in \mathbf{R}^{n\times n}$.

Proof. Let us first complete the mapping T by generating a nonsingular mapping $\widetilde{T}$:

$$\begin{pmatrix} x \\ \bar{x} \end{pmatrix} = \overbrace{\begin{pmatrix} T \\ \overline{T} \end{pmatrix}}^{\tilde{T}} y \tag{7.17}$$

such that $\tilde{T} \in \mathbf{R}^{k\times k}$ has rank k. Using $\widetilde{T}$, we have that

$$y^T P_y^{-1} y < \chi \Longleftrightarrow \begin{pmatrix} x \\ \bar{x} \end{pmatrix}^T \overbrace{\widetilde{T}^{-T} P_y^{-1} \widetilde{T}^{-1}}^{P^{-1}} \begin{pmatrix} x \\ \bar{x} \end{pmatrix} < \chi \tag{7.18}$$

Proving Theorem 7.1 is thus equivalent to proving that (7.16) is the domain where x is constrained to lie when (7.18) holds. This follows immediately from Lemma 7.1, noting that if $P = \widetilde{T} P_y \widetilde{T}^T$, then $P_x = P_{11} = TP_yT^T$. □

Theorem 7.2 *Let us consider the mapping T and the ellipsoids U_y and U_x defined in (7.12), (7.15) and (7.16), respectively. Define the inverse image C_y of U_x using the mapping T as*

$$C_y \stackrel{\Delta}{=} \{y \mid x = Ty \in U_x\}, \tag{7.19}$$

Then C_y is a volume given by

$$C_y = \{y \mid y^T R_C y < \chi\}, \tag{7.20}$$

with $R_C = T^T P_x^{-1} T$, a singular matrix $\in \mathbf{R}^{k\times k}$. Moreover, the volume C_y has the following properties:

- *The matrix R_C defining C_y has rank n i.e. it has $k - n$ zero eigenvalues. The volume C_y has therefore $k - n$ infinite main axes. The directions y_i ($i = 1...k - n$) of these infinite main axes are the eigenvectors corresponding to the null eigenvalues of R_C. Moreover, these eigenvectors y_i belong to the null space of T i.e. $Ty_i = 0$.*

- *The ellipsoid U_y is included in C_y.*

Proof. See Appendix A.2. □

Comments.

- Since the matrix T has rank $n < k$, the mapping (7.12) is not bijective. This explains the fact that the image of U_y by the mapping (7.12) is exactly U_x and that the inverse image of U_x is a larger volume C_y containing U_y.
- In the particular case where $k = 3$ and $n = 2$, U_x is then an ellipse (Theorem 7.1) and C_y is a cylinder with infinite axis. The axis of the cylinder is in the direction of the eigenvector corresponding to the single null eigenvalue (Theorem 7.2).

7.4 Image of $\mathcal{D}$ in the Nyquist plane

Theorem 7.1 tells us that the image of an ellipsoid by a linear mapping into a smaller dimensional space is also an ellipsoid. This theorem will now be used in order to find the frequency domain region (or dynamic region) that is the image of $\mathcal{D}$ in the Nyquist plane. This frequency domain region is defined via a constraint on the frequency response of the plants in this region at every frequency. The general expression of a frequency domain region can e.g. be written as follows:

$$\mathcal{L} = \{G(z) \mid g(e^{j\omega}) \in U(\omega)\ \forall\omega\}, \tag{7.21}$$

where $g(e^{j\omega}) = \begin{pmatrix} Re(G(e^{j\omega})) & Im(G(e^{j\omega})) \end{pmatrix}^T$ and $U(\omega)$ is the particular domain where the frequency response vector of the plants $G(z) \in \mathcal{L}$ is constrained to lie at the frequency ω.

We are thus looking for the frequency domain region $\mathcal{L}$ that corresponds to the image of the set $\mathcal{D}$ in the Nyquist plane. Let us first define this notion properly.

Definition 7.2 (image of $\mathcal{D}$ in the Nyquist plane) *Consider the set $\mathcal{D}$ of transfer functions defined in (7.7) and the general expression of a frequency domain region $\mathcal{L}$ given in (7.21). The image of $\mathcal{D}$ in the Nyquist plane is the frequency domain region $\mathcal{L}$ defined by (7.21) with $U(\omega)$ defined as follows, at each frequency ω:*

$$U(\omega) = \{g(e^{j\omega}) \mid g(e^{j\omega}) = g(e^{j\omega}, \theta) \ for \ some \ \theta \in U_\theta\} \qquad (7.22)$$

with $g(e^{j\omega}, \theta)$ *defined in (7.4).*

Important comments. Definition 7.2 tells us

- that the image $\mathcal{L}$ of $\mathcal{D}$ in the Nyquist plane is a set containing the image of all plants in $\mathcal{D}$;
- that all "points $g(e^{j\omega}) \in U(\omega)$" at a frequency ω are the image of some plant in $\mathcal{D}$.

However, if we randomly select frequency functions $f(e^{j\omega}) \in \mathcal{L}$, for $\omega \in [0 \ \pi]$, then most of such functions will not be in $\mathcal{D}$, i.e. for most of such functions $f(e^{j\omega}) \in \mathcal{L}$, there will not exist a θ such that $f(e^{j\omega}) = g(e^{j\omega}, \theta)$ $\forall\omega$ with $g(e^{j\omega}, \theta)$ defined by (7.4).

Using the mapping (7.4) between the space of parametrized transfer functions $G(z, \theta)$ (or parameter space) and the frequency domain space, and the results of Theorem 7.1, we can construct an explicit expression of the image $\mathcal{L}$ of $\mathcal{D}$ in the Nyquist plane.

Theorem 7.3 *Consider the set* $\mathcal{D}$ *of transfer functions* $G(z, \theta) = \bar{G}(z) + \Lambda(z)\theta$ *presented in Definition 7.1, and the mapping (7.4) between parameter space and frequency domain space. The image of* $\mathcal{D}$ *in the Nyquist plane (see Definition 7.2) is a frequency domain region* $\mathcal{L}$ *having the following expression.*

$$\mathcal{L} = \{G(z) \mid g(e^{j\omega}) \in U(\omega) \ \forall\omega\} \qquad (7.23)$$

$$U(\omega) = \{g \in \mathbf{R}^{2\times 1} \mid (g - \bar{g}(e^{j\omega}))^T P(\omega)^{-1} (g - \bar{g}(e^{j\omega})) < \chi\} \qquad (7.24)$$

with $P(\omega) = T(e^{j\omega}) P_\theta T(e^{j\omega})^T$,

$$g(e^{j\omega}) = \begin{pmatrix} Re(G(e^{j\omega})) \\ Im(G(e^{j\omega})) \end{pmatrix} \quad and \quad \bar{g}(e^{j\omega}) = \begin{pmatrix} Re(\bar{G}(e^{j\omega})) \\ Im(\bar{G}(e^{j\omega})) \end{pmatrix} .$$

The image $\mathcal{L}$ *of* $\mathcal{D}$ *in the Nyquist plane is thus made up of ellipses* $U(\omega)$ *at each frequency around the frequency response of the known transfer function* $\bar{G}(z)$. *The ellipse* $U(\omega)$ *at a particular frequency can therefore be considered as the image of* $\mathcal{D}$ *in the Nyquist plane at this frequency.*

Proof. In order to establish the proof of Theorem 7.3, we need to prove that the expression (7.24) of $U(\omega)$ is equivalent with (7.22). The result follows directly from Theorem 7.1 by considering the mapping (7.4) (i.e. $g(e^{j\omega},\theta) - \bar{g}(e^{j\omega}) = T(e^{j\omega})\theta$) at a particular frequency ω. □

Remarks. It is to be noted that the matrix $P(\omega)$ defining $U(\omega)$ is equal to the covariance matrix $P_g(\omega)$ of $g(e^{j\omega},\theta)$ (see (7.5)). It is also to be noted that, at the frequencies $\omega = 0$ and $\omega = \pi$, the ellipse $U(\omega)$ degenerates into a line segment. The matrix $P(\omega)$ is no longer nonsingular. However, because $Im(G(e^{j\omega})) = 0$ at $\omega = 0$ and $\omega = \pi$, one only need the first entry of $P(\omega)$ to be nonzero.

7.5 Inverse image of $\mathcal{L}$

In the previous section, we have determined the frequency domain region $\mathcal{L}$, image of the set $\mathcal{D}$ of parametrized transfer functions $G(z,\theta)$. This set $\mathcal{L}$, made up of ellipses $U(\omega)$ at each frequency, is defined by the property (7.22). In particular, $\mathcal{L}$ contains all plants in $\mathcal{D}$. The set $\mathcal{L}$ is nevertheless not equivalent to $\mathcal{D}$. Indeed, we prove that there are more plants in $\mathcal{L}$ than those in $\mathcal{D}$. These additional plants obviously include plants having a structure different from $G(z,\theta)$ (i.e. they cannot be described as $G(z,\theta)$ for any θ (see (7.1))), but surprisingly, also include plants having the structure $G(z,\theta)$ but for $\theta \notin U_\theta$.

In this chapter, we will focus on the additional plants in $\mathcal{L}$ having the structure $G(z,\theta)$ given in (7.1) but for $\theta \notin U_\theta$. The fact that such additional plants exist in $\mathcal{L}$ is a consequence of the fact that the mapping (7.4) is not bijective[1] since (7.4) maps a k-dimensional space into the 2-dimensional frequency domain space. In order to establish that additional plants $G(z,\theta)$ lie in $\mathcal{L}$, the inverse image of $\mathcal{L}$ in the space of parametrized transfer functions $G(z,\theta)$ has to be determined. For this purpose, it is useful to first analyze the inverse image $\mathcal{D}(U(\omega))$, via the mapping (7.4), of one ellipse $U(\omega)$ of $\mathcal{L}$ in the space of parametrized transfer functions $G(z,\theta)$.

Proposition 7.1 *Consider a particular frequency ω and the ellipse $U(\omega)$ defined in (7.24) which is the image of the set $\mathcal{D}$ in the Nyquist plane at*

[1] The mapping $T(e^{j\omega})$ is only bijective if the size k of the vector θ is equal to two.

the frequency ω. Using the mapping (7.4) from θ to $g(e^{j\omega}, \theta)$, define the inverse image of $U(\omega)$ in the parameter space as

$$C_\theta(U(\omega)) = \{\theta \mid g(e^{j\omega}, \theta) \in U(\omega)\}. \tag{7.25}$$

Correspondingly, define the inverse image of $U(\omega)$ in the space of parametrized transfer functions $G(z, \theta)$ as

$$\mathcal{D}(U(\omega)) = \{G(z, \theta) \mid g(e^{j\omega}, \theta) \in U(\omega)\}. \tag{7.26}$$

Then the set $C_\theta(U(\omega))$ is a volume in the θ-space with $k-2$ infinite axes defined as:

$$C_\theta(U(\omega)) = \{\theta \in \mathbf{R}^{k\times 1} \mid \theta^T T(e^{j\omega})^T P(\omega)^{-1} T(e^{j\omega})\theta < \chi\}. \tag{7.27}$$

Moreover, $U_\theta \subset C_\theta(U(\omega))$ and $\mathcal{D} \subset \mathcal{D}(U(\omega))$.

Proof. The expression (7.27) of $C_\theta(U(\omega))$ follows directly from Theorem 7.2 by substituting $U(\omega)$ for U_x, U_θ for U_y and $C_\theta(U(\omega))$ for C_y. It then follows from the last part of Theorem 7.2 that U_θ is a subset of $C_\theta(U(\omega))$. Now observe from (7.25) and (7.26) that $\mathcal{D}(U(\omega))$ can equivalently be described as

$$\mathcal{D}(U(\omega)) = \{G(z, \theta) \mid \theta \in C_\theta(U(\omega))\} \tag{7.28}$$

It then follows from $U_\theta \subset C_\theta(U(\omega))$ and the definitions (7.7) and (7.28) that $\mathcal{D} \subset \mathcal{D}(U(\omega))$. □

Proposition 7.1 tells us that the ellipse $U(\omega)$ is the image of more plants $G(z, \theta)$ than those in $\mathcal{D}$. These additional plants $G(z, \theta_{out})$ with $\theta_{out} \in C_\theta(U(\omega)) \setminus U_\theta$, have the property that $\exists\ \theta_{in} \in U_\theta$ such that, *at frequency* ω,

$$g(e^{j\omega}, \theta_{out}) = g(e^{j\omega}, \theta_{in}),$$

since $U(\omega)$ is defined by (7.22).

It is also important to note that the inverse image $\mathcal{D}(U(\omega))$ of $U(\omega)$ in the space of parametrized transfer functions $G(z, \theta)$ is different at each frequency, because the inverse image $C_\theta(U(\omega))$ in parameter space is different at each frequency. In other words, $U(\omega)$ is the image of a set $\mathcal{D}(U(\omega))$ of plants $G(z, \theta)$ that are different at each frequency.

In Proposition 7.1, we have computed the inverse image $C_\theta(U(\omega))$ in parameter space of one ellipse $U(\omega)$, via the inverse of mapping (7.4). We now determine the inverse image $U_\theta(\mathcal{L})$ in parameter space of the whole set $\mathcal{L}$ defined by (7.23) and (7.24).

Theorem 7.4 *Consider the frequency domain set $\mathcal{L}$ defined by (7.23) and (7.24). Define the inverse image $U_\theta(\mathcal{L})$ of $\mathcal{L}$ in parameter space, via the mapping (7.4), as:*

$$U_\theta(\mathcal{L}) = \{\theta \mid G(z,\theta) \in \mathcal{L}\}. \tag{7.29}$$

Then

$$U_\theta(\mathcal{L}) = \bigcap_{\omega \in [0 \ \ \pi]} C_\theta(U(\omega)), \tag{7.30}$$

where $C_\theta(U(\omega))$ is defined in (7.25) and (7.27). Moreover,

$$U_\theta \subseteq U_\theta(\mathcal{L}). \tag{7.31}$$

Proof. First observe that, by the definition of $\mathcal{L}$ in (7.23), the set $U_\theta(\mathcal{L})$ defined in (7.29) is equivalent with

$$U_\theta(\mathcal{L}) = \{\theta \mid g(e^{j\omega},\theta) \in U(\omega) \ \forall\omega\}.$$

The result (7.30) then follows immediately from Definition (7.25). The inclusion (7.31) then follows from the main result of Proposition 7.1, namely $U_\theta \subset C_\theta(U(\omega)) \ \forall\omega$. □

Corollary 7.1 *Consider the frequency domain set $\mathcal{L}$ defined by (7.23) and (7.24). Define the inverse image $\mathcal{D}(\mathcal{L})$ of $\mathcal{L}$ in the space of parametrized transfer functions $G(z,\theta)$, via the mapping (7.4), as*

$$\mathcal{D}(\mathcal{L}) = \{G(z,\theta) \mid G(z,\theta) \in \mathcal{L}\}. \tag{7.32}$$

Then $\mathcal{D} \subseteq \mathcal{D}(\mathcal{L})$.

Proof. By (7.32) and (7.29), it follows that

$$\mathcal{D}(\mathcal{L}) = \{G(z,\theta) \mid \theta \in U_\theta(\mathcal{L})\}. \tag{7.33}$$

The result then follows from the result (7.31) of Theorem 7.4, and the definition (7.7) of $\mathcal{D}$. □

Corollary 7.2 *With definitions as above, we have:*

$$U_\theta \subseteq U_\theta(\mathcal{L}) \subset C_\theta(U(\omega)) \ \forall\omega \tag{7.34}$$

$$\mathcal{D} \subseteq \mathcal{D}(\mathcal{L}) \subset \mathcal{D}(U(\omega)) \ \forall\omega. \tag{7.35}$$

Proof. The first inclusions follow from Theorem 7.4 and Corollary 7.1. The second inclusion in (7.34) follows from (7.30), and the second inclusion of (7.35) from (7.33), (7.28) and (7.34). □

Theorem 7.4 tells that the ellipsoid U_θ which defines $\mathcal{D}$ is a subset of $U_\theta(\mathcal{L}) = \bigcap_{\omega\in[0\ \pi]} C_\theta(U(\omega))$. We shall illustrate by an example in Section 8 that it may be a strictly proper subset of $U_\theta(\mathcal{L})$. As a consequence, $\mathcal{D}$ may be a strictly proper subset of $\mathcal{D}(\mathcal{L})$, and the frequency domain region $\mathcal{L}$ is therefore the image in the Nyquist plane of a set $\mathcal{D}(\mathcal{L})$ containing more plants $G(z,\theta)$ than those in $\mathcal{D}$. It is to be noted that, according to the definition of $\mathcal{L}$ (Definition 7.2), these additional plants $G(z,\theta_{out})$ with $\theta_{out} \in U_\theta(\mathcal{L}) \setminus U_\theta$, must have the property that, at each frequency ω, there exists θ_{in} in U_θ such that $G(e^{j\omega},\theta_{out}) = G(e^{j\omega},\theta_{in})$. Note that it is not possible to have a single value of θ_{in} which applies at all frequencies.

7.6 Probability level linked to the confidence region $\mathcal{L}$

In the previous sections, we have shown that the image of a set $\mathcal{D}$ in the Nyquist plane is a frequency domain region $\mathcal{L}$ made up of ellipses $U(\omega)$ at each frequency. We have also shown that the sets $U(\omega)$ and the whole region $\mathcal{L}$ are (or may be) the image of more plants $G(z,\theta)$ than those in $\mathcal{D}$. Let us now consider both sets (i.e. $U(\omega)$ and $\mathcal{L}$) as confidence regions. The ellipse $U(\omega)$ is a confidence region for the frequency response vector $g(e^{j\omega},\theta)$ of the plants $G(z,\theta)$ and the set $\mathcal{L}$ is a confidence region for the plants $G(z,\theta)$. Since the parameter vector θ has a probability density function (see (7.2)), we can relate a probability level to both confidence regions.

Definition 7.3 *Consider the parametrized transfer functions $G(z,\theta)$ given in (7.1), whose parameter vector θ has the probability density function (7.2). Consider also the sets $U(\omega)$ and $\mathcal{L}$ defined in (7.23)-(7.24).*

The probability level $\alpha(U(\omega))$ linked to $U(\omega)$ is defined as :

$$\alpha(U(\omega)) = Pr(g(e^{j\omega}, \theta) \in U(\omega)),$$

where $g(e^{j\omega}, \theta)$ is defined in (7.4). The probability level $\alpha(\mathcal{L})$ linked to $\mathcal{L}$ is defined as:

$$\alpha(\mathcal{L}) = Pr(G(z, \theta) \in \mathcal{L}).$$

These probability levels $\alpha(U(\omega))$ and $\alpha(\mathcal{L})$ will be larger than the probability level $\alpha(\mathcal{D})$ linked to $\mathcal{D}$ (i.e. $\alpha(\mathcal{D}) = 0.95$) since $\mathcal{D} \subseteq \mathcal{D}(\mathcal{L}) \subset \mathcal{D}(U(\omega))\ \forall\omega$ (see Corollary 7.2). Theorem 7.5 gives an exact computation of $\alpha(U(\omega))$, as well as upper and lower bounds for $\alpha(\mathcal{L})$.

Theorem 7.5 *Consider the parametrized transfer functions $G(z, \theta)$ given in (7.1), whose parameter vector θ has the probability density function (7.2). Consider also the sets $U(\omega)$ and $\mathcal{L}$ defined in (7.23)-(7.24). Then the probability level $\alpha(U(\omega))$ linked to $U(\omega)$ (see Definition 7.3) is given by:*

$$\begin{aligned} \alpha(U(\omega)) &= Pr(G(z, \theta) \in \mathcal{D}(U(\omega))) && (7.36) \\ &= Pr(\chi^2(2) < \chi)\ \forall\omega, && (7.37) \end{aligned}$$

where $\mathcal{D}(U(\omega))$ is defined in (7.26). The probability level $\alpha(\mathcal{L})$ linked to $\mathcal{L}$ (see Definition 7.3) is bounded by:

$$\alpha(\mathcal{D}) \leq \alpha(\mathcal{L}) < \alpha(U(\omega)) \qquad (7.38)$$

where $\alpha(\mathcal{D})$ is the probability level linked to the set $\mathcal{D}$ presented in Definition 7.1 and of which the set $\mathcal{L}$ is the image in the Nyquist plane ($\alpha(\mathcal{D}) = 0.95$).

Proof. That $\alpha(U(\omega))$ is equal to $Pr(G(z, \theta) \in \mathcal{D}(U(\omega)))$ follows from Proposition 7.1. That $\alpha(U(\omega))$ is also equal to (7.37) is a direct consequence of the probability density function of $g(e^{j\omega}, \theta)$ given in (7.5) since the covariance matrix $P_g(\omega)$ of $g(e^{j\omega}, \theta)$ is equal to the matrix $P(\omega)$ defining the ellipse $U(\omega)$.

Since the inverse image of $\mathcal{L}$ in the space of parametrized transfer functions $G(z, \theta)$ is $\mathcal{D}(\mathcal{L})$, we can write the following about the probability level $\alpha(\mathcal{L})$ linked to $\mathcal{L}$:

$$\alpha(\mathcal{L}) = Pr(G(z, \theta) \in \mathcal{D}(\mathcal{L})).$$

The upper bound in (7.38) proceeds then from the fact that $\mathcal{D}(\mathcal{L}) \subset \mathcal{D}(U(\omega))\ \forall\omega$ and the lower bound from the fact that $\mathcal{D} \subseteq \mathcal{D}(\mathcal{L})$ (see Theorem 7.4). □

Important comments. Theorem 7.5 shows that the probability level $\alpha(\mathcal{L})$ linked to the image of $\mathcal{D}$ in the Nyquist plane is larger than the probability level linked to $\mathcal{D}$ (i.e. $\alpha(\mathcal{D}) = 0.95$). This is a consequence of the fact that $\mathcal{L}$ is the image of more plants than those in $\mathcal{D}$ because of the singularity of the mapping (7.4).

It is also interesting to note that if we consider the ellipses $U(\omega)$ frequency by frequency, these ellipses are the image in the Nyquist plane of a set $\mathcal{D}(U(\omega))$, different at each frequency, and having a probability level $\alpha(U(\omega))$ which follows from the probability density function (7.5) of $g(e^{j\omega}, \theta)$. However, since the sets $\mathcal{D}(U(\omega))$ are different at each frequency, when we collect together all ellipses $U(\omega)$ to make up $\mathcal{L}$, the probability level $\alpha(\mathcal{L})$ is smaller than $\alpha(U(\omega))$. This last remark shows that the probablility density function of $g(e^{j\omega}, \theta)$ given in (7.5) is only relevant for one particular frequency. Theorem 7.5 shows therefore that, in order to design a confidence region $\mathcal{L}$ with a probability level $\alpha(\mathcal{L})$ larger than 95%, one has to first design a confidence region $\mathcal{D}$ having the desired probability level (i.e. $\alpha(\mathcal{D}) = 0.95$) and then take its image $\mathcal{L}$ in the Nyquist plane.

Remarks. The plants having another structure than $G(z, \theta)$ and that lie in $\mathcal{L}$ do not modify the probability level $\alpha(\mathcal{L})$ since only the parameter vector θ has a probability density function.

7.7 Summary and consequences for the uncertainty region deduced from PE identification

In the previous section, we have considered the set $\mathcal{D}$ of linearly parametrized transfer functions $G(z, \theta)$ that is constructed from a 95% confidence ellipsoid U_θ in parameter space. We have shown that the image $\mathcal{L}$ of this set $\mathcal{D}$ is a frequency domain region $\mathcal{L}$ made up of ellipses at each frequency. We have also shown that the inverse image of $\mathcal{L}$ in the space of parametrized transfer functions $G(z, \theta)$ is a set $\mathcal{D}(\mathcal{L})$ larger than the set $\mathcal{D}$ because of the singularity of the mapping between parameter space

and frequency domain space. If we consider the set $\mathcal{L}$ as a confidence region for the plants $G(z,\theta)$, the probability level $\alpha(\mathcal{L})$ linked to $\mathcal{L}$ is thus larger than the probability level $\alpha(\mathcal{D})$ linked to $\mathcal{D}$ (i.e. $\alpha(\mathcal{D}) = 0.95$).

These results can apply to the case of the uncertainty region $\mathcal{D}_{pei}$ containing the (linearly parametrized) true system G_0 at a probability level of 0.95. This set has been introduced in Section 7.2. Indeed, the set $\mathcal{D}_{pei}$ has the same structure as the set $\mathcal{D}$ presented in Definition 7.1. Therefore, we can construct the image $\mathcal{L}_{pei}$ of $\mathcal{D}_{pei}$ in the Nyquist plane using Theorem 7.3. If we consider then the set $\mathcal{L}_{pei}$ as an uncertainty region for the true system G_0, Theorem 7.5 shows that the probability level of the presence of the true system G_0 in the frequency domain uncertainty region $\mathcal{L}_{pei}$ is larger than 0.95.

7.8 Case of not linearly parametrized model structures

Until now, we have treated the case of systems $G(z,\theta)$ that can be written as in (7.1) and whose parameters have the probability density function (7.2). We have shown for this type of model structure the link between a set $\mathcal{D}$ of transfer functions $G(z,\theta)$ and its image $\mathcal{L}$ in the Nyquist plane. If the model structure is not linearly parametrized as in (7.1), our conclusions do not hold i.e. the image at a frequency ω is not guaranteed to be an ellipse. In [62, 43, 10], a first order approximation was used to map the parametric confidence ellipsoid into ellipses in the Nyquist plane. However, using such an approach, no probablity level can be guaranteed for the obtained frequency domain region.

As a consequence, it is very difficult to have a clear idea of the image in the Nyquist plane of a set $\mathcal{D}_{gen}$ of rational transfer functions with parameters appearing in both numerator and denominator like the set defined in (2.44). Some partial results have been presented in [20, 40]. In [20], the authors have presented a way to compute, at each frequency, the largest and the smallest modulus and phase of the plants in a region $\mathcal{D}_{gen}$. In [40], we have given an LMI procedure that computes at each frequency the smallest overbounding ellipse that contains the frequency response of the plants in such set $\mathcal{D}_{gen}$.

7.9 Simulation example

In order to illustrate the results of this chapter, we present the following example. Let us consider the following system description:

$$\begin{aligned} G(z,\theta) &= \frac{0.08z^{-1}+0.1009z^{-2}+0.0359z^{-3}}{1-1.5578z^{-1}+0.5769z^{-2}} + \frac{\theta_1 z^{-1}+\theta_2 z^{-2}+\theta_3 z^{-3}}{1-1.5578z^{-1}+0.5769z^{-2}} \\ &= \bar{G}(z) + \overbrace{\frac{1}{1-1.5578z^{-1}+0.5769z^{-2}} \times \begin{pmatrix} z^{-1} & z^{-2} & z^{-3} \end{pmatrix}}^{\Lambda(z)} \overbrace{\begin{pmatrix} \theta_1 \\ \theta_2 \\ \theta_2 \end{pmatrix}}^{\theta} \end{aligned}$$

where the parameter vector θ is assumed to have a Gaussian probability density function with zero mean and covariance P_θ given by:

$$P_\theta = 10^{-3} \times \begin{pmatrix} 1.0031 & 0.0263 & -0.0111 \\ 0.0263 & 1.0039 & 0.0268 \\ -0.0111 & 0.0268 & 1.0039 \end{pmatrix}.$$

We consider the 95 % confidence ellipsoid U_θ in the parameter space that defines a corresponding region $\mathcal{D}$ in the space of transfer function:

$$U_\theta = \{\theta \mid \theta^T P_\theta^{-1} \theta < 7.81\},$$

$$\mathcal{D} = \{G(z,\theta) \mid \theta \in U_\theta\}$$

Using Theorem 7.3, we can design the image $\mathcal{L}$ of $\mathcal{D}$ in the Nyquist plane. This image $\mathcal{L}$ is made up of ellipses at each frequency around the frequency response of $\bar{G}(z)$ and is represented in Figure 7.1. According to Theorem 7.3, the expression of the ellipse $U(\omega)$ at the frequency ω is given by:

$$U(\omega) = \{g \in \mathbf{R}^{2\times 1} \mid (g - \bar{g}(e^{j\omega}))^T P(\omega)^{-1} (g - \bar{g}(e^{j\omega})) < 7.81\}$$

with $P(\omega) = T(e^{j\omega}) P_\theta T(e^{j\omega})^T$ and

$$\bar{g}(e^{j\omega}) = \begin{pmatrix} Re(\bar{G}(e^{j\omega})) \\ Im(\bar{G}(e^{j\omega})) \end{pmatrix}, \quad T(e^{j\omega}) = \begin{pmatrix} Re(\Lambda(e^{j\omega})) \\ Im(\Lambda(e^{j\omega})) \end{pmatrix}.$$

All plants in $\mathcal{D}$ lie in $\mathcal{L}$, and $\mathcal{L}$ has the property (7.22). However, the mappings between $\mathcal{D}$ and $\mathcal{L}$ and between $\mathcal{D}$ and $U(\omega)$ are not bijective

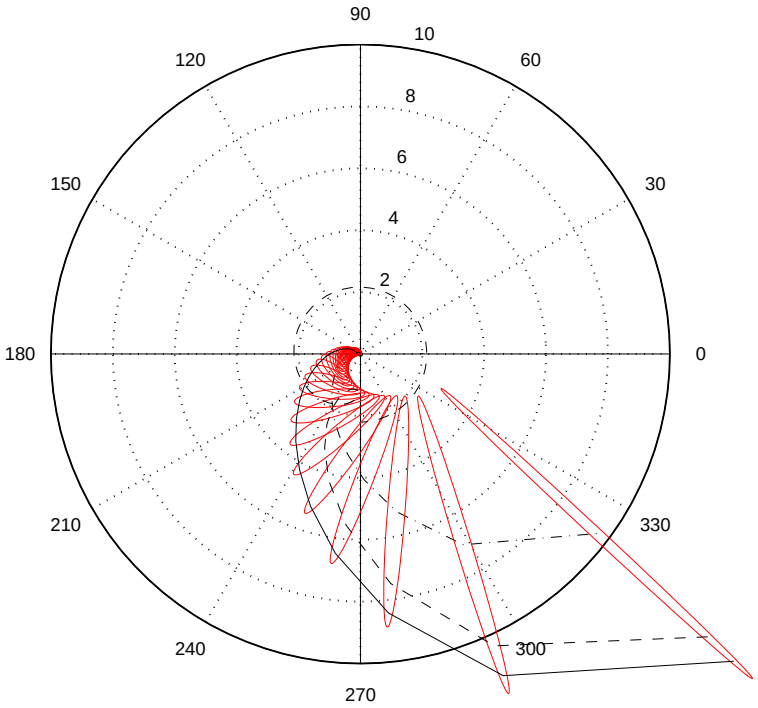

Figure 7.1: Frequency domain representation of $\mathcal{D}$ in the Nyquist plane with ellipses $U(\omega)$ at some frequencies, frequency response of $\bar{G}(z)$ (dash-dot), frequency response of $G(z, \theta_{out})$ (dashed) and frequency response of $G(z, \theta_{bis})$ (solid)

as shown in Theorem 7.4 and Proposition 7.1, respectively. In order to illustrate the results presented in these theorems, we will show two things:

1. there exist plants $G(z, \theta_{out})$ outside $\mathcal{D}$ whose frequency response vector $g(e^{j\omega}, \theta_{out})$ lies in some ellipses $U(\omega)$ but not in all of them;

2. there exist plants $G(z, \theta_{bis})$ outside $\mathcal{D}$ that lie in the whole region $\mathcal{L}$.

Since the size of θ is 3, we know that the vectors θ that are projected into $U(\omega)$ at the frequency ω are those lying in the cylinder $C_\theta(U(\omega))$ whose axis direction is given by the normed eigenvector $\theta_{null}(\omega)$ corresponding to the null eigenvalue of the mapping $T(e^{j\omega})$ (see Theorem 7.2

and Proposition 7.1). Using this property, we can find a plant $G(z, \theta_{out})$ such that $\theta_{out} \notin U_\theta$, but such that its frequency response $g(e^{j\omega_0}, \theta_{out})$ at ω_0 lies in $U(\omega_0)$ for a particular frequency ω_0, say $\omega_0 = 0.25$. Indeed, let us choose as vector θ_{out} a vector in the same direction as $\theta_{null}(0.25)$ but outside the ellipsoid U_θ:

$$\theta_{out} = \begin{pmatrix} 1.8084 \\ -3.5043 \\ 1.8084 \end{pmatrix}$$

This vector is well outside the ellipsoid U_θ since we have that:

$$\theta_{out}^T P_\theta^{-1} \theta_{out} = 19525 > 7.81$$

but we also have that:

$$g(e^{j0.25}, \theta_{out}) = \bar{g}(e^{j0.25}) + \overbrace{T(e^{j0.25})\theta_{out}}^{=0} = \bar{g}(e^{j0.25}),$$

and therefore $g(e^{j0.25}, \theta_{out})$ lies in $U(0.25)$. However, this plant does not lie in all ellipses as can be seen in Figure 7.1 where it circles around the origin at high frequencies.

There also exist plants $G(z, \theta_{bis})$ whose parameter vectors $\theta_{bis} \notin U_\theta$, but that lie completely in $\mathcal{L}$. According to Theorem 7.4 and Corollary 7.1, these are the plants whose parameter vectors θ_{bis} lie in $U_\theta(\mathcal{L}) = \bigcap_{\omega \in [0\ \pi]} C_\theta(U(\omega))$ but not in U_θ. In order to find one of those particular vectors θ_{bis}, we proceed like we did to find θ_{out}. We choose a particular frequency ω_0 and we choose a vector in the direction $\theta_{null}(\omega_0)$ of the axis of the cylinder $C_\theta(U(\omega_0))$. But, here, we choose this frequency ω_0 in the middle of the frequency range: $\omega_0 = \pi/2$ and we choose the vector **just** outside the ellipsoid U_θ:

$$\theta_{bis} = \begin{pmatrix} 0.0684 \\ 0 \\ 0.0684 \end{pmatrix}, \quad \theta_{bis}^T P_\theta^{-1} \theta_{bis} = 9.4501 > 7.81 \ .$$

In Figure 7.1, we see that the frequency response of the plant $G(z, \theta_{bis})$ lies in $U(\omega)$ for each of the plotted ellipses. Since we only plot the ellipses at a certain number of frequencies, Figure 7.1 alone does not prove that $G(z, \theta_{bis})$ is in $\mathcal{L}$. In Figure 7.2, we have therefore plotted the value of the function

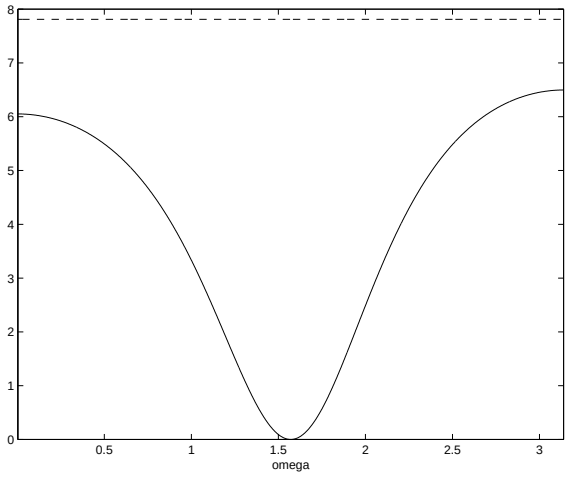

Figure 7.2: Values of $(g(e^{j\omega}, \theta_{bis}) - \bar{g}(e^{j\omega}))^T P(\omega)^{-1}(g(e^{j\omega}, \theta_{bis}) - \bar{g}(e^{j\omega}))$ as a function of the frequency (solid) and size of the ellipses $U(\omega)$ (dashed)

$$(g(e^{j\omega}, \theta_{bis}) - \bar{g}(e^{j\omega}))^T P(\omega)^{-1}(g(e^{j\omega}, \theta_{bis}) - \bar{g}(e^{j\omega}))$$

at each frequency. We see that these values are, at each frequency, smaller than 7.81, the size of the ellipses $U(\omega)$. As a consequence, we can conclude that $G(z, \theta_{bis})$ has its frequency response in $\mathcal{L}$ even though $G(z, \theta_{bis})$ does not lie in $\mathcal{D}$.

7.10 Conclusions

In this chapter, we have considered linearly parametrized plants $G(z, \theta)$ whose parameters are normally distributed and we have presented results about the image $\mathcal{L}$ in the Nyquist plane of a confidence region $\mathcal{D}$ in the space of parametrized transfer functions. We have shown that this image is made of ellipses at each frequency. However, since the mapping between these two spaces is not bijective, the image $\mathcal{L}$ in the Nyquist plane contains more plants $G(z, \theta)$ than the initial confidence region $\mathcal{D}$. The image in the Nyquist plane is thus also a confidence region for the parametrized plants $G(z, \theta)$ but with a probability level larger than that of the initial confidence region $\mathcal{D}$.

Chapter 8

Extension to biased model structures using stochastic embedding

In Chapter 2, we have introduced an uncertainty set $\mathcal{D}$ delivered by classical prediction error identification methods and to which the true system G_0 is known to belong with some prescribed probability. This uncertainty set $\mathcal{D}$ is defined as a set of parametrized rational transfer functions whose parameter vector lies in an ellipsoidal confidence region. In Chapters 3, 4 and 5, we have developed some robustness tools for that uncertainty set $\mathcal{D}$. In the previous chapter, we have analyzed the image of $\mathcal{D}$ in the Nyquist plane for the particular case of linearly parametrized systems.

The only important restriction in the approach yielding $\mathcal{D}$ is that we assume that the model structure used for the identification is unbiased and therefore that the true system lies in the chosen model structure. In this chapter, we show that we can also design an uncertainty set containing the true system using PE identification with *biased model structures* provided that this model structure is linearly parametrized (e.g. FIR or Laguerre model structure [65, 88]) and that the identification is performed using the stochastic embedding assumptions [47]. The key idea of PE identification with stochastic embedding assumptions is to consider the unmodelled dynamics just as the noise i.e. as the realization of a zero mean stochastic process. Using this assumption, the authors of [47] show that, at each frequency, an ellipse containing the frequency

response of the stable true system at a certain probability level (e.g. α) can be designed in the Nyquist plane around the frequency response of the identified model. The ellipse at a particular frequency is constructed using the probability density function of the frequency response of the identified model deduced from the stochastic embedding assumptions. In [1, 79], the ellipses at each frequency have been collected together in order to make up a dynamic (or frequency domain) uncertainty region [1]. The problem with the uncertainty region design presented in the papers [1, 79] is that, if each ellipse contains the frequency response of the true system at a probability of α, the probability level of the presence of the Nyquist plot of G_0 in the tube of ellipses is much smaller as proved in Chapter 7.

One of the contribution of the present chapter is thus to review the design of uncertainty sets for a PE identification procedure with stochastic embedding assumptions. We first show that PE identification with stochastic embedding assumptions allows one to design a set $\mathcal{D}_{se}$ of (linearly) parametrized transfer functions that contains the true system at a certain probability level (e.g. α) and whose parameter vector is constrained to lie in an ellipsoid. This uncertainty set has thus the same structure as the uncertainty set $\mathcal{D}$ presented in Chapter 2. However, we also show that the parametric description of $\mathcal{D}_{se}$ is not really "optimal" in this case and we therefore propose another uncertainty region: a dynamic uncertainty region $\mathcal{L}$ corresponding to the image of $\mathcal{D}_{se}$ in the Nyquist plane. The image of $\mathcal{D}_{se}$ is obtained using the results of Chapter 7. The uncertainty region $\mathcal{L}$ is made up of a tube of ellipses in the Nyquist plane around the Nyquist plot of the identified model. According to Chapter 7, the uncertainty set $\mathcal{L}$ has also the property of containing the true system at a probability larger than the probability α related to $\mathcal{D}_{se}$. It is to be noted that the matrices defining the ellipses in our uncertainty set $\mathcal{L}$ are exactly the same as those defining the ellipses deduced in [47, 1, 79]. However, the size χ of our ellipses [2] is different of the size of the ellipses deduced in these papers.

Another contribution of the present chapter is to extend the stochastic embedding technique to indirect closed-loop identification. In closed-

[1] In the sequel, we will use the term "dynamic uncertainty region" instead of "frequency domain uncertainty region".

[2] If we define an ellipse as $U = \{\theta \mid \theta^T R \theta < \chi\}$, the size of the ellipse is the value χ and the matrix defining the ellipse is R.

loop, we construct a dynamic uncertainty region of closed-loop transfer functions containing the true closed-loop transfer function. The uncertainty region containing the true *open-loop* system G_0 is then computed using the knowledge of the controller present in the loop.

The last contribution of the chapter is to give a general expression of this uncertainty region $\mathcal{L}$ (valid for both the open-loop and closed-loop cases) that will ease the robustness analysis of $\mathcal{L}$ developed in the next chapter. In this general expression, the uncertainty part takes the form of a transfer vector which represents the real and imaginary parts of the dynamic uncertainty and whose frequency response is therefore real. This vector appears linearly in both the numerator and denominator.

Chapter outline. In Section 8.1, we briefly review the assumptions of stochastic embedding. In Section 8.2, we show how we can perform a PE identification procedure using the stochastic embedding assumptions. In Section 8.3, we then present the way to construct an uncertainty set with PE identification with stochastic embedding assumptions in open loop. In Section 8.4, we show that such an uncertainty region can also be deduced using data collected in closed loop. We then give the general expression of the uncertainty region deduced from PE identification with stochastic embedding assumptions in Section 8.5.

8.1 General assumptions on the true system

In the previous chapters, we have reduced the gap between PE identification with unbiased model structures and Robustness theory. Indeed, we have shown that such an identification procedure delivers an uncertainty set that contains the true system and for which we have developed some robustness tools. The aim of this chapter is to extend the results of the previous chapters to the case of biased model structures using stochastic embedding [47]. In this first section, we will present the assumptions we need to make for this purpose on the used model structure $\mathcal{M}$ and on the stable, LTI, rational true system G_0:

$$y(t) = G_0(z)u(t) + v(t). \tag{8.1}$$

Let us consider that we want to identify a model of the true system in the following *linearly parametrized* model structure $\mathcal{M}$:

$$\mathcal{M} = \{G(z,\theta) \in \mathcal{R}H_\infty \mid G(z,\theta) = \overbrace{\begin{pmatrix} \Lambda_1(z) & \Lambda_2(z) & \dots & \Lambda_k(z) \end{pmatrix}}^{\Lambda(z)} \theta\}, \tag{8.2}$$

where $\theta \in \mathbf{R}^{k\times 1}$ is the parameter vector and the $\Lambda_i(z)$ $(i = 1...k)$ are stable transfer functions (e.g. FIR of Laguerre functions [65, 88]). This model structure is biased i.e. there does not exist a θ_0 such that $G_0 = G(z,\theta_0)$.

The property that allowed us to design an uncertainty set containing the true system with PE identification with unbiased model structures was the fact that the only source of error between the identified model and the true system (i.e. the measurement noise $v(t)$) was assumed to be the realization of a zero mean stochastic process. With biased model structures, the measurement noise is not the only source of error. The undermodeling is also another one. The key idea of stochastic embedding is to consider this second source of error just as the first one i.e. as the realization of a zero mean stochastic process, independent of the noise. Note that although this assumption is nonstandard in classical PE identification, this remains in the general philosophy of PE identification since the bias error is considered in the same way as the measurement noise in classical PE identification. Let us now recall this key idea more formally.

Assumption 8.1 ([47]) *The key assumption in stochastic embedding is that (8.1) can be decomposed in the following expression:*

$$y(t) = G(z,\theta_0)u(t) + G_\Delta(z)u(t) + H_0(z)e(t) \tag{8.3}$$

where $G(z,\theta_0) \in \mathcal{R}H_\infty$ is a transfer function lying in $\mathcal{M}$ and parametrized by an unknown vector θ_0. $G_\Delta(z) \in \mathcal{R}H_\infty$ represents the (possibly infinite) unmodelled dynamics that is assumed to be the realization of a stochastic process with zero mean, independent of the additive noise $v(t) = H_0(z)e(t)$. It is further assumed that the impulse response coefficients η_n of $G_\Delta(z) = \sum_{n=1}^{\infty}\eta_n z^{-n}$ have a variance that dies at an exponential rate : $\mathcal{E}(\eta_n^2) = \beta\lambda^n$ $(\mathcal{E}(\eta_n) = 0)$. As a consequence, there exists a number L [3] such that G_Δ can be approximated sufficiently closely by

[3] The choice of L will be discussed in the sequel.

$$G_\Delta(z) = \sum_{n=1}^{L} \eta_n z^{-n} \stackrel{\Delta}{=} \Pi(z)\eta, \tag{8.4}$$

where $\Pi(z) = \begin{pmatrix} z^{-1} & z^{-2} & \dots & z^{-L} \end{pmatrix}$ *and* $\eta^T = \begin{pmatrix} \eta_1 & \eta_2 & \dots & \eta_L \end{pmatrix}$.

8.2 PE identification with stochastic embedding assumptions

Using Assumptions 8.1, we can perform a PE identification procedure on the true system G_0 using N input and output data. This identification delivers a model $G(z,\hat{\theta}) \in \mathcal{M}$. As the unmodelled dynamics are considered as the realization of a zero mean stochastic process, the total error between the true system and the identified model $G(z,\hat{\theta})$ is made up of the sum of variance contributions only, wherein the contribution of the unmodelled dynamics is computed by estimating the parameters describing its variance (i.e. β and λ). The total error is thus a function of the stochastic parameters describing $G_\Delta(z)$ (i.e. β and λ) and of the stochastic parameters γ describing $v(t)$ [4]. These parameters can be estimated from the data $y(t)$ and $u(t)$ using a maximum likelihood technique. In that sense, the computation of the total error follows a procedure very similar to the one used to compute the variance error in classical prediction error identification theory with unbiased model structures (see [63] and Sections 2.1.2 and 2.1.3). Let us now summarize the results of PE identification with stochastic embedding assumptions in the following proposition.

Proposition 8.1 ([47]) *Let us consider a stable true system G_0 satisfying Assumptions 8.1 and the model structure $\mathcal{M}$ defined in (8.2). Let us also consider N measured inputs $u(t)$ and the corresponding N outputs $y(t)$ generated by (8.3). A PE identification procedure delivers then an identified parameter vector $\hat{\theta}$ defining a model $G(z,\hat{\theta}) \in \mathcal{M}$. Moreover, if we rewrite the error between $G_0(z)$ and the identified model*

[4] The stochastic parameters γ describing $v(t)$ may contain the parameters of the noise model $H_0(z)$ as proposed in [1]. Alternatively, it is possible to use a high order identified model of $H_0(z)$ as approximation of this noise model; and then the only stochastic parameter of the noise $v(t)$ is the variance σ_e^2 of the white noise $e(t)$: $\gamma = \sigma_e^2$.

$G(z,\hat{\theta})$ as follows using (8.2) and (8.4):

$$G_0(z) - G(z,\hat{\theta}) = \overbrace{\begin{pmatrix} \Lambda(z) & \Pi(z) \end{pmatrix}}^{\Gamma(z)} \overbrace{\begin{pmatrix} \theta_0 - \hat{\theta} \\ \eta \end{pmatrix}}^{\tilde{\rho}}, \tag{8.5}$$

the vector $\tilde{\rho}$ is then asymptotically a random vector with Gaussian distribution, zero mean and covariance C_ρ:

$$\tilde{\rho} \sim As\mathcal{N}(0, C_\rho) \tag{8.6}$$

where $C_\rho \in \mathbf{R}^{(k+L)\times(k+L)}$ is an unknown symmetric positive definite matrix which is a function of the stochastic parameters β, λ and γ. Besides the identified parameter vector $\hat{\theta}$, the PE identification procedure also delivers an estimate P_ρ of C_ρ obtained using the estimates $\hat{\beta}$, $\hat{\lambda}$ and $\hat{\gamma}$ of β, λ and γ derived from a maximum likelihood procedure.

Remarks.

- More details can be found in Appendix B.
- The quality of the description of the error between G_0 and $G(z,\hat{\theta})$ is of course influenced by the number N of measured data, the quality of the estimates ($\hat{\beta}$, $\hat{\lambda}$ and $\hat{\gamma}$) of the stochastic parameters resulting from a nonlinear optimization (i.e. the maximum likelihood technique) and by the relevance of the stochastic embedding assumptions (choice of L, ...).
- In [37], the authors present a new version of stochastic embedding where the undermodeling is represented by a multiplicative perturbation. One of the main advantage of this new stochastic embedding is that the procedure to estimate the stochastic parameters is linear.
- The choice of L can now be discussed. This choice can be divided in two steps. In a first step, we choose L large (e.g. $L = N$) and we use the maximum likelihood technique to find estimates $\hat{\beta}$ and $\hat{\lambda}$ of β and λ. Using these "accurate estimates", the "final" L is chosen such that:

  $$\hat{\beta}\hat{\lambda}^L < \varepsilon$$

  where ε is very small.

8.3 Design of uncertainty regions using stochastic embedding in open loop

In the previous section, we have presented the results related to a PE identification procedure with *biased model structure* and stochastic embedding assumptions. These results allow one to design different types of uncertainty regions containing the true system at a certain probability level. We first show that one of these types is an uncertainty set $\mathcal{D}_{se}$ having the same structure as the uncertainty set $\mathcal{D}$ delivered by PE identification with *unbiased model structures.*

8.3.1 Design of the uncertainty set $\mathcal{D}_{se}$

The properties presented in Proposition 8.1 are equivalent to those presented in Proposition 2.2 that have allowed us to construct a uncertainty set containing the true system at a certain probability level in Chapter 2. Using a similar procedure, an uncertainty set $\mathcal{D}_{se}$ having the following form is constructed.

$$\mathcal{D}_{se} = \{G(z,\rho) \mid G(z,\rho) = \hat{G}(z) + \Gamma(z)\rho \textit{ with } \rho \in U_{se}\} \tag{8.7}$$

$$U_{se} = \{\rho \mid \rho^T P_\rho^{-1} \rho < \chi\} \tag{8.8}$$

where $\hat{G}(z) \triangleq G(z,\hat{\theta})$ and ρ is a real parameter vector of size $k+L$. This uncertainty set has the following property.

Proposition 8.2 *Let us consider a true system G_0 satisfying Assumptions 8.1. Then, the uncertainty region $\mathcal{D}_{se}$ defined in (8.7) contains G_0 at a probability level $\alpha(k+L,\chi)$: $Pr(\chi^2(k+L) < \chi) = \alpha(k+L,\chi)$.*

Proof. According to (8.6), the vector $\tilde{\rho}$ defined in Proposition 8.1 lies in U_{se} with probability $\alpha(k+L,\chi)$. We can then conclude that G_0 lies in $\mathcal{D}_{se}$ at the same probability level since, using (8.5), we can rewrite G_0 as $G(z,\tilde{\rho})$. □

The uncertainty region $\mathcal{D}_{se}$ has the general structure presented in (2.44). As a consequence, the results of Chapters 3, 4 and 5 can be used to assess the quality of $\mathcal{D}_{se}$ and/or to validate a controller for stability and performance with respect to $\mathcal{D}_{se}$. However, the statement

$G_0 \in \mathcal{D}_{se}$ given in Proposition 8.2 is based on the approximation (8.4) that boils down to neglect the part $\sum_{n=L+1}^{\infty} \eta_n z^{-n}$ of the undermodeling $G_\Delta = \sum_{n=1}^{\infty} \eta_n z^{-n}$. This can be misleading for robust control design since (8.4) is only an approximation in practice. A solution to avoid this problem is to use a dynamic uncertainty region as we will see in the next section. A dynamic uncertainty region is an uncertainty region that is not bounded by a constraint on a parameter vector but by a constraint on the frequency response of the plants in that uncertainty region.

8.3.2 Dynamic uncertainty region $\mathcal{L}_{ol}$

A possibility to design such dynamic uncertainty region is to take the image $\mathcal{L}_{ol}$ [5] of $\mathcal{D}_{se}$ in the Nyquist plane using the results presented in Chapter 7. Using Theorem 7.3, this image $\mathcal{L}_{ol}$ is given by

$$\mathcal{L}_{ol} = \{G(z) \mid g(e^{j\omega}) \in U(\omega)\ \forall\omega\} \tag{8.9}$$

$$U(\omega) = \{g \in \mathbf{R}^{2\times 1} \mid (g - \hat{g}(e^{j\omega}))^T P(\omega)^{-1} (g - \hat{g}(e^{j\omega})) < \chi\} \tag{8.10}$$

with $P(\omega) = T(e^{j\omega}) P_\rho T(e^{j\omega})^T$, χ as defined in (8.8) and

$$\hat{g}(e^{j\omega}) = \begin{pmatrix} Re(\hat{G}(e^{j\omega})) \\ Im(\hat{G}(e^{j\omega})) \end{pmatrix}, \quad T(e^{j\omega}) = \begin{pmatrix} Re(\Gamma(e^{j\omega})) \\ Im(\Gamma(e^{j\omega})) \end{pmatrix}.$$

In order to clear up and to simplify the notations, let us rewrite the dynamic uncertainty set $\mathcal{L}_{ol}$ as follows.

$$\begin{aligned} \mathcal{L}_{ol} = \{G_{in}(z) \mid G_{in}(z) = G(z,\hat{\theta}) + \Delta(z) \quad & with\ \Delta(z) \in \mathcal{R}H_\infty \\ & and \begin{pmatrix} Re(\Delta(e^{j\omega})) \\ Im(\Delta(e^{j\omega})) \end{pmatrix} \in U_{ol}(\omega)\ \forall\omega\} \end{aligned} \tag{8.11}$$

$$U_{ol}(\omega) = \{g \in \mathbf{R}^{2\times 1} \mid g^T P(\omega)^{-1} g < \chi\}. \tag{8.12}$$

The dynamic uncertainty region $\mathcal{L}_{ol}$ that we have just designed has the following property.

[5] We have changed the subscript "se" into the subscript "ol" in order to may differentiate $\mathcal{L}_{ol}$ obtained with open-loop stochastic embedding from $\mathcal{L}_{cl}$ that will be deduced from closed-loop stochastic embedding.

Proposition 8.3 *Let us consider a true system G_0 satisfying Assumption 8.1. Then, the uncertainty set $\mathcal{L}_{ol}$ defined in (8.11) contains G_0 with a probability larger than $\alpha(k+L,\chi)$: $Pr(\chi^2(k+L) < \chi) = \alpha(k+L,\chi)$.*

Proof. According to Proposition 8.2, G_0 lies in $\mathcal{D}_{se}$ with probability $\alpha(k+L,\chi)$. Since $\mathcal{L}_{ol}$ is the image of $\mathcal{D}_{se}$ in the Nyquist plane, the true system G_0 lies therefore in $\mathcal{L}_{ol}$ with a probability larger than $\alpha(k+L,\chi)$ (see Theorem 7.5). □

The true system G_0 lies thus in $\mathcal{L}_{ol}$ and in $\mathcal{D}_{se}$. So, if we stay in the framework defined in (8.4), there is no need to use $\mathcal{L}_{ol}$ instead of $\mathcal{D}_{se}$. However, the expression (8.4) is only an approximation. In practice, we do not have that:

$$\sum_{n=L+1}^{\infty} \eta_n z^{-n} = 0,$$

As a consequence, the structure of $\mathcal{D}_{se}$ may not contain the "real" true system as opposed to the structure of $\mathcal{L}_{ol}$. Indeed, with respect to $\mathcal{D}_{se}$, the dynamic uncertainty region $\mathcal{L}_{ol}$ has the complementary advantage of containing systems having a more complicated structure than $G(z,\rho)$ but whose frequency response is sufficiently close to the frequency response of the plants in $\mathcal{D}_{se}$... such as the "real" true system. Indeed we have that:

$$G_0(z) = \overbrace{G(z,\tilde{\rho})}^{\in \mathcal{D}_{se}} + \sum_{n=L+1}^{\infty} \eta_n z^{-n}$$

$$G_0(e^{j\omega}) \approx G(e^{j\omega},\tilde{\rho}) \quad \forall \omega.$$

In the sequel, we will therefore always use $\mathcal{L}_{ol}$ instead of $\mathcal{D}_{se}$.

Let us summarize. Using the stochastic embedding assumptions, we have developed a methodology that has allowed us to design a dynamic uncertainty region $\mathcal{L}_{ol}$ containing the true system with a probability larger than a given level in the case of an open-loop identification with a *biased* model structure $\mathcal{M}$. In the next section, we will show that such uncertainty set can also be deduced from an indirect closed-loop identification with biased model structure.

8.4 Extension to indirect closed-loop PE identification with stochastic embedding assumptions

Let us consider again the closed-loop experiment design presented in Section 2.2.4. We consider thus a controller K which forms a stable closed loop with the stable true system G_0 defined in (8.1). Our procedure to design an uncertainty set $\mathcal{L}$ with stochastic embedding in closed loop is very similar to the one used in the case of unbiased model structures: it consists of first designing a frequency domain uncertainty region containing one of the four transfer functions of the matrix $T(G_0, K)$ defined in (2.27) and then to back-compute the uncertainty region containing G_0. We give here the procedure for the closed-loop transfer function T_0^1 defined in (2.29). We then have to assume that K and K^{-1} are stable [21]. Similar procedures exist for the other three closed-loop transfer functions.

Let us thus collect N experimental data $r_1(t)$ and $y(t)$ on the closed loop presented in Figure 2.1 and composed of the true system G_0 and the stabilizing controller K:

$$y(t) = \frac{G_0 K}{1 + G_0 K} r_1(t) + \frac{H_0}{1 + G_0 K} e(t) = T_0^1 r_1(t) + \tilde{v}(t) \tag{8.13}$$

As the loop $[K\ G_0]$ is stable, it is possible to use the procedure presented in Section 8.3 to design an uncertainty region $\mathcal{L}_T$ of closed-loop transfer functions containing T_0^1. For this purpose, we define a *biased* model structure for T_0^1 as follows

$$\mathcal{M}_{cl} = \{T(z, \xi) \in \mathcal{R}H_\infty \mid T(z, \xi) = \Lambda_{cl}(z)\xi\}, \tag{8.14}$$

where ξ is a parameter vector and $\Lambda_{cl}(z)$ a row vector containing known transfer functions. We rewrite also (8.13) in a way similar to (8.3):

$$y(t) = T(z, \xi_0) r_1(t) + T_\Delta(z) r_1(t) + \tilde{v}(t) \tag{8.15}$$

where T_0^1 is decomposed into a model $T(z, \xi_0) \in \mathcal{M}_{cl}$ and the unmodelled dynamics $T_\Delta(z)$. Using the procedure given in Section 8.3, we may deduce the uncertainty region $\mathcal{L}_T$ containing T_0^1 with a probability larger than a given level:

$$\mathcal{L}_T = \{T_{in}(z) \mid T_{in}(z) = \overbrace{T(z,\hat{\xi})}^{\hat{T}(z)} + \Delta(z) \quad with\ \Delta(z) \in \mathcal{R}H_\infty \quad and \begin{pmatrix} Re(\Delta(e^{j\omega})) \\ Im(\Delta(e^{j\omega})) \end{pmatrix} \in U_{cl}(\omega)\ \forall\omega\} \tag{8.16}$$

where $\hat{T} = T(z,\hat{\xi}) \in \mathcal{R}H_\infty$ is the identified model and $U_{cl}(\omega)$ is an ellipse having the same form as the one defined in (8.12).

The set $\mathcal{L}_T$ is a set of closed-loop transfer functions. The corresponding set of open-loop transfer functions is now constructed. As $G_0 = T_0^1/(K(1-T_0^1))$, the open-loop transfer function $G_{in}(z)$ corresponding to $T_{in}(z)$ is given by:

$$G_{in}(z) = \frac{1}{K} \times \frac{T_{in}(z)}{1 - T_{in}(z)}. \tag{8.17}$$

In particular, the nominal open-loop model $G(z,\hat{\xi})$ corresponding to $\hat{T} = T(z,\hat{\xi})$ is given by:

$$G(z,\hat{\xi}) = \frac{1}{K} \times \frac{T(z,\hat{\xi})}{1 - T(z,\hat{\xi})} \tag{8.18}$$

As we assume that the true system G_0 is stable, we also assume that this open-loop model $G(z,\hat{\xi})$ is stable. The set $\mathcal{L}_{cl}$ of open-loop plants G_{in} corresponding to the set $\mathcal{L}_T$ of closed-loop transfer functions T_{in} is:

$$\mathcal{L}_{cl} = \{G_{in}(z) \mid G_{in}(z) = \frac{\frac{\hat{T}}{K-K\hat{T}} + \frac{1}{K-K\hat{T}}\Delta}{1 + \frac{-1}{1-\hat{T}}\Delta} \quad with\ \Delta(z) \in \mathcal{R}H_\infty \quad and \begin{pmatrix} Re(\Delta(e^{j\omega})) \\ Im(\Delta(e^{j\omega})) \end{pmatrix} \in U_{cl}(\omega)\ \forall\omega\} \tag{8.19}$$

The frequency domain uncertainty region $\mathcal{L}_{cl}$ can be rewritten as follows using (8.18).

$$\mathcal{L}_{cl} = \{G_{in}(z) \mid G_{in}(z) = \frac{G(z,\hat{\xi}_N)+\frac{1+KG(z,\hat{\xi}_N)}{K}\Delta}{1+(-1-KG(z,\hat{\xi}_N))\Delta} \quad with\ \Delta(z) \in \mathcal{R}H_\infty$$
$$and \begin{pmatrix} Re(\Delta(e^{j\omega})) \\ Im(\Delta(e^{j\omega})) \end{pmatrix} \in U_{cl}(\omega)\ \forall\omega\} \tag{8.20}$$

Properties of $\mathcal{L}_{cl}$. According to the results of the previous section, the true closed-loop transfer function T_0^1 lies in $\mathcal{L}_T$ with a probability larger than a given level. As a consequence, the true system $G_0 = T_0^1/(K(1-T_0^1))$ lies in the frequency domain uncertainty region $\mathcal{L}_{cl}$ with the same probability.

8.5 General structure of the uncertainty regions obtained from PE identification with biased model structures

In the previous subsections, uncertainty regions $\mathcal{L}_{ol}$ and $\mathcal{L}_{cl}$ containing the true system have been obtained as a result of open-loop or "indirect" closed-loop PE identification with biased model structures and stochastic embedding assumptions, respectively. In both cases, these uncertainty regions take the form of a set of open-loop transfer functions (around some center) defined by a dynamic uncertainty $\Delta(z) \in \mathcal{R}H_\infty$ whose frequency response is bounded at each frequency by an ellipsoid in the Nyquist plane. In the following proposition, we show that $\mathcal{L}_{ol}$ and $\mathcal{L}_{cl}$ can be described using the same generic expression $\mathcal{L}$. The form of this generic expression has been chosen very similar to the structure of the uncertainty region $\mathcal{D}$ defined in (2.44) in order to ease the robustness analysis of $\mathcal{L}$ that will be developed in the next chapter. For this purpose, let us define the RI vector $\delta(z)$ corresponding to the uncertainty transfer function $\Delta(z)$.

Definition 8.1 (The RI vector $\delta(z)$ corresponding to $\Delta(z)$) *Let $\Delta(z)$ be the stable uncertainty transfer function present in (8.11) and (8.20). We define the RI vector $\delta(z)$ as follows:*

$$\delta(z) = \begin{pmatrix} Re(\Delta(z)) \\ Im(\Delta(z)) \end{pmatrix}. \tag{8.21}$$

Note that the frequency response $\delta(e^{j\omega})$ of $\delta(z)$ is, at each frequency, **real***: $\delta(e^{j\omega}) \in \mathbf{R}^{2\times 1} \quad \forall\omega$.*

Proposition 8.4 *Consider the true open-loop dynamics G_0. The uncertainty regions $\mathcal{L}_{ol}$ and $\mathcal{L}_{cl}$ given in (8.11) and (8.20), respectively, and containing G_0 with a probability larger than a given level have the general form of a frequency domain uncertainty region $\mathcal{L}$ where the uncertainty part is the RI vector $\delta(z)$ (see Definition 8.1).*

$$\mathcal{L} = \left\{ G(z,\delta(z)) \mid G(z,\delta(z)) = \frac{\hat{G}(z) + Z_N(z)\delta(z)}{1 + Z_D(z)\delta(z)} \quad with\ \delta(e^{j\omega}) \in U(\omega)\ \forall\omega \right\} \tag{8.22}$$

$$U(\omega) = \{\delta(e^{j\omega}) \in \mathbf{R}^{2\times 1} \mid \delta(e^{j\omega})^T R(\omega)\delta(e^{j\omega}) < 1\} \tag{8.23}$$

where

- *$R(\omega)$ are symmetric positive definite matrices $\in \mathbf{R}^{2\times 2}$. These matrices are different at each frequency ω.*
- *$Z_N(z)$ and $Z_D(z)$ are stable row vectors of length 2 containing known transfer functions.*
- *$\hat{G}(z) \in \mathcal{R}H_\infty$ is a known transfer function that can be considered as the center of $\mathcal{L}$* [6].

Proof. Let us first prove that $\mathcal{L}_{ol}$ can be expressed as in (8.22). This can be done by considering Expression (8.12) of $U_{ol}(\omega)$ and by rewriting expression (8.11) of $\mathcal{L}_{ol}$ using (8.21):

$$\mathcal{L}_{ol} = \left\{ G_{in}(z) \mid G_{in}(z) = G(z,\hat{\theta}) + \begin{pmatrix} 1 & j \end{pmatrix} \delta(z)\ with\ \delta(e^{j\omega}) \in U_{ol}(\omega)\ \forall\omega \right\} \tag{8.24}$$

which is in the form (8.22) with $Z_N = (1\ j)$, $Z_D = (0\ 0)$, $\hat{G}(z) = G(z,\hat{\theta}) \in \mathcal{R}H_\infty$ and $R(\omega) = P(\omega)^{-1}/\chi$.

[6] we call "center of the uncertainty region $\mathcal{L}$" the system corresponding to $\delta(z) = 0$

Now consider $\mathcal{L}_{cl}$ and rewrite expression (8.20) using (8.21) and denoting $\hat{G}(z) = G(z, \hat{\xi})$:

$$\mathcal{L}_{cl} = \{G_{in}(z) \mid G_{in}(z) = \frac{\hat{G}(z) + \frac{1+K\hat{G}(z)}{K}\begin{pmatrix} 1 & j \end{pmatrix}\delta(z)}{1+(-1-K\hat{G}(z))\begin{pmatrix} 1 & j \end{pmatrix}\delta(z)} \quad and \quad \delta(e^{j\omega}) \in U_{cl}(\omega)\ \forall\omega\} \tag{8.25}$$

which is clearly in the form (8.22). Note that $\hat{G}(z) = G(z, \hat{\xi})$ is assumed stable; hence, $Z_N(z)$ and $Z_D(z)$ are also stable since the controller K is stable and non-minimum phase according to [21]. This completes the proof. □

Remarks.

- The center $\hat{G}(z)$ of the uncertainty region $\mathcal{L}$ is given by the identified model $G(z, \hat{\theta})$ in the open-loop case and, in the closed-loop case, by $G(z, \hat{\xi})$, the open-loop model corresponding to the identified closed-loop model $T(z, \hat{\xi})$: see (8.18).
- The uncertainty set $\mathcal{L}$ has a particularity with respect to the classical linear fractional dynamic uncertainty regions such as additive or multiplicative uncertainty sets (see (2.45) for the additive uncertainty set). Indeed, the uncertainty part $\delta(z)$ is not a classical transfer function but is a "transfer vector" whose frequency response is real[7]. Therefore, the classical tools of Robustness Theory can not be used for $\mathcal{L}$. However, the uncertainty set $\mathcal{L}$ has a structure that is very similar to the one of the uncertainty region $\mathcal{D}$ delivered by PE identification with unbiased model structures and for which we have developed robustness tools in the previous chapters. The only difference is that the uncertainty domain of $\delta(z)$ is here different at each frequency. This similarity will help us to develop robustness tools for this uncertainty region $\mathcal{L}$.

8.6 Conclusions

In this chapter, we have shown that a PE identification procedure with a biased model structure allows one to design a dynamic uncertainty

[7]Such a description is due to the ellipsoidal uncertainty domain $U(\omega)$ at each frequency.

set $\mathcal{L}$ containing the true system with a probability larger than a given level. Moreover, we have also shown that this particular uncertainty region presents similarities with the uncertainty region $\mathcal{D}$ delivered by PE identification with unbiased model structures.

Chapter 9

Robustness analysis of $\mathcal{L}$

In the previous chapter, we have introduced a dynamic uncertainty region $\mathcal{L}$. This uncertainty region containing the true system with a probability larger than a given level is the uncertainty region obtained after a PE identification with biased model structure and stochastic embedding assumptions. The uncertainty region $\mathcal{L}$ is made up of transfer functions parametrized by a transfer vector[1] $\delta(z)$ which represents the real and imaginary parts of the dynamic uncertainty and whose frequency response is real. The uncertainty vector $\delta(z)$ is constrained to lie at each frequency in an ellipse.

Let us now consider that a PE identification procedure has delivered such uncertainty set $\mathcal{L}$. Let us also consider that we have chosen a model G_{mod} for control design (e.g. the center of $\mathcal{L}$) and that we have designed a controller C from that model G_{mod}. In order to validate the controller C with respect to the uncertainty region $\mathcal{L}$, we will develop, in this chapter, robust stability and performance analysis tools for such uncertainty set. These tools are the same as those developed for the uncertainty set $\mathcal{D}$ in Chapters 4 and 5 i.e. a necessary and sufficient condition for the stabilization of all plants in $\mathcal{L}$ by the controller C (*controller validation for stability*) and a procedure to compute the worst case performance achieved by C over all plants in $\mathcal{L}$ (*controller validation for performance*). These robustness tools give therefore a condition guaranteeing the stabilization of the unknown true system G_0 by the controller C and a lower bound of the performance achieved by the

[1] We use the term "transfer vector" with some abuse. The vector $\delta(z)$ is in fact a function of a complex variable.

controller C on the true system.

In order to obtain these robustness tools, we will use the similarities between the structure of $\mathcal{L}$ and $\mathcal{D}$. In that sense, our main contribution concerning the robustness analysis of uncertainty sets deduced from PE identification with stochastic embedding assumptions, has been achieved in the last section of Chapter 8. In that section, we have indeed expressed the general structure of $\mathcal{L}$ so that the tools developed in Chapters 4 and 5 for $\mathcal{D}$ can be easily adapted for $\mathcal{L}$.

Robust stability analysis. Just as for the uncertainty region $\mathcal{D}$, the necessary and sufficient condition for the stabilization of all plants in $\mathcal{L}$ by C is thus derived from the LFT framework of the uncertainty region $\mathcal{L}$. Indeed, we show that one can rewrite the closed-loop connection of the controller C and all plants in the uncertainty region $\mathcal{L}$ as a particular LFT where the uncertainty part is a transfer vector whose frequency response is real. In that particular LFT, the (real) stability radius can be computed exactly, using the result presented in [53, 72].

Our robust stability analysis tool is "better" than the one obtained in [79]. In [79], the authors present an LFT description of the closed-loop connection of the controller C and all plants in an uncertainty region $\mathcal{L}$, where the ellipsoids at each frequency are approximated by a mixed perturbation set. The main advantage of our LFT description is that it exactly represents the closed-loop connection of the controller C and all plants in the uncertainty region $\mathcal{L}$ without any approximation.

Robust performance analysis. Just as for $\mathcal{D}$, our robust performance analysis tool for $\mathcal{L}$ is based on the computation of the worst case performance of a closed-loop made up of the considered controller and a system in the uncertainty region $\mathcal{L}$. The performance of a particular loop made up of the controller C and a plant in $\mathcal{L}$ is here also defined as the largest singular value of a weighted version of the matrix containing the four closed-loop transfer functions of this loop. Our definition of the worst case performance is thus very general and, by an appropriate choice of the weights, allows one to derive most of the commonly used worst case performance measures such as e.g. the largest modulus of the sensitivity function. Our contribution is to show that the computation of the worst case performance can be formulated as an LMI-based

optimization problem. Just as in the case of $\mathcal{D}$, the LMI formulation of the problem uses the fact that the uncertainty part (i.e. the transfer vector $\delta(z)$) of the uncertainty region $\mathcal{L}$ appears linearly in the expression of both the numerator and the denominator of the systems in the uncertainty region $\mathcal{L}$ and, as a consequence, also appears linearly in the expression of the different closed-loop transfer functions.

If you are only interested by the largest modulus of one closed-loop transfer function (e.g. the sensitivity function), our LMI-optimization is not necessary. Indeed, in this case, the computation of the worst case performance can also be achieved by using the fact that an ellipse of uncertainty for the open-loop system maps into an ellipse of uncertainty for the closed-loop system (see [81, 30] for the case of a disk). However, this result can not be used to compute our more general worst case performance criterion. Our optimization approach has also the further advantage that it can easily be extended to the multivariable case.

Chapter outline. In Section 9.1, we present our procedure to validate a controller for stability with respect to an uncertainty set $\mathcal{L}$. In Section 9.2, we present the LMI procedure allowing the exact computation of the worst case performance achieved by a controller C over all plants in $\mathcal{L}$. In Section 9.3, we present a simulation example and we finish by drawing some conclusions in Section 9.4.

9.1 Robust stability analysis of $\mathcal{L}$

As said in the introduction, the aim of this first section is to validate a given controller for stability i.e. to find a necessary and sufficient condition for the stabilization of all plants in an uncertainty region $\mathcal{L}$ by this controller. Robust stability theory provides such necessary and sufficient conditions [34, 31, 92, 68, 53]. But for the application of robust stability results, it is required that the closed loop connections of this controller to all plants in the uncertainty region be rewritten as a set of loops that connect a known fixed dynamic matrix $M(z)$ to an uncertainty part $\Delta(z)$ of known structure that belongs to a prescribed uncertainty domain.

9.1.1 LFT framework for the uncertainty region $\mathcal{L}$ and a controller C

Just as was done for the uncertainty set $\mathcal{D}$ in Chapter 4, a first step is to find the particular set of loops, given in the general LFT framework, that correspond to the closed-loop connections of all plants in $\mathcal{L}$ with C. This is achieved using the following theorem which is very similar to Theorem 4.1.

Theorem 9.1 (LFT framework for $\mathcal{L}$) *Consider an uncertainty region $\mathcal{L}$ of plant transfer functions given by (8.22) and a controller $C(z) = X(z)/Y(z)$ [2]. The set of closed-loop connections $[G(z,\delta(z))\ C]$ for all $G(z,\delta(z)) \in \mathcal{L}$ can be rewritten into to the set of loops $[M_{\mathcal{L}}(z)\ \delta(z)]$ which obey the following system of equations*

$$\begin{cases} p = \delta(z)q \\ q = M_{\mathcal{L}}(z)p \end{cases} \tag{9.1}$$

The uncertainty part (i.e. the RI vector $\delta(z)$) has a real frequency response $\delta(e^{j\omega})$ that is constrained to lie, at the frequency ω, in the normalised uncertainty domain: $|T(\omega)\delta(e^{j\omega})|_2 < 1$. $T(\omega) \in \mathbf{R}^{2\times 2}$ is a square root of the matrix $R(\omega)$ defining $U(\omega)$ in (8.22): $R(\omega) = T(\omega)^T T(\omega)$. $M_{\mathcal{L}}(z)$ is a row vector of transfer functions of length 2 defined as:

$$M_{\mathcal{L}}(z) = -(Z_D + \frac{X(Z_N - \hat{G}Z_D)}{Y + \hat{G}X}). \tag{9.2}$$

Proof. The closed-loop connection of C and a particular plant $G(z,\delta(z)) = (\hat{G} + Z_N\delta(z))/(1 + Z_D\delta(z))$ in $\mathcal{L}$ (see (8.22)) is given by

$$\begin{cases} y = \frac{\hat{G}+Z_N\delta(z)}{1+Z_D\delta(z)}u = (\hat{G} + \frac{(Z_N-\hat{G}Z_D)\delta(z)}{1+Z_D\delta(z)})u \\ u = -Cy \end{cases} \tag{9.3}$$

By introducing two new signals q and p, we can restate (9.3) as

$$\begin{cases} \begin{pmatrix} q \\ y \end{pmatrix} = \overbrace{\begin{pmatrix} -Z_D & 1 \\ Z_N - \hat{G}Z_D & \hat{G} \end{pmatrix}}^{H(z)} \begin{pmatrix} p \\ u \end{pmatrix} \\ p = \delta(z)q \\ u = -Cy \end{cases} \tag{9.4}$$

[2] $X(z)$ and $Y(z)$ are the polynomials corresponding to the numerator and to the denominator of $C(z)$, respectively

By doing so, we have isolated the uncertainty vector $\delta(z)$ from the known matrix $H(z)$ and the controller $C(z)$. The variables y and u are now eliminated from (9.4), yielding the following system of equations which is equivalent to (9.1):

$$\begin{cases} p = \delta(z)q \\ q = \overbrace{(-Z_D - \dfrac{C(Z_N - \hat{G}Z_D)}{1+\hat{G}C})}^{M_{\mathcal{L}}(z)}\, p \end{cases} \tag{9.5}$$

The system (9.5) is equivalent with the closed-loop connection of a particular $G(z, \delta(z))$ in $\mathcal{L}$ with the controller C. In order to consider the closed-loop connections for all plants in $\mathcal{L}$, we have to consider all $\delta(z)$ such that $\delta(e^{j\omega}) \in \mathbf{R}^{2\times 1}$ lies in the ellipsoid $U(\omega)$ given by:

$$U(\omega) = \{\delta(e^{j\omega}) \mid \delta(e^{j\omega})^T R(\omega)\delta(e^{j\omega}) < 1\}. \tag{9.6}$$

This last expression is the uncertainty domain of the uncertainty vector $\delta(z)$ at the frequency ω. This uncertainty domain can be normalized. Using $R(\omega) = T(\omega)^T T(\omega)$, we see that

$$\delta(e^{j\omega}) \in U(\omega) \Leftrightarrow (T(\omega)\delta(e^{j\omega}))^T (T(\omega)\delta(e^{j\omega})) < 1 \Longleftrightarrow |T(\omega)\delta(e^{j\omega})|_2 < 1 \tag{9.7}$$

The set of loops $[M_{\mathcal{L}}\ \delta(z)]$ for all $\delta(z)$ such that $\delta(e^{j\omega}) \in \mathbf{R}^{2\times 1}$ lies in the uncertainty domain $|T(\omega)\delta(e^{j\omega})|_2 < 1$ is therefore equivalent to the set of closed-loop connections $[G(z, \delta(z))\ C]$ for all plants $G(z, \delta(z))$ in $\mathcal{L}$. This completes the proof. □

9.1.2 Robust stability condition for the uncertainty region $\mathcal{L}$

Theorem 9.1 allows us to "transform" our problem of testing if the controller C stabilizes all the plants in the uncertainty region $\mathcal{L}$ into the *equivalent* problem of testing if the set of loops $[M_{\mathcal{L}}(z)\ \delta(z)]$ are stable for all $\delta(z)$ such that $\delta(e^{j\omega}) \in \mathbf{R}^{2\times 1}$ lies in the uncertainty domain $|T(\omega)\delta(e^{j\omega})|_2 < 1$. This equivalent set of loops is very similar to the set of loops $[M(z)\ \beta]$ presented in Section 4.1 and for which there exists a robust stability theorem (see Proposition 4.1). The only difference is the size of the uncertainty domain which is here different at each frequency. As a consequence, Proposition 4.1 can not be used to find a necessary

and sufficient robust stability condition for the uncertainty set $\mathcal{L}$. However, we can derive the necessary and sufficient robust stability condition after a last effort of normalisation and using the following property of the stability radius of the loop $[M(z)\ \beta]$ (which is a direct consequence of its definition (4.3)).

Proposition 9.1 *Consider a known complex vector $M \in \mathbf{C}^{1\times b}$ and $\beta \in \mathbf{R}^{b\times 1}$. We have that $1 - M\beta \neq 0$ for all β such that $|\beta|_2 < 1$ if and only if*

$$\mu(M) \leq 1 \tag{9.8}$$

where μ is the stability radius defined in (4.3).

Theorem 9.2 (robust stability condition) *Consider an uncertainty region $\mathcal{L}$ of plant transfer functions having the general form (8.22) and let C be a controller that stabilizes the center $\hat{G}(z)$ of $\mathcal{L}$. All the plants in the uncertainty region $\mathcal{L}$ are stabilized by the controller C if and only if, at each frequency ω,*

$$\mu(M_{\mathcal{L}}(e^{j\omega})T^{-1}(\omega)) \leq 1. \tag{9.9}$$

with μ, the stability radius defined in (4.3), $R(\omega) = T(\omega)^T T(\omega)$ and $M_{\mathcal{L}}(z)$ as defined in (9.2).

Proof. By Theorem 9.1, our problem of testing if the controller C stabilizes all the plants in the uncertainty region $\mathcal{L}$ is equivalent to testing if the set of loops $[M_{\mathcal{L}}(z)\ \delta(z)]$ are stable for all $\delta(z)$ such that $\delta(e^{j\omega}) \in \mathbf{R}^{2\times 1}$ lies in the uncertainty domain $|T(\omega)\delta(e^{j\omega})|_2 < 1$.

A first step of this proof is to observe

- that $M_{\mathcal{L}}(z)$ is stable. Indeed, its denominator contains the denominator of the sensitivity function of the closed loop $[C\ \hat{G}(z)]$, which is stable by assumption, and the denominators of $Z_N(z)$ and $Z_D(z)$ which are also stable according to Proposition 8.4;
- that, by Definition 8.1, $\Delta(z) = (1\ j)\delta(z)$ with $\Delta(z) \in \mathcal{R}H_\infty$;
- and that the uncertainty domain of $\delta(z)$ i.e. $Dom(\delta(z)) = \{\delta(z) \mid |T(\omega)\delta(e^{j\omega})|_2 < 1\ \forall\omega\}$ is connected and contains $\delta(z) = 0$.

A first conclusion that follows from these observations is that one of the considered loops i.e. $[M_{\mathcal{L}}(z)\ \delta(z) = 0]$ is guaranteed to be stable. As a consequence, using the fact that $Dom(\delta(z))$ is connected and the fact that $\Delta(z) \in \mathcal{R}H_\infty$, the set of loops $[M_{\mathcal{L}}(z)\ \delta(z)]$ are internally stable for all $\delta(z) \in Dom(\delta(z))$ if and only if, at each frequency ω,

$$1 - M_{\mathcal{L}}(e^{j\omega})\delta(e^{j\omega}) \neq 0 \ \ \forall \delta(e^{j\omega}) \ \ \textit{such that} \ \ |T(\omega)\delta(e^{j\omega})|_2 < 1. \quad (9.10)$$

A final normalisation shows that expression (9.10) is equivalent with the statement (9.9). Indeed, if, at each frequency ω, we define a *real* vector $\phi(e^{j\omega}) \triangleq T(\omega)\delta(e^{j\omega})$, then, (9.10) is equivalent with:

$$1 - M_{\mathcal{L}}(e^{j\omega})T^{-1}(\omega)\phi(e^{j\omega}) \neq 0 \ \ \forall \phi(e^{j\omega}) \ \ \textit{such that} \ \ |\phi(e^{j\omega})|_2 < 1 \quad (9.11)$$

Since $\phi(e^{j\omega})$ is real, this last expression is equivalent with (9.9), by Proposition 9.1. □

Theorem 9.2 gives a necessary and sufficient condition for the stabilization of all plants in $\mathcal{L}$ by any controller that stabilizes $\hat{G}(z)$, the "center" of $\mathcal{L}$. This necessary and sufficient condition involves the computation at each frequency of the stability radius $\mu(M_{\mathcal{L}}(e^{j\omega})T^{-1}(\omega))$, which is achieved using Definition 4.1. Since the true system lies in $\mathcal{L}$, Theorem 9.2 gives also a condition guaranteeing that the controller C stabilizes the unknown true system G_0.

9.2 Robust performance analysis of $\mathcal{L}$

In this section, we show that we can evaluate the worst case performance achieved by some controller C with all systems in the uncertainty region $\mathcal{L}$, i.e. the worst level of performance of a closed loop made up of the connection of the considered controller and a particular plant in $\mathcal{L}$. This worst case performance is of course a lower bound for the closed-loop performance achieved with the true system. We say that a controller is validated for performance if the worst case performance in $\mathcal{L}$ remains below some threshold.

The worst case performance criterion over all plants in an uncertainty region $\mathcal{L}$ is defined in a similar way as has been defined, in Section 5.1,

the worst case performance achieved by a controller C over the plants in the uncertainty region $\mathcal{D}$.

Definition 9.1 *Consider an uncertainty region $\mathcal{L}$ of systems $G(z, \delta(z))$ whose general structure is given in (8.22). Consider also a controller $C(z)$. The worst case performance achieved by this controller at a frequency ω over all systems in $\mathcal{L}$ is defined as:*

$$J_{WC}(\mathcal{L}, C, W_l, W_r, \omega) = \max_{G(z,\delta(z))\in\mathcal{L}} \sigma_1 \left(W_l T(G(e^{j\omega}, \delta(e^{j\omega})), C(e^{j\omega})) W_r \right), \tag{9.12}$$

where $W_l(z) = diag(W_{l1}, W_{l2})$ and $W_r(z) = diag(W_{r1}, W_{r2})$ are diagonal weights, $\sigma_1(A)$ denotes the largest singular value of A, and $T(G, C)$ is the transfer matrix of the closed-loop system defined in (3.3).

The worst case performance J_{WC} can be computed at a given frequency using an LMI based optimization problem. The LMI procedure is now given in the following theorem. Note that this procedure is very similar to that used in Theorem 5.1 to compute the worst case performance in the uncertainty set $\mathcal{D}$.

Theorem 9.3 *Consider an uncertainty region $\mathcal{L}$ defined in (8.22) and a controller $C(z) = X(z)/Y(z)$ [3]. Then, at frequency ω, the criterion function $J_{WC}(\mathcal{L}, C, W_l, W_r, \omega)$ is obtained as*

$$J_{WC}(\mathcal{L}, C, W_l, W_r, \omega) = \sqrt{\gamma_{opt}}, \tag{9.13}$$

where γ_{opt} is the optimal value of γ for the following standard convex optimization problem involving LMI constraints evaluated at ω:

$$\begin{array}{ll} \textit{minimize} & \gamma \\ \textit{over} & \gamma,\ \tau \\ \textit{subject to} & \tau \geq 0 \quad \textit{and} \\ \multicolumn{2}{c}{\begin{pmatrix} Re(a_{11}) & Re(a_{12}) \\ Re(a_{12}^*) & Re(a_{22}) \end{pmatrix} - \tau \begin{pmatrix} R(\omega) & 0 \\ 0 & -1 \end{pmatrix} < 0} \end{array} \tag{9.14}$$

where

[3] $X(z)$ and $Y(z)$ are the polynomials corresponding to the numerator and to the denominator of $C(z)$, respectively

- $a_{11} = (Z_N^* W_{l1}^* W_{l1} Z_N + Z_D^* W_{l2}^* W_{l2} Z_D) - \gamma(Q Z_1^* Z_1)$
- $a_{12} = Z_N^* W_{l1}^* W_{l1} \hat{G} + W_{l2}^* W_{l2} Z_D^* - \gamma(Q Z_1^* (Y + \hat{G} X))$
- $a_{22} = \hat{G}^* W_{l1}^* W_{l1} \hat{G} + W_{l2}^* W_{l2} - \gamma(Q(Y + \hat{G} X)^* (Y + \hat{G} X))$
- $Q = 1/(X^* W_{r1}^* W_{r1} X + Y^* W_{r2}^* W_{r2} Y)$

Proof. In order to ease the establishment of the proof, we rewrite the weighted matrix $T_w(z, \delta(z)) \stackrel{\Delta}{=} W_l T(G(z, \delta(z)), C(z)) W_r$, using the definition of the closed-loop transfer matrix T in (3.3) and the expression of $G(z, \delta(z))$ in (8.22):

$$T_w(z, \delta(z)) = \frac{\begin{pmatrix} W_{l1} X(\hat{G} + Z_N \delta(z)) W_{r1} & W_{l1} Y(\hat{G} + Z_N \delta(z)) W_{r2} \\ W_{l2} X(1 + Z_D \delta(z)) W_{r1} & W_{l2} Y(1 + Z_D \delta(z)) W_{r2} \end{pmatrix}}{Y + \hat{G} X + (X Z_N + Y Z_D)\delta(z)} \tag{9.15}$$

It is important to note that $T_w(z, \delta(z))$ is of rank one. As a result (9.15) can be written as follows:

$$T_w(z, \delta(z)) = \begin{pmatrix} \frac{W_{l1}(\hat{G} + Z_N \delta(z))}{Y + \hat{G} X + Z_1 \delta(z)} \\ \frac{W_{l2}(1 + Z_D \delta(z))}{Y + \hat{G} X + Z_1 \delta(z)} \end{pmatrix} \begin{pmatrix} X W_{r1} & Y W_{r2} \end{pmatrix} \tag{9.16}$$

with $Z_1 = X Z_N + Y Z_D$. Using the above introduced notations, we can now state that proving Theorem 9.3 is equivalent to proving that the solution γ_{opt} of the LMI problem (9.14), evaluated at ω, is such that:

$$\sqrt{\gamma_{opt}} = \max_{\delta(e^{j\omega}) \in U(\omega)} \sigma_1(T_w(e^{j\omega}, \delta(e^{j\omega}))) \Longleftrightarrow$$

$$\gamma_{opt} = \max_{\delta(e^{j\omega}) \in U(\omega)} \lambda_1(T_w(e^{j\omega}, \delta(e^{j\omega}))^* T_w(e^{j\omega}, \delta(e^{j\omega})))$$

where $U(\omega) = \{\delta(e^{j\omega}) \mid \delta(e^{j\omega})^T R(\omega) \delta(e^{j\omega}) < 1\}$, and where $\sigma_1(A)$ and $\lambda_1(A)$ denote the largest singular value and the largest eigenvalue of A, respectively.

An equivalent and convenient way of restating the problem of computing $\max_{\delta(e^{j\omega}) \in U(\omega)} \lambda_1(T_w(e^{j\omega}, \delta(e^{j\omega}))^* T_w(e^{j\omega}, \delta(e^{j\omega})))$ is as follows:

minimize γ *such that*

$$\lambda_1(T_w(e^{j\omega},\delta(e^{j\omega}))^* T_w(e^{j\omega},\delta(e^{j\omega}))) - \gamma < 0 \quad \forall \delta(e^{j\omega}) \in U(\omega).$$

Since $T_w(e^{j\omega},\delta(e^{j\omega}))$ has rank one, we have:

$$\lambda_1(T_w(e^{j\omega},\delta(e^{j\omega}))^* T_w(e^{j\omega},\delta(e^{j\omega}))) - \gamma < 0 \Longleftrightarrow$$

$$\begin{pmatrix} \frac{W_{l1}(\hat{G}+Z_N\delta(e^{j\omega}))}{Y+\hat{G}X+Z_1\delta(e^{j\omega})} \\ \frac{W_{l2}(1+Z_D\delta(e^{j\omega}))}{Y+\hat{G}X+Z_1\delta(e^{j\omega})} \end{pmatrix}^* \begin{pmatrix} \frac{W_{l1}(\hat{G}+Z_N\delta(e^{j\omega}))}{Y+\hat{G}X+Z_1\delta(e^{j\omega})} \\ \frac{W_{l2}(1+Z_D\delta(e^{j\omega}))}{Y+\hat{G}X+Z_1\delta(e^{j\omega})} \end{pmatrix} \frac{1}{Q} - \gamma < 0 \Longleftrightarrow$$

$$\begin{pmatrix} \frac{W_{l1}(\hat{G}+Z_N\delta(e^{j\omega}))}{Y+\hat{G}X+Z_1\delta(e^{j\omega})} \\ \frac{W_{l2}(1+Z_D\delta(e^{j\omega}))}{Y+\hat{G}X+Z_1\delta(e^{j\omega})} \\ 1 \end{pmatrix}^* \begin{pmatrix} I_2 & 0 \\ 0 & -\gamma Q \end{pmatrix} \begin{pmatrix} \frac{W_{l1}(\hat{G}+Z_N\delta(e^{j\omega}))}{Y+\hat{G}X+Z_1\delta(e^{j\omega})} \\ \frac{W_{l2}(1+Z_D\delta(e^{j\omega}))}{Y+\hat{G}X+Z_1\delta(e^{j\omega})} \\ 1 \end{pmatrix} < 0 \quad (9.17)$$

where $Q = 1/(X^*W_{r1}^*W_{r1}X + Y^*W_{r2}^*W_{r2}Y)$. By pre-multiplying (9.17) by $(Y + \hat{G}X + Z_1\delta(e^{j\omega}))^*$ and post-multiplying the same expression by $(Y + \hat{G}X + Z_1\delta(e^{j\omega}))$, we obtain:

$$\begin{pmatrix} W_{l1}(\hat{G} + Z_N\delta(e^{j\omega})) \\ W_{l2}(1 + Z_D\delta(e^{j\omega})) \\ Y + \hat{G}X + Z_1\delta(e^{j\omega}) \end{pmatrix}^* \begin{pmatrix} I_2 & 0 \\ 0 & -\gamma Q \end{pmatrix} \begin{pmatrix} W_{l1}(\hat{G} + Z_N\delta(e^{j\omega})) \\ W_{l2}(1 + Z_D\delta(e^{j\omega})) \\ Y + \hat{G}X + Z_1\delta(e^{j\omega}) \end{pmatrix} < 0 \quad (9.18)$$

which is equivalent to the following constraint on $\delta(e^{j\omega})$ with variable γ

$$\begin{pmatrix} \delta(e^{j\omega}) \\ 1 \end{pmatrix}^* \begin{pmatrix} a_{11} & a_{12} \\ a_{12}^* & a_{22} \end{pmatrix} \begin{pmatrix} \delta(e^{j\omega}) \\ 1 \end{pmatrix} < 0 \quad (9.19)$$

with a_{11}, a_{12} and a_{22} as defined in (9.14). Since $\delta(e^{j\omega})$ is real, it can be shown that (9.19) is equivalent with

$$\overbrace{\begin{pmatrix} \delta(e^{j\omega}) \\ 1 \end{pmatrix}^T \begin{pmatrix} Re(a_{11}) & Re(a_{12}) \\ Re(a_{12}^*) & Re(a_{22}) \end{pmatrix} \begin{pmatrix} \delta(e^{j\omega}) \\ 1 \end{pmatrix}}^{\psi(\delta(e^{j\omega}))} < 0 \quad (9.20)$$

This last expression is equivalent to stating that $\lambda_1(T_w(e^{j\omega}, \delta(e^{j\omega}))^* T_w(e^{j\omega}, \delta(e^{j\omega}))) - \gamma < 0$ for a particular $\delta(e^{j\omega})$ in $U(\omega)$. However, this must be true for all $\delta(e^{j\omega}) \in U(\omega)$. Therefore (9.20) must be true for all $\delta(e^{j\omega})$ such that

$$\overbrace{\begin{pmatrix} \delta(e^{j\omega}) \\ 1 \end{pmatrix}^T \begin{pmatrix} R(\omega) & 0 \\ 0 & -1 \end{pmatrix} \begin{pmatrix} \delta(e^{j\omega}) \\ 1 \end{pmatrix}}^{\rho(\delta(e^{j\omega}))} < 0 \qquad (9.21)$$

which is equivalent to the statement "$\delta(e^{j\omega}) \in U(\omega)$".

Let us now recapitulate. Computing $\max_{\delta(e^{j\omega})\in U(\omega)} \lambda_1(T_w(e^{j\omega}, \delta(e^{j\omega}))^* T_w(e^{j\omega}, \delta(e^{j\omega})))$ is equivalent to finding the smallest γ such that $\psi(\delta(e^{j\omega})) < 0$ for all $\delta(e^{j\omega})$ for which $\rho(\delta(e^{j\omega})) < 0$. By the $\mathcal{S}$ procedure [55, 17], this problem is equivalent to finding the smallest γ and a positive scalar τ such that $\psi(\delta(e^{j\omega})) - \tau\rho(\delta(e^{j\omega})) < 0$, for all $\delta(e^{j\omega}) \in \mathbf{R}^{2\times 1}$, which is precisely (9.14). To complete this proof, note that since $\lambda_1(T_w(e^{j\omega}, \delta(e^{j\omega}))^* T_w(e^{j\omega}, \delta(e^{j\omega}))) = \sigma_1^2(T_w(e^{j\omega}, \delta(e^{j\omega})))$, the value $\max_{\delta(e^{j\omega})\in U(\omega)} \sigma_1(T_w(e^{j\omega}, \delta(e^{j\omega})))$ at ω is equal to $\sqrt{\gamma_{opt}}$, where γ_{opt} is the optimal value of γ. □

9.3 Simulation example

To illustrate our results, we present an example of controller validation based on an uncertainty region $\mathcal{L}_{ol}$ design using a PE identification procedure with stochastic embedding assumptions in open-loop. The open-loop model $G(z, \hat{\theta})$, center of $\mathcal{L}_{ol}$, is used to design the "to-be-validated" controller C. This controller is then validated for stability using the procedure of Section 9.1, and for performance using the procedure of Section 9.2.

Identification step. Let us consider the same true system G_0 as in [47]:

$$y(t) = \overbrace{\frac{0.0355z^{-1} + 0.0247z^{-2}}{1 - 1.2727z^{-1} + 0.3329z^{-2}}}^{G_0} u(t) + e(t)$$

where $e(t)$ is a white noise with a variance equal to 0.005. The sampling time is 1 second. We simulate this system collecting 300 data from which

we use the last 50 for least-square model fitting (the first 250 are used to get rid of initial condition effects). As in [47], we choose a second order Laguerre model of the form (the pole of the Laguerre model is chosen near the dominant pole of G_0):

$$G(z,[\theta_1,\theta_2]^T) = \frac{0.9063\ \theta_1 z^{-1}}{1-0.8187z^{-1}} + \frac{\theta_2 z^{-1}(0.7311-0.8954z^{-1})}{(1-0.8187z^{-1})^2}$$

Using the 50 data, the identified parameters are:

$$\hat{\theta}_1 = 0.1129 \quad \hat{\theta}_2 = -0.0689$$

Design of the uncertainty region $\mathcal{L}_{ol}$. The uncertainty region $\mathcal{L}_{ol}$ is constructed using the classical assumptions and the classical procedure described in Section 8.3, i.e. the unmodelled dynamic stochastic process is assumed to have impulse response coefficients η_n whose variance dies at an exponential rate: $\mathcal{E}(\eta_n^2) = \beta\lambda^n$, with β and λ determined by the measured data. The parameters β and λ and the variance σ^2 of the white noise $e(t)$ are estimated using the maximum likelihood technique described in [47]. This estimation delivers:

$$\hat{\beta} = 19.96, \quad \hat{\lambda} = 0.002, \quad \hat{\sigma}^2 = 0.006.$$

The number L in (8.4) is chosen equal to 15 as in [47]. These values allow us to design a frequency domain uncertainty region $\mathcal{L}_{ol}$ made up of ellipses at each frequency in the Nyquist plane. The desired probability for the presence of G_0 in $\mathcal{L}_{ol}$ is here chosen equal to 0.9. This uncertainty region is represented in Figure 9.1. Even though $G_0(e^{j\omega})$ seems at each frequency to lie in the ellipses, it is to be noted that, at very few ones, $G_0(e^{j\omega})$ lies slightly outside. This phenomenon can be explained by the nonlinear optimization that delivers the estimate of the stochastic parameters, by the very few data used to design the uncertainty regions, but also by the chosen probabilistic framework.

Control design. The second order Laguerre model $G(z,[\hat{\theta}_1,\hat{\theta}_2]^T)$ is chosen as model G_{mod} for control design. From this model G_{mod}, we have designed a controller with a lead-lag filter:

$$C(z) = \frac{5.2314 - 3.8667z^{-1}}{1-0.6z^{-1}}.$$

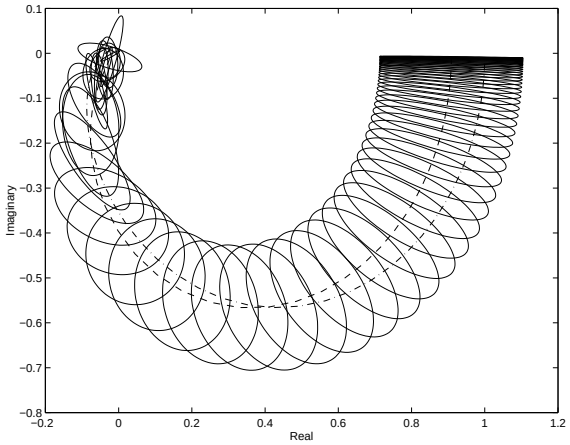

Figure 9.1: Ellipses of $\mathcal{L}_{ol}$ at some frequencies, $G(e^{j\omega}, [\hat{\theta}_1, \hat{\theta}_2]^T)$ (dashed) and $G_0(e^{j\omega})$ (dashdot) in the Nyquist plane

With this controller, the designed closed-loop $[C\ G_{mod}]$ has a phase margin of 85 degrees. The cut-off frequency ω_c is equal to 0.5. Before applying this controller $C(z)$ to the true system, we verify whether it achieves satisfactory behaviour with all plants in an uncertainty region $\mathcal{L}_{ol}$ (and therefore also with the true system G_0).

Validation of C for stability. We can use the procedure presented in Section 9.1 to check whether C stabilizes all plants in $\mathcal{L}_{ol}$. For this purpose, we construct the row vector $M_{\mathcal{L}_{ol}}(z)$ defined in Theorem 9.1 and we compute the corresponding stability radius $\mu(M_{\mathcal{L}_{ol}}(e^{j\omega})T^{-1}(\omega))$ at all frequencies. The stability radii are plotted in Figure 9.2. The maximum over all frequencies in $[0\ \pi]$ is $0.4577 < 1$; thus, we conclude that $C(z)$ stabilizes all plants in $\mathcal{L}_{ol}$ (and therefore also the true system G_0). In other words, C is validated for stability.

Validation of C for performance. In order to verify that C gives satisfactory performance with all plants in $\mathcal{L}_{ol}$, we choose the sensitivity function T_{22} as performance indicator, and we compute, at each frequency, the largest modulus $t_{\mathcal{L}_{ol}}(\omega, T_{22})$ of T_{22}. This can be done by computing $J_{WC}(\mathcal{L}_{ol}, C, W_l, W_r, \omega)$ using Theorem 9.3 with the particular weights $W_l = W_r = diag(0, 1)$. The worst case modulus of all sensitivity functions over $\mathcal{L}_{ol}$ is represented in Figure 9.3. It is compared

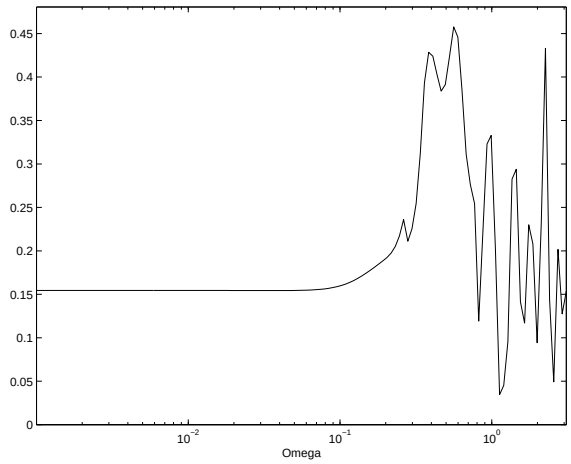

Figure 9.2: $\mu(M_{\mathcal{L}_{ol}}(e^{j\omega})T^{-1}(\omega))$ in $[0\ \pi]$

with the sensitivity functions of the designed closed loop $[C\ G_{mod}]$ and that of the achieved closed loop $[C\ G_0]$. From $t_{\mathcal{L}_{ol}}(\omega, T_{22})$, we can find that the worst case static error $(=t_{\mathcal{L}_{ol}}(0, T_{22}))$ resulting from a constant disturbance of unit amplitude is equal to 0.2889, whereas this static error is 0.2438 in the designed closed-loop and 0.2267 in the achieved closed loop. Using $t_{\mathcal{L}_{ol}}(\omega, T_{22})$, we can also see that the bandwidth of $\omega_c = 0.5$ in the designed closed-loop is almost preserved for all closed loops with a plant in $\mathcal{L}_{ol}$ since $t_{\mathcal{L}_{ol}}(\omega, T_{22})$ is equal to 1 at $\omega_c \simeq 0.33$. The difference between the resonance peak of the designed sensitivity function (i.e. $\max_\omega \parallel T_{22}(G_{mod}, C) \parallel = 1.1626$) and the worst case reasonance peak achieved by a plant in $\mathcal{L}_{ol}$ (i.e. $\max_\omega t_{\mathcal{L}_{ol}}(\omega, T_{22}) = 2.45$) also remains small. Note that the actually achieved resonance peak (i.e. $\max_\omega \parallel T_{22}(G_0, C) \parallel$) is equal to 1.3930. A last remark is to note that the actually achieved sensitivity function is at very few frequencies slightly above the template $t_{\mathcal{L}_{ol}}(\omega, T_{22})$. This is due to the fact that $G_0(e^{j\omega})$ lies slightly outside $\mathcal{L}_{ol}$ at those frequencies.

We may therefore conclude that the controller C is validated for performance since the difference between the nominal and worst case performance level remains very small at every frequency. With such stability and performance analysis results, one would confidently apply the controller to the real system, assuming that the nominal performance

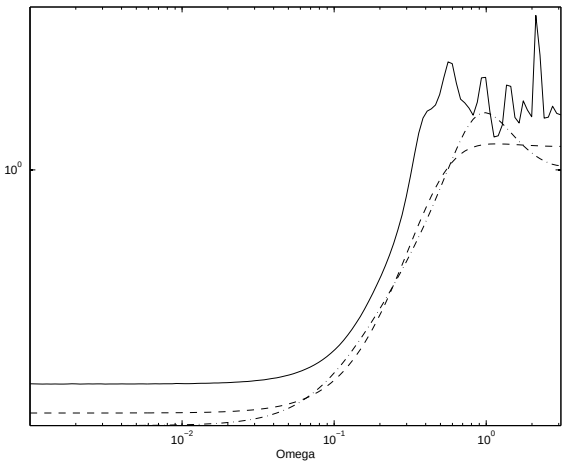

Figure 9.3: $t_{\mathcal{L}_{ol}}(\omega, T_{22})$ (solid) and modulus of the designed sensitivity function $T_{22}(G_{mod}, C)$ (dashed) and actually achieved sensitivity function $T_{22}(G_0, C)$ (dashdot)

is judged to be satisfactory.

9.4 Conclusions

In this chapter, we have developed the robust stability and robust performance analysis tools for the uncertainty region $\mathcal{L}$. This uncertainty region $\mathcal{L}$ is the uncertainty region obtained after a PE identification procedure with biased model structure and with stochastic embedding assumptions. The robust stability analysis tool for $\mathcal{L}$ is a necessary and sufficient condition for the stabilization of all plants in $\mathcal{L}$ by a given controller. The robust performance analysis tool is an LMI procedure that exactly computes the worst case performance achieved by a given controller over all plants in $\mathcal{L}$. It is to be noted that we can compute the worst case chordal distance at each frequency for the set $\mathcal{L}$ (see e.g. our paper [10]). However, the maximum of these worst case chordal distances over the frequencies is not guaranteed to deliver the worst case ν-gap since we do not have a similar result for $\mathcal{L}$ as Lemma 3.1 for $\mathcal{D}$.

Chapter 10

Conclusions

10.1 Contribution of this thesis

This thesis presents a framework to connect PE identification with Robust Control theory. The proposed framework has been initially presented for PE identification with an unbiased model structure, but has been extended, in the last part of the thesis, to PE identification with a biased model structure in the case where this model structure is linearly parametrized.

First, we have shown that PE identification with unbiased model structure yields an uncertainty region $\mathcal{D}$ containing the true system at a certain probability level. We have developed a procedure to compute such uncertainty region for open-loop identification, different types of closed-loop identification methods, but also the MEM approach. This uncertainty region takes the form of a set of transfer functions whose parameter vector is constrained to lie in an ellipsoid. We have then developed robustness tools that are adapted to this uncertainty set. The first robustness tool is a necessary and sufficient condition for the stabilization of all plants in $\mathcal{D}$ by a given controller. The second robustness tool is an LMI procedure to compute exactly the worst case performance achieved by a controller over all plants in $\mathcal{D}$. We have also introduced a measure of the uncertainty set $\mathcal{D}$ that is directly connected to a set of model-based controllers that stabilize all plants in this set $\mathcal{D}$. This measure is used to assess the quality of the uncertainty set with respect to robustly stable control design. From that measure, we have also deduced guidelines for the design of the identification experiment, paving

therefore the way to a new research field i.e. *PE identification for robust control.*

We have also developed results in order to represent $\mathcal{D}$ in the Nyquist plane. Our results are restricted to linearly parametrized uncertainty regions $\mathcal{D}$. We have shown that the mapping between the parameter space and the Nyquist plane is not bijective and that the image of $\mathcal{D}$ in the Nyquist plane contains therefore more plants than $\mathcal{D}$.

In the last part of this thesis, we have extended our framework to the case of PE identification with a biased model structure, provided that this model structure is linearly parametrized. For this purpose, we have used the stochastic embedding assumptions. Our first contribution has been to propose a proper way to design the uncertainty region deduced from stochastic embedding in open-loop. We have then extended the stochastic embedding technique to closed-loop identification and given a general expression of the uncertainty set $\mathcal{L}$ delivered by PE identification with stochastic embedding assumptions that is valid as well in open-loop as in closed-loop. This uncertainty region $\mathcal{L}$ takes the form of a set of transfer functions parametrized by a transfer vector whose frequency response is real and constrained to lie in an ellipse at each frequency. We have then developed the robustness tools adapted to this uncertainty set $\mathcal{L}$ i.e. a necessary and sufficient robust stability condition for $\mathcal{L}$ and an LMI procedure to compute the worst case performance in that set $\mathcal{L}$. It is to be noted that a technical problem has prevented us from computing the worst case ν-gap for $\mathcal{L}$.

10.2 Open questions

Have we closed the gap between PE identification and Robust Control theory. Of course, not ! We have contributed to reduce it, but there remain some open problems. Some are technical, the others are open research fields.

10.2.1 Open technical problems

Let us begin by the problems we have just mentioned at the end of Section 10.1. We still need to find a procedure to derive the worst case ν-gap in the uncertainty region $\mathcal{L}$ obtained by stochatic embedding from the worst case chordal distances at each frequency. The problem is

here that a result in that sense exists for parametric uncertainty regions (like $\mathcal{D}$) but not for frequency domain uncertainty regions (like $\mathcal{L}$). In Chapter 4, we have also mentioned that we are currently investigating the possibility to compute a measure for robust stability $\mu_{min}(\mathcal{D})$ (or $\mu_{min}(\mathcal{L})$) based on the necessary and sufficient result of that chapter in order to improve the result of Chapter 3 that is based on sufficient conditions only. Another and important technical problem is the extension to Multiple Inputs Multiple Outputs (MIMO) systems. Indeed, the result of this thesis has been presented in the SISO context. While many of the new *concepts* carry over to the MIMO case, the extension of a number of our technical and computational results is by no means trivial.

10.2.2 Open research fields

In Chapter 3, we have paved the way to a new research field i.e. *PE identification for robust control*. We have indeed characterized what quality an uncertainty set deduced from PE identification must possess for it to be tuned for robustly stable control design based on the model, and we have drawn guidelines for the design of the identification experiment. Plenty of work is still to be achieved in this direction. In Section 10.2.1, we have already stated the problem that follows from the fact that our result is based on a sufficient condition only. A lot of research has also to be done in order to apply, in practice, the proposed guidelines for the design of the identification experiment. Moreover, our result is restricted to stability purposes. It will be interesting to seek a *robust performance measure* for the uncertainty sets delivered by PE identification.

It would also be interesting to integrate our framework in one of the iterative schemes [24, 90, 75] that alternate control design and identification steps (for example on a real-life plant).

Another possible development may be a procedure to apply when one (or both) controller validation procedure (stability and/or performance) has failed with respect to an uncertainty set $\mathcal{D}$[1]. We have then two possibilities:

- We perform a new identification experiment yielding a new uncertainty set $\mathcal{D}_{bis}$. When we have this new uncertainty set, we try

[1] or $\mathcal{L}$

again to validate the controller with respect to this new uncertainty set $\mathcal{D}_{bis}$.

- We design a new controller and we try to validate this new controller with respect to the uncertainty set $\mathcal{D}$.

In the first case, we are back in the problem of designing the validation experiment in order to obtain an uncertainty set that is tuned for robust control design. In the second case, we face the problem of designing a robust controller with respect to the uncertainty sets $\mathcal{D}$ or $\mathcal{L}$. For this purpose, μ-analysis can be investigated. However, this technique has the drawback of not being guaranteed to converge.

Another possible extension is the extension of our framework to PE identification with a biased model structure in the general case where the model structure is *not linearly parametrized*. Finally, another possible research field is the extension of the results of Chapter 7 to the general case of nonlinearly parametrized uncertainty regions $\mathcal{D}$.

Appendix A

Appendices to Chapter 7

A.1 Proof of Lemma 7.1

The inverse of the block matrix P can be written (see e.g. [92, page 22])

$$P^{-1} = \begin{pmatrix} K_{11} & K_{12} \\ K_{12}^T & K_{22} \end{pmatrix}$$

where $K_{11} = P_{11}^{-1} + P_{11}^{-1}P_{12}\Delta^{-1}P_{12}^T P_{11}^{-1}$, $K_{12} = -P_{11}^{-1}P_{12}\Delta^{-1}$, $K_{22} = \Delta^{-1}$ and $\Delta = P_{22} - P_{12}^T P_{11}^{-1} P_{12}$.

Using these notations and introducing the vector $z = K_{22}^{-1}K_{12}^T x + \bar{x}$, we have the following equivalences:

$$\begin{aligned} \begin{pmatrix} x \\ \bar{x} \end{pmatrix}^T P^{-1} \begin{pmatrix} x \\ \bar{x} \end{pmatrix} < 1 \quad &\Longleftrightarrow \quad x^T(K_{11} - K_{12}K_{22}^{-1}K_{12}^T)x + z^T K_{22} z < 1 \\ &\Longleftrightarrow \quad x^T P_{11}^{-1} x + z^T K_{22} z < 1 \end{aligned} \tag{A.1}$$

Using this last expression, we can now write that

1. if $(x^T \ \bar{x}^T)^T \in U_{x\bar{x}}$, then $x^T P_{11}^{-1} x < 1$. Indeed

$$\begin{pmatrix} x \\ \bar{x} \end{pmatrix}^T P^{-1} \begin{pmatrix} x \\ \bar{x} \end{pmatrix} < 1 \Longrightarrow x^T P_{11}^{-1} x < (1 - z^T K_{22} z) < 1$$

2. if $x^T P_{11}^{-1} x < 1$ then there exists $\bar{x}$ such that $(x^T \ \bar{x}^T)^T \in U_{x\bar{x}}$. Indeed, take as $\bar{x}$, the vector $\bar{x}$ such that $z = 0$ (i.e. $\bar{x} = -K_{22}^{-1}K_{12}^T x$). Then, $\begin{pmatrix} x \\ -K_{22}^{-1}K_{12}^T x \end{pmatrix} \in U_{x\bar{x}}$.

This completes the proof. □

A.2 Proof of Theorem 7.2

We first prove that the inverse image of U_x by the mapping (7.12) is given by (7.20). This follows directly from:

$$x^T P_x^{-1} x < \chi \Longleftrightarrow y^T T^T P_x^{-1} T y < \chi \tag{A.2}$$

The volume C_y is thus the inverse image of U_x since y has to satisfy the right-hand side of (A.2) in order to have x in U_x.

It follows from $R_C = T^T P_x^{-1} T \in \mathbf{R}^{k \times k}$ with T of rank $n < k$ that R_C has $k - n$ null eigenvalues and that the corresponding eigenvectors are in the null-space of the mapping T.

Theorem 7.1 and the definition (7.19) of C_y show that U_y is included in C_y. Indeed, we know by Theorem 7.1 that each y in U_y has an image (i.e. Ty) in U_x. Therefore, each y in U_y lies in C_y defined by (7.19). $\square$

Appendix B

PE identification with stochastic embedding assumptions in open loop

In this appendix, we give some details about the results of PE identification with stochastic embedding assumptions that are presented in Proposition 8.1. The results presented below can be found in [47]. In order to ease the notations, we will assume that $H_0 = 1$. However, it is not a requirement as shown in [47].

According to Proposition 8.1, a PE identification procedure with Assuptions 8.1 delivers a model $G(z, \hat{\theta}) \in \mathcal{M}$ and an estimate P_ρ of the covariance matrix C_ρ of the vector $\tilde{\rho}$ parametrizing the error between G_0 and the identified model $G(z, \hat{\theta})$.

B.1 Identification of a model in $\mathcal{M}$

In order to identify a model $G(z, \hat{\theta})$, we collect N input signals $u(t)$ and the N corresponding output signals $y(t)$ generated by (8.3). Just as was done in Section 2.1.3, we can write the relation between the N signals $y(t)$ and the N signals $u(t)$ as follows using the approximation (8.4):

$$\overbrace{\begin{pmatrix} y(1) \\ y(2) \\ \vdots \\ y(N) \end{pmatrix}}^{Y} = \overbrace{\begin{pmatrix} \phi(1) \\ \phi(2) \\ \vdots \\ \phi(N) \end{pmatrix}}^{\Phi} \theta_0 + \overbrace{\begin{pmatrix} \psi(1) \\ \psi(2) \\ \vdots \\ \psi(N) \end{pmatrix}}^{\Psi} \eta + \overbrace{\begin{pmatrix} e(1) \\ e(2) \\ \vdots \\ e(N) \end{pmatrix}}^{E} \tag{B.1}$$

where $\phi(t) \in \mathbf{R}^{1\times k}$ $(t = 1...N)$ is equal to $\Lambda(z)u(t)$ and $\psi(t) \in \mathbf{R}^{1\times L}$ $(t = 1...N)$ is defined by:

$$\psi(t) = \begin{pmatrix} u(t-1) & u(t-2) & ... & u(t-L) \end{pmatrix}.$$

Since the predicted output of a system $G(z,\theta)$ in $\mathcal{M}$ is given by $\hat{y}(t,\theta) = \phi(t)\theta$, the estimate $\hat{\theta}$ minimizing the criterion (2.3) is:

$$\hat{\theta} = (\Phi^T\Phi)^{-1}\Phi^T Y = QY. \tag{B.2}$$

Let us now analyze the mean and the covariance of the estimate $\hat{\theta}$. These values will be used in the sequel in order to express the matrix C_ρ defined in (8.6). The mathematical expectation $\mathcal{E}\hat{\theta}$ of $\hat{\theta}$ can be computed as follows:

$$\begin{aligned} \mathcal{E}\hat{\theta} &= \mathcal{E}[(\Phi^T\Phi)^{-1}\Phi^T \overbrace{(\Phi\theta_0 + \Psi\eta + E)}^{Y}] \\ &= \theta_0 + Q\mathcal{E}(\Psi\eta + E) \\ &= \theta_0 \end{aligned} \tag{B.3}$$

The fact that the unmodeling is considered as the realization of a zero mean stochastic process independent of the noise $e(t)$ has as consequence that the estimate $\hat{\theta}$ has a mean equal to θ_0. Using the same property, the covariance matrix C of the estimate $\hat{\theta}$ can now be derived as follows:

$$\begin{aligned} C = \mathcal{E}[(\hat{\theta} - \theta_0)(\hat{\theta} - \theta_0)^T] &= \mathcal{E}[(Q(\Psi\eta + E))(Q(\Psi\eta + E))^T] \\ &= Q(\Psi C_\eta \Psi^T + \sigma^2 I_N)Q^T, \end{aligned} \tag{B.4}$$

where σ^2 is the variance of the white noise $e(t)$ and $C_\eta \stackrel{\Delta}{=} \mathcal{E}(\eta\eta^T)$ is, according to Assumptions 8.1, equal to

$$C_\eta = diag(\beta\lambda, \beta\lambda^2, ..., \beta\lambda^L) \tag{B.5}$$

B.2 Error between $G_0(z)$ and $G(z,\hat{\theta})$

After having identified a model $G(z,\hat{\theta})$, we can now express the error between the true system G_0 and the identified model. For this purpose, let us rewrite $G_0(z)$ and the model $G(z,\hat{\theta})$ as follows using (8.2) and (8.4):

$$G_0(z) = G(z,\theta_0) + \sum_{n=1}^{L} \eta_n z^{-n} = \begin{pmatrix} \Lambda(z) & \Pi(z) \end{pmatrix} \begin{pmatrix} \theta_0 \\ \eta \end{pmatrix} \tag{B.6}$$

$$G(z,\hat{\theta}) = \begin{pmatrix} \Lambda(z) & \Pi(z) \end{pmatrix} \begin{pmatrix} \hat{\theta} \\ 0 \end{pmatrix} \tag{B.7}$$

The difference between these two transfer functions is thus equal to

$$G_0(z) - G(z,\hat{\theta}) = \begin{pmatrix} \Lambda(z) & \Pi(z) \end{pmatrix} \overbrace{\begin{pmatrix} \theta_0 - \hat{\theta} \\ \eta \end{pmatrix}}^{\tilde{\rho}} \tag{B.8}$$

If we assume that the impulse response coefficients η_n of $G_\Delta(z)$ are Gaussian distributed, $\tilde{\rho} \in \mathbf{R}^{(k+L)\times 1}$ has (asymptotically) a Gaussian distribution. Using (B.3) and the fact that $\mathcal{E}(\eta_n) = 0$, the mean of this Gaussian distribution is zero. The covariance matrix C_ρ can be deduced from (B.4), (B.5), and the fact that

$$\mathcal{E}[(\theta_0 - \hat{\theta})\eta^T] = \mathcal{E}[(-Q\Psi\eta - QE)\eta^T] = -Q\Psi C_\eta$$

The covariance matrix C_ρ is thus equal to:

$$C_\rho = \begin{pmatrix} C & -Q\Psi C_\eta \\ -C_\eta \Psi^T Q^T & C_\eta \end{pmatrix}.$$

The matrix C_ρ is unknown since the variance σ^2 of the white noise $e(t)$ and C_η are unknown. However, we can obtain estimates $\hat{\sigma}^2$, $\hat{\beta}$ and $\hat{\lambda}$ of the stochastic parameters σ^2, β and λ by using a maximum likelihood technique [47]. As a consequence, we also obtain an estimate P_ρ of C_ρ:

$$P_\rho = \begin{pmatrix} P_\theta & -Q\Psi\hat{C}_\eta \\ -\hat{C}_\eta \Psi^T Q^T & \hat{C}_\eta \end{pmatrix}.$$

where $\hat{C}_\eta = diag(\hat{\beta}\hat{\lambda}, \hat{\beta}\hat{\lambda}^2, ..., \hat{\beta}\hat{\lambda}^L)$ and P_θ is the estimate of the matrix C given by

$$P_\theta = Q(\Psi\hat{C}_\eta\Psi^T + \hat{\sigma}^2 I_n)Q^T$$

Bibliography

[1] P. Andersen, S. Toffner-Clausen, and T.S. Pedersen. Estimation of frequency domain model uncertainties with application to robust control design. In *Proc. IFAC Symposium on System Identification*, pages 603–608, Copenhagen, 1994.

[2] B.D.O. Anderson, X. Bombois, M. Gevers, and C. Kulcsar. Caution in iterative modeling and control design. In *Proc. IFAC Workshop on Adaptative Systems in Control and Signal Processing*, pages 13–19, Glasgow, 1998.

[3] K.J. Åström and J. Nilsson. Analysis of a scheme for iterated identification and control. In *Proc. IFAC Symp. on Identification*, pages 171–176, Copenhagen, Denmark, 1994.

[4] B.R. Barmish. *New Tools for Robustness of Linear Systems.* MacMillan, 1994.

[5] S.P. Bhattacharyya, H. Chapellat, and L.H. Keel. *Robust Control - The Parametric Approach.* Prentice Hall, Upper Saddle River, New Jersey, 1995.

[6] G. Bianchini, P. Falugi, A. Tesi, and A. Vicino. Restricted complexity robust controllers for uncertain plants with rank one real perturbations. In *Proc. IEEE Conference on Decision and Control*, pages 1213–1218, Tampa, Florida, 1998.

[7] R.M. Biernacki, H. Hwang, and S.P. Bhattacharyya. Robust stability with structured real parameter perturbations. *IEEE Transactions on Automatic Control*, 32(6):495–506, 1987.

[8] X. Bombois, B.D.O. Anderson, and M. Gevers. Frequency domain image of a set of linearly parametrized transfer functions. Submitted to the European Control Conference (ECC01), Porto, 2001.

[9] X. Bombois, M. Gevers, and G. Scorletti. A measure of robust stability for a set of parametrized transfer functions. To appear in IEEE Transactions on Automatic Control, December 2000.

[10] X. Bombois, M. Gevers, and G. Scorletti. Controller validation for a validated model set. In *CD-ROM Proc. European Control Conference*, paper 869, Karlsruhe, Germany, 1999.

[11] X. Bombois, M. Gevers, and G. Scorletti. Controller validation for stability and performance based on a frequency domain uncertainty region obtained by stochastic embedding. In *CD-ROM Proc. 39th Conference on Decision and Control*, paper TuM06-5, Sydney, Australia, 2000.

[12] X. Bombois, M. Gevers, and G. Scorletti. Controller validation based on an identified model. In *Proc. IEEE Conference on Decision and Control*, pages 2816–2821, Phoenix, Arizona, 1999.

[13] X. Bombois, M. Gevers, G. Scorletti, and B.D.O. Anderson. Controller validation for stability and performance based on an uncertainty region designed from an identified model. CESAME Technical Report 99.36.

[14] X. Bombois, M. Gevers, G. Scorletti, and B.D.O. Anderson. Robustness analysis tools for an uncertainty set obtained by prediction error identification. Revised version submitted to Automatica, April 2000.

[15] X. Bombois, M. Gevers, G. Scorletti, and B.D.O. Anderson. Controller validation for stability and performance based on an uncertainty region designed from an identified model. In *CD-ROM Proc. IFAC Symposium on System Identification*, paper WePM1-6, Santa Barbara, California, 2000.

[16] B. Boulet and B.A. Francis. Consistency of open-loop experimental frequency-response data with coprime factor plant models. *IEEE Transactions on Automatic Control*, 43(12):1680–1691, 1998.

[17] S. Boyd, L. El Ghaoui, E. Feron, and V. Balakrishnan. *Linear Matrix Inequalities in Systems and Control Theory*, volume 15 of *Studies in Appl. Math.* SIAM, Philadelphia, June 1994.

[18] H. Chapellat, M. Dahleh, and S. Bhattacharyya. Robust stability under structured and unstructured perturbations. *IEEE Transactions on Automatic Control*, 35(10):1100–1107, 1990.

[19] J. Chen. Frequency-domain tests for validation of linear fractional uncertain models. *IEEE Transactions on Automatic Control*, 42(6):748–760, 1997.

[20] G. Chesi, A. Garulli, A. Tesi, and A. Vicino. Exact bounds for the frequency response of an uncertain plant with ellipsoidal perturbations. In *CD-ROM Proc. IFAC Symposium on System Identification*, paper WeMD1-5, Santa Barbara, California, 2000.

[21] B. Codrons, B.D.O. Anderson, and M. Gevers. Closed-loop identification with an unstable or nonminimum phase controller. In *CD-ROM Proc. IFAC Symposium on System Identification*, paper ThPM1-3, Santa Barbara, California, 2000.

[22] B. Codrons, X. Bombois, M. Gevers, and G. Scorletti. A practical application of recent results in model and controller validation to a ferrosilicon production process. In *CD-ROM Proc. 39th Conference on Decision and Control*, paper WeP07-6, Sydney, Australia, 2000.

[23] M. Dahleh, A. Tesi, and A. Vicino. An overview of extremal properties for robust control of interval plants. *Automatica*, 29(3):707–721, 1993.

[24] R.A. de Callafon. *Feedback Oriented identification for enhanced and robust control: a fractional approach applied to a wafer stage*. PhD thesis, Delft University of Technology, 1998.

[25] R.A. de Callafon and P.M.J. Van den Hof. Suboptimal feedback control by a scheme of iterative identification and control design. *Mathematical Modelling of Systems*, 3(1):77–101, 1997.

[26] D.K. de Vries and P.M.J. Van den Hof. Quantification of uncertainty in transfer function estimation: a mixed probabilistic - worst-case approach. *Automatica*, 31:543–558, 1995.

[27] P. Van den Hof and R.A. de Callafon. Multivariable closed-loop identification: from indirect identification to dual-youla parametrization. In *Proc. Conference on Decision and Control*, pages 1397–1402, Kobe, Japan, 1996.

[28] P.M.J. Van den Hof. Closed-loop issues in system identification. In *Proc. IFAC Symposium on Sytem Identifiaction*, pages 1651–1664, Kitakyushu, Japan, 1997.

[29] C. Desoer, R. Liu, J. Murray, and R. Saeks. Feedback system design: the fractional representation approach to analysis and synthesis. *IEEE Transactions on Automatic Control*, 25:399–412, 1980.

[30] H. Dötsch. *Identification for control design with application to a compact disk mechanism.* PhD thesis, Delft University of Technology, The Netherlands, 1998.

[31] J.C. Doyle. Analysis of feedback systems with structured uncertainties. *IEE Proc.*, 129-D(6):242–250, November 1982.

[32] L. El Ghaoui, R. Nikoukhah, and F. Delebecque. `LMITOOL`*: A front-end for LMI optimization, users's guide*, February 1995. Avalaible via anonymous ftp to `ftp.ensta.fr`, under `/pub/elghaoui/lmitool`.

[33] M. K. H. Fan and A. L. Tits. A measure of worst-case H_∞ performance and of largest acceptable uncertainty. *Syst. Control Letters*, 18:409–421, 1992.

[34] M. K. H. Fan, A. L. Tits, and J. C. Doyle. Robustness in the presence of mixed parametric uncertainty and unmodeled dynamics. *IEEE Trans. Aut. Control*, 36(1):25–38, January 1991.

[35] G. Ferreres and V. Fromion. Computation of the robustness margin with the skewed μ-tool. *Syst. Control Letters*, 32:193–202, 1997.

[36] P. Gahinet, A. Nemirovsky, A. L. Laub, and M. Chilali. *LMI Control Toolbox.* The Mathworks Inc., 1995.

[37] J.H. Braslavsky G.C. Goodwin and M. Seron. Nonstationnary stochastic embedding for transfer function estimation. In *Proc. IFAC World Congress*, Beijing, 1999.

[38] M. Gevers. Towards a joint design of identification and control? In H.L. Trentelman and J.C. Willems, editors, *Essays on Control: Perspectives in the Theory and its Applications, Birkhauser, New York*, pages 111–151, New York, 1993. Birkhauser.

[39] M. Gevers, B. D.O. Anderson, and B. Codrons. Issues in modeling for control. In *Proc. American Control Conference*, pages 1615–1619, Philadelphia, USA, 1998.

[40] M. Gevers, X. Bombois, B. Codrons, F. De Bruyne, and G. Scorletti. The role of experimental conditions in model validation for control. In A. Garulli, A. Tesi, and A. Vicino, editors, *Robustness in Identification and Control - Proc. of Siena Workshop, July 1998*, volume 245 of *Lecture Notes in Control and Information Sciences*, pages 72–86. Springer Verlag, 1999.

[41] M. Gevers, X. Bombois, B. Codrons, F. De Bruyne, and G. Scorletti. Model validation for robust control and controller validation in a prediction framework. In *CD-ROM Proc. IFAC Symposium on System Identification*, paper WeAM1-1, Santa Barbara, California, 2000.

[42] M. Gevers, X. Bombois, B. Codrons, G. Scorletti, and B.D.O. Anderson. Model validation for control and controller validation: a prediction error identification approach. Submitted to Automatica.

[43] M. Gevers, B. Codrons, and F. De Bruyne. Model validation in closed-loop. In *Proc. American Control Conference,*, pages 326–330, San Diego, California,1999.

[44] M. Gevers, P.M.J. Van den Hof, and L. Ljung. Asymptotic variance expressions for closed-loop identification and their relevance in identification for control. In *Proc. 11th IFAC Symp. on System Identification (SYSID'97)*, pages 1449–1454, Fukuoka, Japan, 1997.

[45] L. Giarré and M. Milanese. Model quality evaluation in H_2 identification. *IEEE Trans. Automatic Control*, 42(5):691–698, 1997.

[46] L. Giarré, M. Milanese, and M. Taragna. H_∞ identification and model quality evaluation. *IEEE Trans. Automatic Control*, 42(2):188–199, 1997.

[47] G.C. Goodwin, M. Gevers, and B. Ninness. Quantifying the error in estimated transfer functions with application to model order selection. *IEEE Trans. Automatic Control*, 37:913–928, 1992.

[48] G.C. Goodwin and M.E. Salgado. A stochastic embedding approach for quantifying uncertainty in the estimation of restricted

complexity models. *Int. J. of Adaptive Control and Signal Processing*, 3(4):333–356, 1989.

[49] R.G. Hakvoort. *System Identification for Robust Process Control - PhD Thesis.* Delft University of Technology, Delft, The Netherlands, 1994.

[50] R.G. Hakvoort and P.M.J. Van den Hof. Identification of probabilistic system uncertainty regions by explicit evaluation of bias and variance errors. *IEEE Trans. Automatic Control*, 42(11):1516–1528, 1997.

[51] F. Hansen. *A fractional representation approach to closed loop system identification and experiment design.* PhD thesis, Stanford University, 1989.

[52] F. Hansen and G. Franklin. On a fractional representation approach to closed-loop experiment design. In *Proc. American Control Conference*, pages 1319–1320, Atlanta, Georgia, 1988.

[53] D. Hinrichsen and A.J. Pritchard. New robustness results for linear systems under real perturbations. In *Proc. Conference on Decision and Control,*, pages 1375–1378, Austin, Texas,1988.

[54] H.T. Ingason and G.R. Jonsson. Control of the silicon ratio in ferrosilicon production. *Control Engineering Practice*, 6:1015–1020, 1998.

[55] V.A. Jakubovič. The $\mathcal{S}$-procedure in nonlinear control theory. *Vestnik Leningrad Univ. (russian) Vestnik Leningrad Univ. Math. (amer.)*, 4 (amer.)(1 (russian)), 1971 (russian) 1977 (amer.).

[56] R.L. Kosut. Uncertainty model unfalsification : a sytem identification paradigm compatible with robust control design. In *Proc. Conference on Decision and Control*, pages 3492–3497, New Orleans, LA, 1995.

[57] R.L. Kosut and B.D.O. Anderson. Least-squares parameter set estimation for robust control design. In *Proc. American Control Conference*, pages 3002–3006, Baltimore, Maryland, 1994.

[58] I.D. Landau, A. Karimi, A. Voda, and D. Rey. Robust digital control of flexible transmissions using the combined pole placement/sensititvity function shaping method. *European Journal of Control*, 1(2):122–133, 1995.

[59] I.D. Landau, D. Rey, A. Karimi, A. Voda, and A. Franco. A flexible transmission system as a benchmark for robust digital control. *European Journal of Control*, 1(2):77–96, 1995.

[60] W.S. Lee, B.D.O. Anderson, R.L. Kosut, and I.M.Y Mareels. A new approach to adaptive robust control. *Int. Journal of Adaptive Control and Signal Processing*, 7:183–211, 1993.

[61] L. Ljung. Identification, model validation and control. *36th IEEE Conf. on Decision and Control, plenary lecture*, 1997.

[62] L. Ljung. Identification for control - what is there to learn ? *Workshop on Learning, Control and Hybrid Systems, Bangalore*, 1998.

[63] L. Ljung. *System Identification: Theory for the User, 2nd Edition*. Prentice-Hall, Englewood Cliffs, NJ, 1999.

[64] L. Ljung. Model error modeling and control design. In *CD-ROM Proc. IFAC Symposium on system identification*, paper WeAM1-3, Santa Barbara, California, 2000.

[65] P.M. Makila. Approximation of stable systems by Laguerre filters. *Automatica*, 26(2):333–345, 1990.

[66] M. Milanese. Learning models from data: the set membership approach. In *Proc. American Control Conference*, pages 178–182, Philadelphia, USA, 1998.

[67] M. Nordin and P.O. Gutman. Digital QFT design for the benchmark problem. *European Journal of Control*, 1(2):97–103, 1995.

[68] A. Packard and J.C. Doyle. The complex structured singular value. *Automatica*, 29(1):71–109, 1993.

[69] A.G. Partanen and R.R. Bitmead. The application of an iterative identification and controller design to a sugar cane crushing mill. *Automatica*, 31:1547–1563, 1995.

[70] K. Poolla, P. Khargonekar, A. Tikku, J. Krause, and K. Nagpal. A time-domain approach to model validation. *IEEE Transactions on Automatic Control*, 39(5):951–959, 1994.

[71] L. Qiu, B. Bernhardsson, A. Rantzer, E.J. Davison, P.M. Young, and J.C. Doyle. A formula for computation of the real stability radius. *Automatica*, 31(6):879–890, 1995.

[72] A. Rantzer. Convex robustness specifications for real parametric uncertainty in linear systems. In *Proc. American Control Conference*, pages 583–585, 1992.

[73] A. Rantzer and A. Megretski. A convex parametrization of robustly stabilizing controllers. *IEEE Trans. Aut. Control*, 39(9):1802–1808, September 1994.

[74] M.G. Safonov and T.C. Tsao. The unfalsified control concept and learning. *IEEE Trans. Automatic Control*, 42(6):843–847, June 1997.

[75] R. Schrama. *Approximate Identification and Control Design*. PhD thesis, Delft Universtity of Technology, 1992.

[76] R. S. Smith and M. Dahleh. *The Modeling of Uncertainty in Control Systems*. Lecture Notes in Control and Information Sciences, vol. 192, Springer-Verlag, 1994.

[77] R.S. Smith and J.C Doyle. Model invalidation: A connection between robust control and identification. *IEEE Trans. Automatic Control*, 37:942–952, July 1992.

[78] T. Söderström and P. Stoica. *System Identification*. Prentice Hall International, Hemel Hempstead, Hertfordshire, UK, 1989.

[79] S. Toffner-Clausen, P. Andersen, J. Stoustrup, and H.H. Niemann. Estimated frequency domain model uncertainties used in robust controller design - a μ-approach. In *Proc. IEEE Conference on Control Applications*, pages 1585–1590, Glasgow, 1994.

[80] P.M.J. Van den Hof and R.J.P. Schrama. Identification and control - closed-loop issues. *Automatica*, 31:1751–1770, December 1995.

[81] P.M.J. Van den Hof, E.T. van Donkelaar, H.G.M. Dötsch, and R.A. de Callafon. Control-relevant uncertainty modelling directed towards performance robustness. In *IFAC World Congress, paper 3a-043*, pages 103–108, San Francisco, 1996.

[82] L. Vandenberghe and S. Boyd. Semidefinite programming. *SIAM Review*, 38(1):49–95, March 1996.

[83] M. Vidyasagar. *Control System Synthesis: A Factorization Approach.* MIT Press, Cambridge, Massachusetts, 1985.

[84] G. Vinnicombe. Frequency domain uncertainty and the graph topology. *IEEE Trans Automatic Control*, AC-38:1371–1383, 1993.

[85] G. Vinnicombe. *Measuring the Robustness of Feedback Systems.* PhD thesis, Cambridge University, 1993.

[86] G. Vinnicombe. *Uncertainty and Feedback - H_∞ loop-shaping and the ν-gap metric.* Book to be published, 2000.

[87] D. De Vries. *Identification of model uncertainty for control design.* PhD thesis, Delft University of Technology, The Netherlands, 1994.

[88] B. Wahlberg. System identification using Laguerre models. *IEEE Transactions on Automatic Control*, 36(5):551–562, May 1991.

[89] G. Zames. Feedback and optimal sensitivity: Model reference transformations, multiplicative seminorms, and approximate inverses. *IEEE Trans. Aut. Control*, AC-26(2):301–320, April 1981.

[90] Z. Zang, R.R. Bitmead, and M. Gevers. Iterative weighted least-squares identification and weighted LQG control design. *Automatica*, 31(11):1577–1594, 1995.

[91] K. Zhou and J. Doyle. *Essentials of Robust Control.* Prentice Hall, Upper Saddle River, New Jersey, 1998.

[92] K. Zhou, J.C. Doyle, and K. Glover. *Robust and Optimal Control.* Prentice Hall, New Jersey, 1995.